Islamic University of Gaza

Deanery of Higher Studies

Faculty of Science

Department of Physics

DYE-SENSITIZED SOLAR CELLS USING ZnO AS A SEMICONDUCTING LAYER

الخلايا الشمسية ذات الأصباغ باستخدام أكسيد الزنك كطبقة شبه موصلة

By

Hatem S. El-Ghamri

B.Sc. In Physics, Islamic University of Gaza

Supervisors

Dr. Sofyan A. Taya

Dr. Taher M. El-Agez

Submitted to the Faculty of Science as a Partial Fulfillment of the Master of Science (M. Sc.) in Physics

1433 – 2012

Dedication

To my parents, my wife, my brother, my sisters, my children.

To my homeland Palestine the only place in which I feel alive.

Hatem S. El-Ghamri

ACKNOWLEDGMENTS

In the name of Allah to whom I am overwhelmed with gratitude for his continuous help and guidance throughout the path of knowledge. I would like to express my gratitude to all those who gave me the possibility to complete this thesis.

I am extremely indebted to supervisors Dr. Sofyan Taya and Dr. Taher El-Agez for their constant support and whose help, and encouragement helped me in all time of research for arranging and writing of this thesis. Also, I would like to express my thanks to Dr. Naji Al-Doahida, and Dr. Amal El-kahlot for their support and guidance.

Personally, I'd like to thank all those who have helped with their advice and efforts .

ABSTRACT

Dye-sensitized solar cell (DSSC) was developed by Grätzel in 1991 which was named "Grätzel Cell". DSSC is considered the third generation of photovoltaic devices for the conversion of visible light into electric energy. These new types of solar cells are based on the photosensitization produced by the dyes on wide band-gap semiconductors such as TiO_2. This sensitization is produced by the dye absorption of part of the visible light spectrum. One advantage of DSSCs is the low cost of the solar energy conversion into electricity because of inexpensive materials and the relative ease of the fabrication processes. Recent studies have shown that metal oxides such as TiO_2, have been successfully used as photo-anode when a dye is absorbed in the interior of the porous layer of the semiconductor.

In this work, DSSCs were prepared using Zinc oxide (ZnO) as a semiconducting layer with eight natural and eight chemical dyes. Thin films of nanocrystalline ZnO was spread on transparent conducting FTO coated glass using doctor blade method. The absorption spectra of all dyes were performed. The I-V characteristic curves of the fabricated cells were measured and studied at different light intensity. All photovoltaic parameters of the cells were defined. The results revealed that the extract of safflower and Eosin Y corresponds to the highest efficiency. Optimization of the fabricated cells were conducted concerning the sintering temperature and the thickness of the ZnO layer.

List of Figure Captions

CHAPTER ONE

CHAPTER TWO

CHAPTER THREE

CHAPTER FOUR

CHAPTER FIVE

List of Table Captions

CHAPTER THREE

CHAPTER FOUR

CHAPTER FIVE

CONTENTS

CHAPTER ONE
INTRODUCTION AND MOTIVATION

1.1. Renewable Energy

Energy is the capacity of a physical system to perform work. Energy exists in several forms such as heat, kinetic or mechanical energy, light, potential energy, electrical, or other forms. The need for inexpensive, clean energy is increasing everyday. As more and more countries develop and the world's population increases, the need to power increases. One of the most promising sources of energy for powering the planet was solar energy. Approximately 120,000 terawatts (TW) of solar energy strike the earth everyday. In 2008, the current world energy consumption is approximately 15 TW [1]. The sun is a huge, untapped resource. Currently, only 0.05% of the world's energy production is from solar energy. This brings us to the question, "Why we don't use the sun to power the planet?" The basic fundamental answer to the question is the cost. Solar energy is relatively more expensive than conventional means of energy, such as coal and fossil fuels. According to the California levelized energy costs in 2007, the cost of electricity produced by coal was 0.074-0.088 cents per kilowatt hour. The high cost of solar energy explains why 70 to 80 percent of the world's energy comes from fossil fuels [2].

1.2. Renewable and Non-renewable Energy Resources

Renewable energy is energy which comes from natural resources such as sunlight, wind, rain, tides, and geothermal heat, which are renewable (naturally replenished). The renewable energy sources include solar energy, wind energy, energy waves of the sea, the energy of gravity, and magnetic energy. Human world energy consumption is made up of about 76% fossil fuels, 14% biomass (wood etc. − a form

of solar energy), 6% hydroelectricity (also a form of solar energy), 4% nuclear and tiny fraction from other solar energy sources [2]. Fossil energy (petrol and the like) cannot be a renewable energy resource. The crude oil found on our planet was formed over periods of several tens of thousands of years. However, we have used almost all of it within only a few decades and it becomes clear that this does not meet the requirements of our definition of a renewable energy source.

Nuclear energy obtained from nuclear fission is also clearly not a renewable energy because its main resources, e.g. uranium, were formed during the birth of our planet and are therefore limited. Similarly, nuclear fusion is not a renewable energy resource, since it depends on the presence of deuterium, a hydrogen isotope. It reacts to give helium and hydrogen and simultaneously releases heat. However, these fusion reactions are similar to those that occur in the sun and other stars, and provide a much greater energy potential than nuclear fission. The use of nuclear power as energy source is not accepted by wide section of the population anymore because of security and health risks. Further, the disposal of nuclear waste is still an unsolved problem, worldwide. Over the last decades, there have been big efforts for developing new alternative energy sources. The sun, on the other hand, matches all requirements of an ideal energy source. It is reliable, ubiquitous and for free. The nature uses the sun as its nearly only energy source in photosynthesis since millions of years.

1.3. Types of Solar Energy Conversions

Solar energy emitted by the sun and reaching the earth's surface is a form of electromagnetic radiation that is available over a wide spectral range (300−2100nm). In order to be used, the radiation needs to be converted into an energy form suitable for our needs. Four different types of solar energy conversion methods are currently available for this purpose [3]:

a. Thermal Solar Energy Conversion

The most used type of solar energy include the use of solar radiation to heat water directly. It has been observed this type as black spots (mirrors assembly) on the roofs of houses, and is used only for heating water for domestic purposes. This system is

not so efficient in winter due to the low intensity of sun radiation. As an alternative electricity and gas are used in heating water process.

b. Thermoelectric Solar Energy Conversion

Solar energy is converted into heat which is used to generate electricity. It is well known that electricity producing turbines can be rotated by steam which is produced by heating water using the conventional fuel (cool, gas,...). In thermoelectric solar energy conversion, solar energy is used to heat water and convert it steam which in turn rotates the turbines.

c. Photoelectric Solar Energy Conversion

The direct conversion of solar energy into electricity is the best known type of solar energy conversion. This type of energy conversion makes use of devices called solar cells. The high cost of solar cells is the main limiting factor for large scale use of solar electricity. An intensive scientific research is now conduced to lower the solar cell cost.

d. Chemical Solar Energy Conversion

Solar energy can be transformed into many types of energy. One of these types is the chemical energy. The importance of this kind of energy comes from their ability to overcome problems with long-term storage and transfer of energy.

1.4. Solar Radiation and Air Mass

The sun in a huge nuclear fusion reactor in which the energy of the sun is created. The fusion of hydrogen to give helium inside the sun at several million degrees is the source of sun energy . In this process, there is a mass difference between reactants. This mass difference is converted into energy according to $E = mc^2$. This gives rise to its surface temperature of 6000 ^{0}k. Because all elements are ionized to some degree at

this temperature, their spectral lines are strongly broadened so that the gaseous surface of the sun radiates like a black body. The solar energy that reaches earth is determined by the radiation of the sun and the distance between the earth and the sun. The solar radiation power just outside the earth's atmosphere is 1.367 kWm^{-2} and this value is known as the solar constant [4] . On its way from the sun to the earth through the atmosphere, radiation is partly absorbed and scattered . Ozone absorbs ultraviolet radiation whereas carbon dioxide and water vapor absorb in the infrared region. Molecules, aerosols, and clouds are the main agents causing radiation scattering. Scattering of radiation caused by molecules, aerosols and clouds are, respectively, called Rayleigh, Mie, and Cirrus scattering. Specific solar radiation conditions are defined by the Air Mass (AM) value. The spectral distribution and total flux of radiation just outside the Earth's atmosphere, similar to the radiation of a black body of 6000 ^0k, has been defined as AM-0. In passing through the atmosphere the radiation becomes attenuated by complex and varying extinction processes mentioned above. At the equator at sea level at noon when the incidence of sunlight is vertical (α=90°, sun in zenith) and the light travels the shortest distance through the atmosphere and air ("air-mass") to the surface, the spectral solar radiance and flux (1.07 kWm^{-2}) is defined as AM-1. However, if the angle of light incidence is smaller than 90°, the light has to travel through more air-mass than under AM-1 conditions. The relative path length through the atmosphere by the shortest geometrical path is given by:

$$AM = 1/\cos\alpha \,, \qquad (1.1)$$

where α is the incident angle of light. The so-called AM-1.5 conditions are achieved when the sun is at an angle of 41.8° above the horizon and results in the spectral distribution shown in Fig. 1.1 and a solar flux of 963 Wm^{-2}. This angle of incidence is commonly encountered in western countries and hence AM-1.5 is taken as a standard condition for solar cell testing and referencing [5].

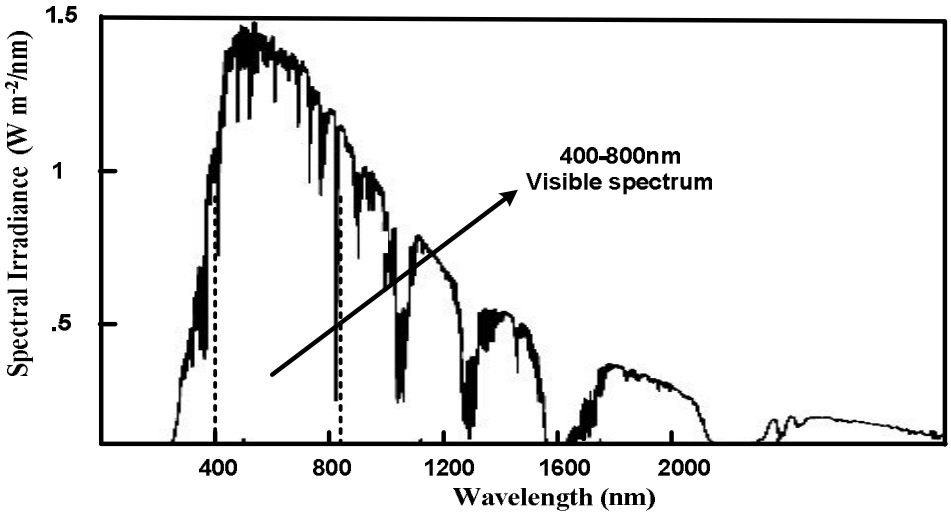

Figure 1.1. Spectral distribution of solar radiation .

1.5. Solid State Solar Cells

The history of the photovoltaic effects began in 1839 when Becquerel detected a photovoltage when sunlight was allowed to shine on one of the two electrodes he had placed in an electrolytic solution . In 1954, researchers at the Bell Telephone Laboratories demonstrated the first practical conversion of solar radiation into electric energy via use of a *p-n* junction type solar cell with 6% efficiency [6]. With the advent of the space program, photovoltaic cells made from semiconductor-grade silicon rapidly became the power source of choice for use on satellites. The systems were very reliable, and cost was of little concern. In the early 1970s, some troubles took place in the oil supply to the industrial world. This led to a significant consideration of photovoltaics as an alternative power source. The main problems where improving performance, lowering cost, and increasing reliability. These three points are still hot research topics until today. It's very significant to understand the physical mechanism associated with the photovoltaic power generation. The most common photovoltaic cell is based on the use of a semi-conducting material to convert sunlight directly into electrical energy. The electricity obtained is direct current and can be used directly to operate direct current devices, converted to an alternating current, or stored for later use. Furthermore, there are no moving parts, the operation is environmentally clean and if the device is correctly insulated, caring

against harm from the environment, there is nothing to worry. Because sunlight is universally available, photovoltaic devices provide many benefits that make it very important to understand the operation principle of photovoltaic cells.

1.5.1. Semiconductor

A semiconductor is a material with electrical conductivity intermediate in magnitude between that of a conductor and an insulator. This means it has a conductivity roughly in the range of 10^3 to 10^{-8}siemens per centimeter. Semiconducting materials are the foundation of modern electronics including radio, computers, telephones, and many other devices. Such devices include transistors, solar cells, many kinds of diodes including the light-emitting diodes (LEDs), the silicon controlled rectifiers, photo-diode, and digital and analog integrated circuits. In a metallic conductor, current is carried by the flow of electrons**.** In a semiconductor, the electrons reside within two energetic values or bands; the valence band and the conduction band. These two bands are separated by the forbidden energy gap (E_g). According to band theory, a solid body is characterized by a unified electron spectrum in which each electron belongs to the entire body but not to an individual band. The energy band diagram of that part of the spectrum which determines the electrical and optical characteristics of a semiconductor in the range of interest is shown in Fig. 1.2.

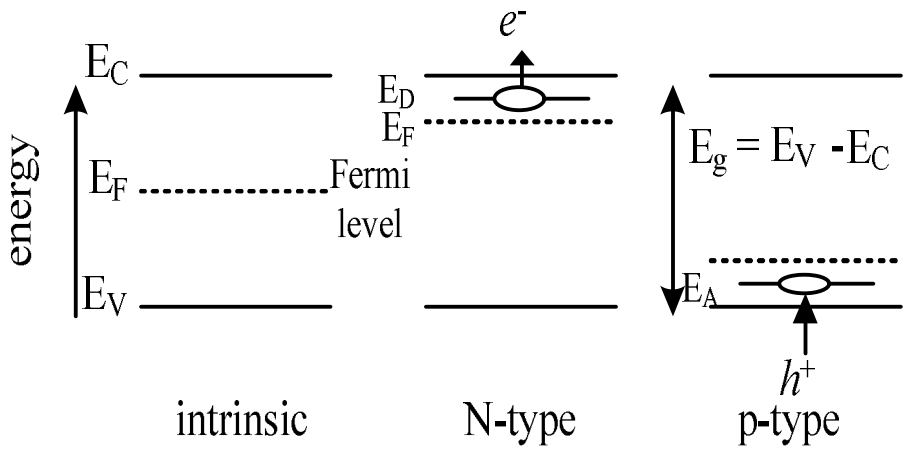

Figure 1.2. Energy diagram of semiconductors with intrinsic, n-type and p-type properties.

1.5.2. Light Absorption

When an intrinsic semiconductor is irradiated with light of energy larger than the bandgap energy ($h\upsilon \geq E_g$), an electron from the valence band can be promoted into the conduction band (see Figure 1.3). This process creates non-equilibrium carriers in pairs, so that $D_n=D_p$, where D_n and D_p are the excess concentrations of electrons and holes, compared to the equilibrium concentrations (n_0 and p_0), and is called the intrinsic or fundamental absorption. The amount of light absorbed by a semiconductor is given by Lambert's law of extinction:

$$I = I_0 e^{-\beta x}, \qquad (1.2)$$

where x is the coordinate, I_0 is the intensity of non-reflected light incident on the surface of the semiconductor at x=0, and β is the linear coefficient of light absorption. The dimension of this coefficient is the inverse of length, thus, β^{-1} is often arbitrarily called the depth or length of penetration and is a measure of distance over which the incident light attenuates e times.

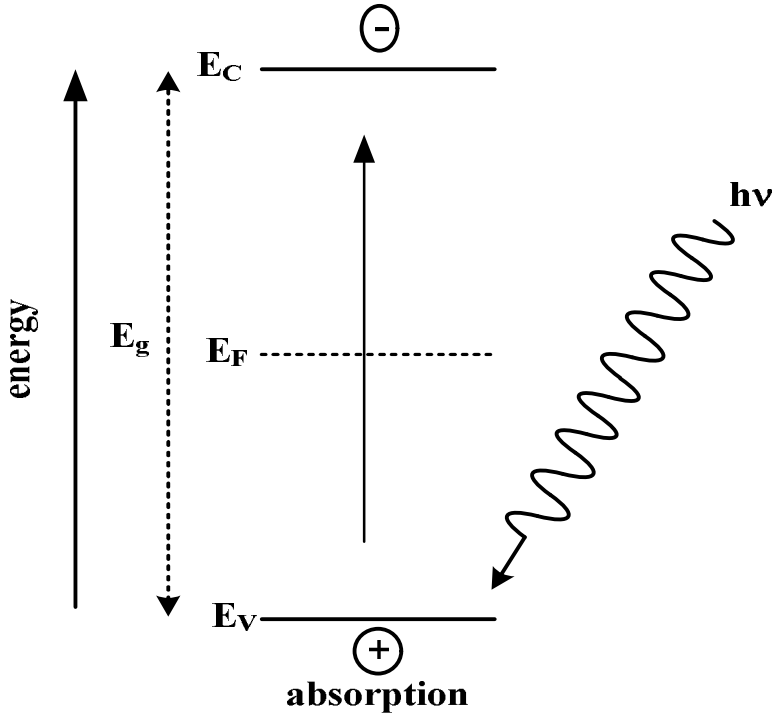

Figure 1.3**.** Light absorption by an intrinsic semiconductor. The impinging photon induces an electron transition from the valence band into the conduction band if hν $\geq E_g$.

1.5.3. The p-n Junction

The purpose of a solar cell is to convert the energy of sunlight to electrical energy and to deliver that electrical energy to an external load. This implies that a current has to flow within the semiconductor composed of the positively charged holes and negatively charged electrons which the light has generated.

When an *n*-doped and a *p*-doped semiconductor are joined into a single semiconductor crystal, the Fermi levels (chemical potential) of the *n*- and *p*-type regions must be aligned to the same level, leading to the configuration shown in Fig. 1.4. At the moment of joining, a diffusion gradient is established and carriers will diffuse due to the difference in concentration, that is the holes from the *p*-region will

move into the *n*-region, and the electrons from the *n*-area will move into the *p*-region. This is an uphill reaction, energetically unfavorable, only driven by the concentration gradient. Diffusion currents will arise. The ionized acceptor and donor atoms, which are no longer electrically compensated since they cannot diffuse, remain behind as fixed space charges. As demonstrated in Fig. 1.4, negative space charges will arise on the right hand side in the *p*-region and positive space charges arise on the left hand side in the *n*-region. Correspondingly, as occurs in a plate capacitor, an electric field is generated at the *p*-*n* junction, which is directed so that it drives the diffusing charge carriers in the opposite direction of the diffusion. Hence, the diffusion continues until an equilibrium is established, in other words until the diffusional flow is compensated by a field current of equal magnitude. The resulting (extremely large) internal field exists, even if both sides of the semiconductor are grounded.

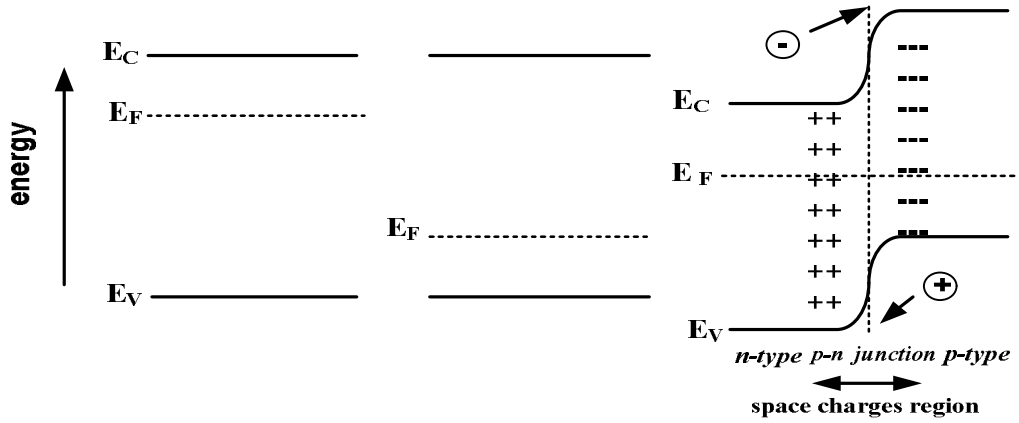

Figure 1.4**.** The charge dipole and space charge region produced at a p-n junction.

The current versus voltage characteristic of an ideal *p*-*n* junction is quantitatively given by diode equation ,

$$I = I_s[\, e^{(-qE/kT)} - 1] \quad . \qquad (1.3)$$

where q is the elemental charge, k is the Boltzmann constant, T is the absolute temperature and I_s is the saturation current of the junction.

1.5.4. Photovoltaic Processes in a Solar Cell

A semiconductor containing a *p-n* junction generates a hole-electron pair as shown in Fig. 1.5. The electron will be drawn to the *n*-side when illuminated by light of proper wavelength (the *n*-side is the side of the junction with minimum energy for electrons) and the hole to the *p*-side (this side exhibits minimum energy for holes) of the *p-n* junction. As illustrated in Fig. 1.5, continuous irradiation leads to a reduction of the energy barrier (E_B) created by the *p-n* junction which generates the desired photovoltage E_P. Eventually a steady-state condition will be reached between holes and electrons generated by light and their recombination. The band gap energy determines the maximum photovoltage that can be generated, which is called the open circuit potential, V_{oc}. The qualitative description of a *p-n* junction under illumination is illustrated in Fig. 1.5.

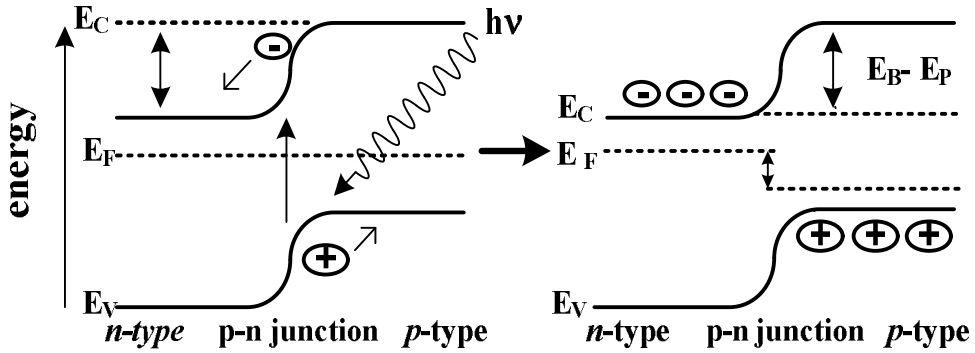

Figure 1.5. The p-n junction under illumination. Left: A photon induced hole-electron pair is separated by the local field of the junction. Right: The origin of the photovoltage E_P. E_B = Energy barrier created by the p-n junction, E_P = Energy equivalent of the photovoltage.

1.5.5. Parameters of Solar Cells

A number of important parameters of the solar cell have to be clarified. These parameters are short circuit current , open circuit voltage, optimum voltage, optimum Current, fill factor, efficiency, and parasitic resistances.

a. Short Circuit Current I_{sc}:

It is the current obtained if the solar cell is short circuited, that is there is no potential differences across the cell. The short circuit current is equal to the absolute number of photons converted to hole-electron pairs.

b. Open Circuit Potential V_{oc} :

The open circuit potential is obtained when no current is drawn from the solar cell.

c. Optimum voltage V_m :

V_m is the voltage at the optimum operating point .

d. Optimum Current I_m :

I_m is the current at the optimum operating point.

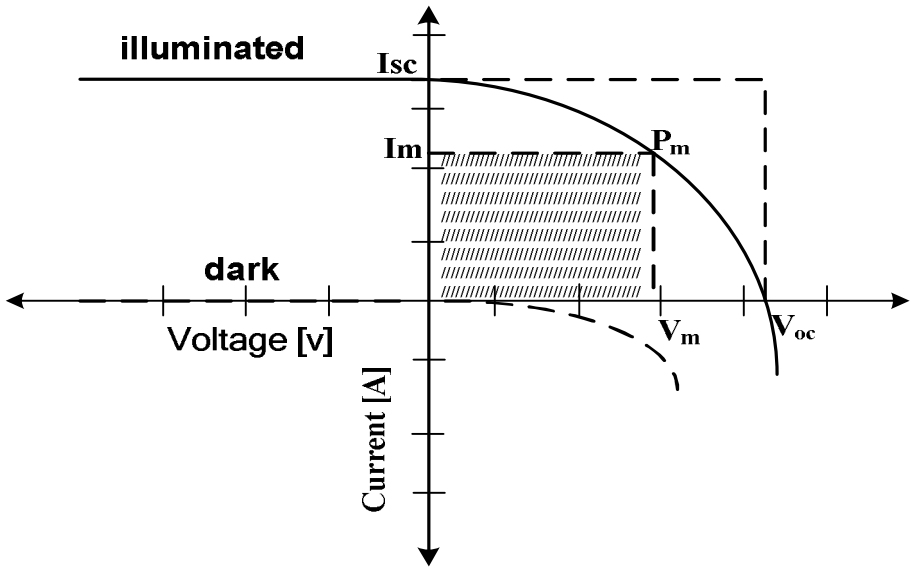

Figure 1.6. Voltage−current characteristics of a solar cell. Shaded area represents the maximum achievable output power.

e. Fill Factor FF :

Optimal power output requires a suitable resistor, which corresponds to the ratio V_m/I_m, where V_m and I_m are the voltage and current at the optimum operating point and $P_m=V_mI_m$ is the maximum achievable power output. The ratio of peak output V_mI_m to $V_{oc}I_{sc}$ is called the fill factor (FF) of a solar cell and is an important quality criterion.

$$FF = I_m V_m / I_{sc} V_{oc} \quad . \tag{1.4}$$

The meaning of fill factor can be understood from its graphical representation. It indicates how much area underneath the I−V characteristic curve is filled by the rectangle described by V_mI_m (shaded area in Fig. 1.6) in relation to the rectangle $V_{oc}I_{sc}$. The theoretically maximum obtainable FF is a function of the open circuit potential, the higher the V_{oc} the higher FF. Fill factors for optimized solar cells are typically within the range of 0.6−0.75.

f. Efficiency η :

The efficiency of a solar cell is the ratio of the electrical power it delivers to the load the optical power incident on the cell . Maximum efficiency is reached when power delivered to the load is P_{max}. Incident optical power is normally specified as the solar power on the surface of the earth which is approximately $1mW/mm^2$. Spectral distribution of sunlight is close to a blackbody spectrum at 6000^0C minus the atmospheric spectrum [7]. Maximum efficiency may be written as:

$$\eta = FF.I_{sc}.V_{oc} /P_{light} \quad , \tag{1.5}$$

where P_{light} is the energy of the light shining on the solar cell and is obtained when the light intensities of the whole spectral range are integrated. I_{sc} is directly proportional to the incident optical power P_{light} but V_{oc} increases logarithmically with the incident power. So the overall efficiency of solar cell is expected to increase logarithmically with incident power. However, at high light concentration thermal effect and electrical losses in the series resistance of solar cell limit the efficiency enhancement that can be achieved, so the efficiency of practical solar cell peaks at some finite concentration level [8].

The efficiency of the solar cell depends on the temperature of the cell, and which is even more important, on the quality of the illumination, i.e., the total light intensity and the spectral distribution of the intensity. For this reason, a standard measure mentcondition has been developed to facilitate comparable testing of the solar cells between different laboratories. The Standard Test Condition (STC) for solar cells is the Air Mass 1.5 spectrum, an incident power density of 1000 W m^{-2}, and temperature of the cell is 25°C. The power output of the solar cell at these conditions is the nominal power of the cell, or module, and is reported in peak watts, W_p. In practice, special solar simulator light sources are used for the standard measurements.
These four quantities: I_{sc}, V_{oc}, FF and ŋ are the key performance characteristics of a solar cell. All of these should be defined for particular illumination conditions.

g. Parasitic Resistances R_{sh}, R_s :

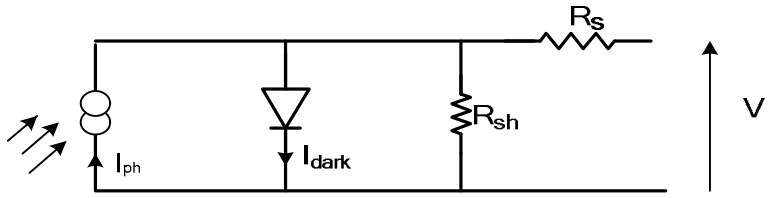

Figure 1.7. Equivalent circuit including series and shunt resistances.

In real cells, there is power dissipation through the resistance of the contacts and through leakage currents around the sides of the device. These effects are equivalent electrically to two parasitic resistances in series (R_s) and in parallel (R_{sh}) with the cell as shown in Fig. 1.7. The series resistance arises from the resistance of the cell material to current flow, particularly through the front surface to the contacts, and from resistive contacts. Series resistance is a particular problem at high current densities, for instance under concentrated light. The parallel or shunt resistance arises from leakage of current through the cell, around the edges of the device, and between contacts of different polarity. It is a problem in poorly rectifying devices. Series and parallel resistances reduce the fill factor as shown in Fig. 1.8. For an efficient cell we need R_s to be as small and R_{sh} to be as large as possible.

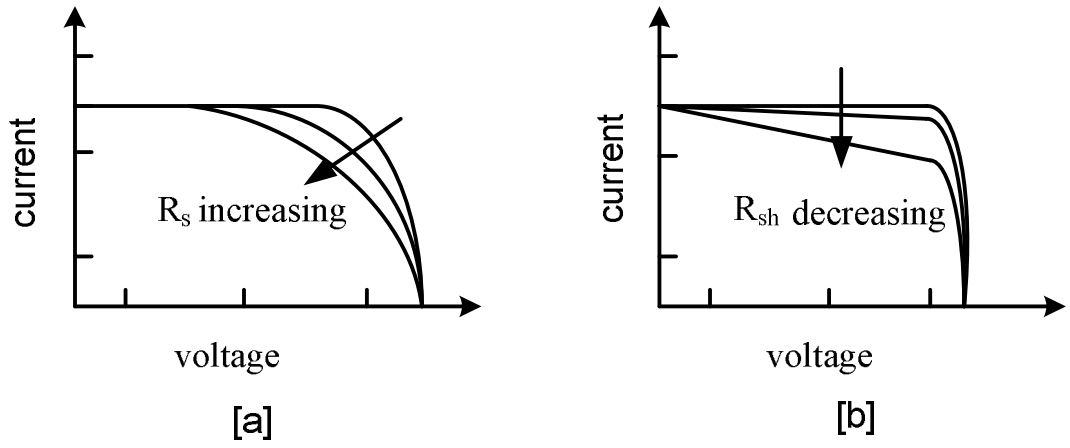

Figure 1.8. Effect of (a) increasing series and (b) reducing parallel resistances. In each case the outer curve has $R_s = 0$ and $R_{sh} = 1$. In each case the effect of the resistances is to reduce the area of the maximum power rectangle compared to $I_{sc} \times V_{oc}$.

1.6. This Work

chapter one presents, an introduction to renewable energy, solar radiation, solar energy conversion, semiconductor properties, and photovoltaic processes in a solar cell are presented.

In chapter two, DSSC is studied. The operation of DSSC, materials of dye sensitized solar cell, factors that affect the efficiency of the cell, and basic difference between the DSSCs and p-n-junction solar cells in operation principal are presented.

In chapter three DSSCs were prepared using natural dyes extracted from plants. The ZnO film is prepared using doctor blade method, absorption spectra of all dyes are performed. Photovoltaic parameters are measured and studied.

In chapter four, DSSCs were prepared using eight chemical dyes. Absorption spectra of all dyes are performed and plotted. Photovoltaic parameters are measured and calculated.

In chapter five, optimization of the sintering temperature and thickness of the ZnO layer using Safflower and Eosin Y dyes are studied.

CHAPTER TWO

DYE SENSITIZED SOLAR CELLS

2.1. Introduction

The dye-sensitization dates back to the 19th century, when photography was invented. The first studies on dye-sensitized titanium dioxide (TiO_2) photoelectrode were done in 1960's and 1970's, because the limited amount of dyes that could be adsorbed on macrocrystalline semiconductors, and the too narrow spectral absorbance range of the dyes, the photocurrent and the cell efficiency stayed on very modest level. The use of dye-sensitization in photovoltaic remained however rather unsuccessful until a breakthrough at the early 1990's in the Laboratory of Photonics and Interfaces in the Switzerland. By the successful combination of nanostructured electrodes and efficient charge injection dyes, Grätzel and his co-workers developed a solar cell with energy conversion efficiency exceeding 7% in 1991[9], and 10% in 1993 [10]. This solar cell is called the dye sensitized solar cell.

Dye-sensitized solar cells (DSSCs) are the third generation of photovoltaic devices for the conversion of visible light into electric energy. These new types of solar cells are based on the photosensitization produced by dyes on wide band-gap mesoporous metal oxide semiconductors. This sensitization is produced by the dye absorption of part of the visible light spectrum. One aspect of these DSSCs photocells that is particularly attractive, is the low cost of the solar energy conversion into electricity; this is possible mainly due to the use of inexpensive materials and the relative ease of the fabrication processes. The low production cost and promising efficiency are ideal for solar cells. Since the breakthrough in 1991, other cheap, wide bandgap materials such as ZnO, SnO_2, Nb_2O_5, and In_2O_3 have been widely investigated. Zinc oxide has received much attention due to its similar bandgap to that of titanium dioxide.

2.2. Operating Principle

The DSSC differs from other solar cell types both by its basic construction and the physical processes behind its operation. Unlike the first and second generation photovoltaic devices based on solid semiconductor materials, the typical DSSC configuration combines solid and liquid phases. Electricity is generated on the photoelectrode, which is a nonporous TiO_2 or ZnO film sensitized with a monolayer of visible light absorbing dye and penetrated with a redox electrolyte. The TiO_2 or ZnO -electrolyte network is sandwiched between two conductive substrates that also work as current collectors. The opposite substrate to the TiO_2 or ZnO layer, the counter electrode is coated with a material capable of catalyzing the redox reaction in the electrolyte. Thus, the DSSC resembles more an electrochemical cell than a conventional p-n junction solar cell.

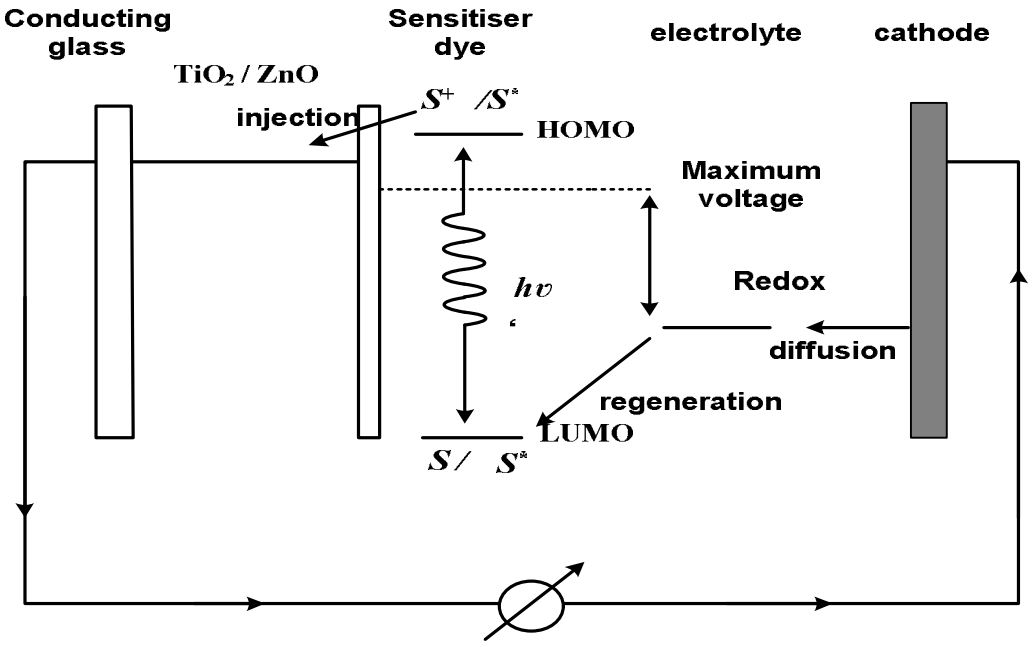

Figure 2.1. Energetics of operation of DSSCs

The operation of dye sensitized solar cell is shown in Fig. 2.1. Photon absorption induces a metal-to-ligand type electronic transition between the highest occupied molecular orbital (HOMO) and lowest unoccupied molecular orbital(LUMO) of the

dye, and this leads to excitation of the dye form the state (S) to an electronically excited state (S*).

❖ Light absorption $S + h\upsilon \rightarrow S^*$. (2.1)

The excited dye molecule injects an electron into the conduction band of the TiO_2 or ZnO electrode and is oxidized (S^+) .

❖ Electron injection $S^* \rightarrow S^+ + e^-$. (2.2)

The amount of current that the cell is able to generate is determined by the energetic difference between of the HOMO and LUMO of the dye, which equals the band gap in inorganic semiconductors. The maximum voltage, on the other hand, is defined as the difference between the redox level of the electrolyte and the Fermi level of the TiO_2 or ZnO electrolyte through the reduction of iodide.

❖ Dye reduction and iodide oxidation $2S^+ + 3I^- \rightarrow 2S + I^{-3}$. (2.3)

The regeneration of the dye by iodide inhibits the recapture of the conduction band electrons by the oxidized dye. The iodide is in turn regenerated at the counter electrode by the reduction of triiodide.

❖ Triiodide reduction $I^{-3} + 2e_{pt}^- \rightarrow 3\, I^-$. (2.4)

The circuit is completed by electron migration through an external load. In an ideal cell, no chemical substances are permanently transmuted. The most often used counter electrode catalyst for the triiodide/iodide reduction reaction is platinum, though also carbon materials and certain conductive polymers have been successfully employed in this function [11].

2.3. Materials of the Dye-Sensitized Solar Cell

The materials of DSSC will be presented in this section. The components of the cell are described one by one.

2.3.1. Substrates

The electrodes of the standard DSSC are prepared onto transparent conducting oxide (TCO) coated glass substrates, between which the cell is assembled. The conducting coating of the substrate works as a current collector and the substrate material itself both as a support structure to the cell and as a sealing layer between the cell and the ambient air.

Requirements for a good DSSC substrate are low sheet resistance which should also be independent of temperature, high transparency, and ability to prevent impurities such as water and oxygen from entering into the cell. The traditional approach is to build the DSSC on TCO coated glass sheets. The most often used TCOs are fluorine- and indium-doped tin oxides, whose sheet resistances are around 10 Ω/cm^2. As the only TCO coating stable at high temperatures, the Fluorine-doped tin oxide (SnO_2:F) has been the material of choice for DSSCs. Whilst glass is obviously an effective barrier towards water and oxygen penetration into the cell. Its disadvantages are fragility, rigidity, heavy weight, and high price [12].

2.3.2. Nanoparticle Electrodes

Oxide semiconductors are preferred in photo electrochemistry because of their exceptional stability against photo-corrosion on optical excitation in the band gap. Furthermore, the large bandgap (>3 eV) of the oxide semiconductors is needed in DSSCs for the transparency of the semiconductor electrode for the large part of the solar spectrum.

On the other hand, oxide semiconductor materials have good stability under irradiation in solutions. However, stable oxide semiconductors cannot absorb visible light because they have relatively wide band gaps. Sensitization of wide band gap oxide semiconductor materials, such as TiO_2, ZnO, and SnO_2, with photosensitizers, such as organic dyes, natural dyes, that can absorb visible light has been extensively

studied in relation to the development of photography technology since the late nineteenth century [13].

TiO_2

Titanium dioxide, also known as titanium(IV) oxide or titania, is the naturally occurring oxide of titanium. TiO_2 has some properties of the most important, such as molar mass:79.86g/mol, melting point:1843^{0}C, boiling point:2972^{0}Cand refractive index:2.488. When used as a pigment, it is called titanium white.

ZnO

Zinc oxide (ZnO) has some properties of the most important, such as low cost, non-toxicity, low sheet resistance, high transmittance, melting point: 1975 °C, high electron mobility: >100cm^2/Vs and high exciting binding energy: ~60meV (electron-hole binding energy). ZnO is a direct wide-band gap semiconductor (~3.3-3.4eV), allows for efficient photon emission, as in LED's or laser diodes. It can easily be n-doped with aluminum, indium, or extra zinc. Possesses high photoconductivity– can help speed up currents in semiconductor devices. In the standard preparation method, the nanostructured ZnO electrodes are deposited from a solution or a paste containing ZnO nanoparticles of desired size. Mastering the properties of the nanoparticle solutions and the nanoparticle films obtained from these solutions belongs to the fields of colloid and sol-gel chemistry, which have been the essential enabling technologies for the development of high efficiency DSSCs.

2.3.3. Sensitizing Dyes

The absorption of incident light in the DSSCs is realized by specifically engineered dye molecules placed on the semiconductor electrode surface. To achieve a high light-to energy conversion efficiency in the DSSC, the properties of the dye molecule as attached to the semiconductor particle surface are essential. Such desirable properties can be summarized as:

1. Absorption: The dye should absorb light at wavelengths up to about 920 nanometers, i.e. the energy of the exited state of the molecule should be about 1.35 eV above the electronic ground state corresponding to the ideal band gap of a single band gap solar cell .

2. Energetics: To maximize the photovoltage, the excited state of the adsorbed dye molecule should be only slightly above the conduction band edge of the TiO_2, but yet above enough to present an energetic driving force for the electron injection process. For the same reason, the ground state of the molecule should be only slightly below the redox potential of the electrolyte.

3. Kinetics: The process of electron injection from the excited state to the conduction band of the semiconductor should be fast enough to outrun competing unwanted relaxation and reaction pathways.

4. Stability: The adsorbed dye molecule should be stable enough in the working environment (at the semiconductor-electrolyte interface) to sustain about 20 years of operation at exposure to natural daylight, i.e. at least 10^8 redox turnovers .

These can be considered as the prerequisites for a proper photovoltaic sensitizer. However, the factors that actually make the dye-sensitization work efficiently and yield good photovoltaic performance in the practical cell are much more complicated with all the details not even fully understood at the moment . Absorption of light by other cell components such as the TiO_2 and the electrolyte is undesirable, because it on one hand does not lead to current generation and reduces thereby the efficiency, and on the other hand may induce side reactions with possibly degrading effects on the cell performance in the long term [14].

Ruthenium Dye

In recent years, considerable developments have been made in the engineering of novel dye structures in order to enhance the performance of the DSSC. In particular, amphiphilic homologues of the pioneering ruthenium based N-3 dye have been developed. These amphiphilic dyes display several advantages compared to the N-3 dye such as:

1. A higher ground state pK_a of the binding moiety thus increasing electrostatic binding onto the TiO_2 surface at lower pH values.
2. The decreased charge on the dye attenuating the electrostatic repulsion in between adsorbed dye units and thereby increasing the dye loading.
3. Increasing the stability of solar cells towards water-induced dye desorption.
4. The oxidation potential of these complexes is catholically shifted compared to that of the N-3 sensitizer, which increases the reversibility of the ruthenium III/II couple, leading to enhanced stability [15].

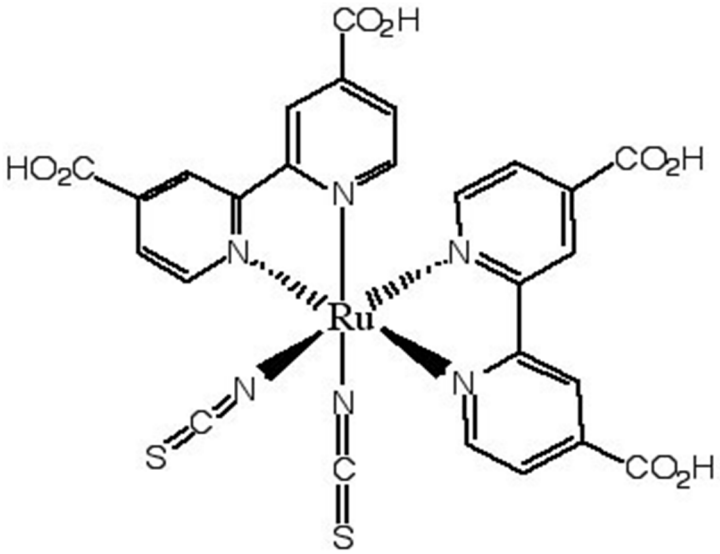

Figure 2.2. Ruthenium organometallic based N-3 Grätzel standard dye used in DSSC applications.

2.3.4. Electrolytes

The electrolyte used in the DSSCs consists of iodine (I^-) and triiodide (I^{-3}) as a redox couple in a solvent with possibly other substances added to improve the properties of the electrolyte and the performance of the operating DSSC.
The ideal characteristics of the redox couple for the DSSC electrolyte are [16]:

1. Redox potential thermodynamically (energetically) favorable with respect to the redox potential of the dye to maximize cell voltage.

2. High solubility to the solvent to ensure high concentration of charge carriers in the electrolyte.

3. High diffusion coefficients in the used solvent to enable efficient mass transport.

4. Absence of significant spectral characteristics in the visible region to prevent absorption of incident light in the electrolyte.

5. High stability of both the reduced and oxidized forms of the couple to enable long operating life.

6. Highly reversible couple to facilitate fast electron transfer kinetics.

7. Chemically inert toward all other components in the DSSC.

The following are the criteria for a suitable solvent for a high efficiency liquid electrolyte DSSC [17]:

1. The solvent must be liquid with low volatility at the operating temperatures (40°C - 80°C) to avoid freezing or expansion of the electrolyte, which would damage the cells.

2. It should have low viscosity to permit the rapid diffusion of charge carriers.

3. The intended redox couple should be soluble in the solvent.

4. It should have a high dielectric constant to facilitate dissolution of the redox couple.

5. The sensitizing dye should not desorb into the solvent.

6. It must be resistant to decomposition over long periods of time.

7. And finally from the point of view of commercial production, the solvent should be of low cost and low toxicity.

The solvent used already in the early DSSCs, acetonitrile, seems to be still the best choice when the cell efficiency is to be maximized. However, with respect to the preferred solvent properties listed above, acetonitrile immediately fails at least in two points. Firstly, it is highly volatile with boiling point of 82°C, which is about the maximum temperature that a roof-top solar cell can reach at full sunlight , and due to the high volatility it easily escapes from the cell through the sealing. Secondly, acetonitrile is highly toxic and cannot be used in the commercial DSSCs . The choice of solvent is thus always a trade-off between low viscosity with better ion diffusion properties and high viscosity with ease of manufacturing and less stringent sealing requirements .

2.3.5. Counter-Electrode Catalysts

For sufficiently fast reaction kinetics for the triiodide reduction reaction at the TCO coated cathode, a catalyst coating is needed such as platinum and carbon.

- **Platinum**

As a traditional and usually most efficient catalyst, platinum has been used almost exclusively in the literature. However, the performance of the catalyst layer depends on the method by which the Pt is deposited onto the TCO surface. Platinum catalyst

coating has been performed for example electrochemically [18], by sputtering [19], pyrolytically [20], or by spin coating [21]. Electrochemically and vapor deposited Pt has been however found unstable in the presence of the iodide electrolyte [22].

- **Carbon**

While showing excellent catalytic action, platinum has the disadvantage of being very expensive. Kay and Grätzel have developed a cell design, which is very interesting with this respect. The design utilizes a porous carbon counter-electrode as a catalyst layer. This carbon electrode is made from a mixture of carbon black, graphite powder and nanocrystalline TiO_2 particles. A high conductivity (sheet resistance of 5 Ω/cm^2 for a 50 μm thick layer) is obtained due to the carbon black particles connecting together separate graphite flakes, while the TiO_2 particles are used as a binder to the structure. It is claimed that thanks to the very high surface area of these electrodes, caused by the carbon black, these electrodes are as active for triiodide reduction as the conventional Pt electrodes.

2.3.6. Electrical Contacts

Similarly to the amorphous silicon and the other thin film solar cells deposited on TCO coated glass, the design of dye cells and modules is affected by the limited conductivity of the TCO layer. To keep the resistive losses in the TCO layer reasonably low, the longest distance from a photoactive point to a current collector should not exceed about 1 cm . For example silver paint and adhesive copper tape can be used to extend the contact area of the current collector to fulfill this geometric requirement. In test cells alligator clips can be easily attached to these conductor strips. Iodine based electrolyte is highly corrosive attacking most metals, such as silver aluminum, copper, nickel and even gold, and can thus be particularly problematic when it comes to designing an electrical contacting of single cells in an integrated DSSC module .

2.3.7. Sealing

Sealing the DSSCs has long been a difficult question because of the corrosive and volatile liquid iodide electrolyte used in the cells. Being directly related to the long term stability of the cells it seems to be one of the main technological challenges of the DSSC technology . A suitable sealing material should at least:

1. be leak-proof to the electrolyte components and impermeable to both ambient oxygen and water vapor,

2. be chemically inert towards the electrolyte and other cell components, and

3. adhere well to the glass substrate and TCO coating.

2.4. Basic Differences Between Dye Sensitized Solar Cell and p-n- Junction Solar Cell in Operation Principals

Since the invention of the nanostructured DSSC, a lot of theoretical and experimental work has been carried out to explain the surprisingly efficient operation of these solar cells. The need for unique theoretical considerations of the photovoltaic effect in the DSSCs arises from the fundamental differences in the operation between the DSSCs and the traditional semiconductor pn-junction solar cells:

1. In contrast to the semiconductor pn-junction solar cells, where light absorption and charge transport occurs in the same material, the DSSC separate these functions: photons are absorbed by the dye molecules and transport of charges is carried out in the TiO_2 or ZnO electrode and electrolyte;

2. While the charge separation in the semiconductor pn-junction cells is induced by the electric field across the junction, no such long-range electric fields exist in the DSSC. The charge separation occurs via other kinds of kinetic and energetic reasons at the dye-covered semiconductor-electrolyte interface;

3. In the semiconductor pn-junction cells, the generated opposite charges travel in the same material, while in the DSSC, electrons travel in the nonporous

TiO_2 or ZnO and holes in the electrolyte. This means that the requirement for a pure and defect free semiconductor material in the case of semiconductor pn junction solar cell is relaxed for the DSSC, where the recombination can occur only at the semiconductor electrolyte interface.

2.5.Efficiency of the Dye Sensitized Solar Cells

There are many factors that affect the efficiency of the DSSC. An efficient DSSC requires:

(1) A dye with efficient electron injection into the semiconductor,

(2) An electrolyte able to penetrate into the porous semiconductor to efficiently reduce oxidized dye molecules,

(3) A semiconductor with a large surface area for maximum dye adsorption,

(4) A long diffusion length (fast electron transport) for the injected electrons to be transported.

For a dye to have an efficient electron injection into the semiconductor it has to contain attachment groups, such as carboxylate or phosphate, and the energy of its excited state should match well to the lower bound of the conduction band of the metal oxide. The most important thing to note about the dye is that these dyes are acidic due to the carboxyl groups. The acidic protons can etch ZnO and, therefore, lower the efficiency. A large surface area is ideal for DSSC because it maximizes the amount of electrons injected into the semiconductor and, therefore, maximizes photocurrent. For an efficient DSSC the semiconductor must also have a large diffusion length, the distance the electron travels before recombining with the photo oxidized dye or electrolyte.

2.6. Aim of This Work

In this thesis, many dye sensitized solar cells have been fabricated, characterized and studied using ZnO as a semiconductor layer. Films of nanocrystalline ZnO were spread on transparent conducting FTO coated glass using doctor blade method. The ZnO layer were dyed using both natural and chemical dyes. The absorption spectra of all dyes will performed. The I-V characteristic curves of the fabricated cells were measured and studied. The output power was also calculated and plotted. Short current circuit, open

circuit voltage, maximum absorption wavelength, maximum power, fill factor, and the power conversion efficiency were calculated. A comparison among all fabricated cells held.

CHAPTER THREE

NATURAL DYES AS PHOTOSENSITIZERS FOR DYE SENSITIZED SOLAR CELLS

Dyeing materials with plants is an old art practiced since early ages. There are many plant materials that can be used for dyeing: roots, bark, leaves, berries, seeds, twigs, branches and tubers. The advantages of natural dyes include their readily availability, low cost, and their simple extraction into cheap organic solvents which can be applied without further purification [23,24].

In this chapter, DSSCs were prepared using natural dyes extracted from seeds, leaves, flowers, and roots of plants. The ZnO layer was dyed using eight natural dyes. The absorption spectra of all dyes were performed. The I-V characteristic curves of the fabricated cells were measured and studied. The output power was calculated and plotted. Short circuit current, open circuit voltage, maximum absorption wavelength, maximum power, fill factor, and power conversion efficiency were presented.

3.1. Absorption Spectra Analysis of Natural Dyes in Dye Sensitized Solar Cells

The size of energy gap of semiconductors determines the absorption frequency of light in solar cells. A significant purpose for using dyes in the DSSC is to shift the absorption spectra to the visible light region. The absorption spectrum of the DSSC is determined by the combination of the photoelectrode's nanoparticles. TiO_2, ZnO and the dyes, where the dyes can expand the absorption spectrum of DSSC.

3.2. Material System

The conductive glass plates (FTO glass, fluorine-doped SnO_2, sheet resistance 15 Ω/cm^2), fluorine-doped tin oxide (SnO_2:F) is most frequently used as transparent conducting oxides (TCOs) in thin film photovoltaic cells. The standard preparation procedure of the nanostructured ZnO electrode includes sintering of the deposited ZnO film at 450-500 °C. FTO is the only transparent conducting oxide stable at these temperatures [25]. Films of nanocrystalline ZnO was spread on transparent

conducting FTO coated glass using doctor blade method. Natural pigments such as Safflower (Cathumus tincrorius), Senna (Cassia angustifolia), Calumus draca (Dracaena oinnabari), Carya illinoensis, Rheum, Roselle (Hibiscas sabdarriffa) and Runica granatum were used as sensitizers. Adsorption of the dye to the mesoporous film was achieved by simple immersion of the ZnO film in the dye solution. The counter electrode is fabricated from FTO-coated glass, with the addition of a platinum catalyst to catalyze the reduction of the redox electrolyte at this electrode. Platinum electrode was used as the counter electrode as it provides a high work function of 5.2 eV. Furthermore, the platinum can improve the short circuit current through a catalytic reduction effect of triiodide. Electrical contact between working and counter electrodes is achieved by the redox electrolyte.

3.3. Experimental

3.3.1 Natural Dyes Extraction

Natural dyes used in this study were extracted from the following plants Safflower (Cathumus tincrorius), Senna (Cassia angustifolia), Calumus draca (Dracaena oinnabari), Carya illinoensis, Rheum, Roselle (Hibiscas sabdarriffa), Rosa damascena, and Runica granatum. The raw natural material were first washed by distilled water then were dried at 40^0C. After crushing into fine powder with a mortar, these materials were immersed ethyl alcohol and poly ethylene glycol at room temperature and in the dark for one day. After filtration of the solutions, natural dyes were obtained [26,27].

3.3.2. Preparation of Dye Sensitized Solar Cells

FTO conductive glass sheet were cut into pieces of dimensions 0.8cm×1.6cm. The samples were cleaned in a detergent solution using an ultrasonic bath for 15 min, rinsed with water and ethanol, and then dried. The ZnO paste was prepared by adding 0.062 g of ZnO nano-powder and 0.072 g of polyethylene glycol (G) then grinding the mixture for half an hour until a homogeneous paste was obtained. Thin films of the prepared ZnO past were spread on the transparent conducting FTO coated glass using doctor blade method, and were placed in an oven at 70 ^{0}C for 20 min. Finally

the samples were sintered at 500 ^{0}C for 40 min. Samples were cooled to about 70 ^{0}C before being placed in dyes for one day under dark. The dyed ZnO electrode and platinum counter electrode were assembled to form a solar cell by sandwiching a redox (I^-/I^3) electrolyte solution. The electrolyte solution is composed of 2ml acetonitrile (ACN), 8ml propylene carbonate (p-carbonate), 0.668gm (LiI), and 0.0634gm (I_2).

3.3.3 Characterization and Measurement

a. Absorption Spectra Analysis

The wavelength range of absorption spectra analysis extends from 350 − 800 nm. The natural dyes extracted from the various plants have complicated mixed constituents. UV-visible absorption measurements of the extracted pigments in ethyl alcohol / polyethylene glycol solution were carried out with continuous wavelength one beam spectrophotometer.

b. I-V Measurements:

In the IV measurements a voltage, usually in the range between –1 to 1 Volts, is applied to the solar cell and the resulting current is measured. To apply the voltage and measure the resulting current, NI USB6251 data acquisition card in combination of a labview program were used. IV –curves were measured in different solar irradiations using high pressure mercury arc lamp.

3.4 Results and Discussions

3.4.1 Absorption of Natural Dyes

Figure 3.1 through 3.8 show the UV–VIS absorption spectra of Safflower (Cathumus tincrorius), Senna (Cassia angustifolia), Calumus draca (Dracaena oinnabari), Rosa damascena, Rheum, Roselle (Hibiscas sabdarriffa) and Runica granatum in ethyl alcohol (E) and polyethylene glycol (G) as solvents. From Fig. 3.1, it can be seen that there is absorption peak at about 428.8 nm for the extracts of Safflower (Cathumus tincrorius) using ethyl alcohol a solvent and a peak at about 414.5nm when using polyethylene glycol as a solvent. The absorption spectrum of Senna (cassia

Angustifolia) is shown in Fig. 3.2. In the case of ethyl alcohol, the absorption spectrum curve shows a peak at 410.8nm and 664.7nm. A small peak appears at 657.1nm using polyethylene glycol as a solvent. As can been seen from Fig. 3.3, there is an absorption peak at 422.2nm for the extract of Rheum when using ethyl alcohol as a solvent and there is a higher absorption peak at 416.5nm when using polyethylene glycol. Figure 3.4 shows that the extract of Calumus draca (Dracaena oinnabari) exhibit absorption peak at 396nm and 384nm for ethyl alcohol and polyethylene glycol solvents respectively. In Fig. 3.5, Rosa damascena extract has a very small peak at 390nm. The extract of Roselle (Hibiscas sabdarriffa) dissolved in ethyl alcohol shows a peak at 512.6nm whereas no apparent peak is found when using polyethylene glycol as a solvent. Figure 3.7 shows the absorption spectrum of Carya illinoensis. As can be seen from the figure, the Carya illinoensis extract shows a peak at 563.4nm for ethyl alcohol and at 576.6nm for polyethylene glycol. Finally, as Fig. 3.8 shows, Runica granatum extract has an absorption peaks in the visible light region at 429nm (ethyl alcohol) and 400nm (polyethylene glycol).

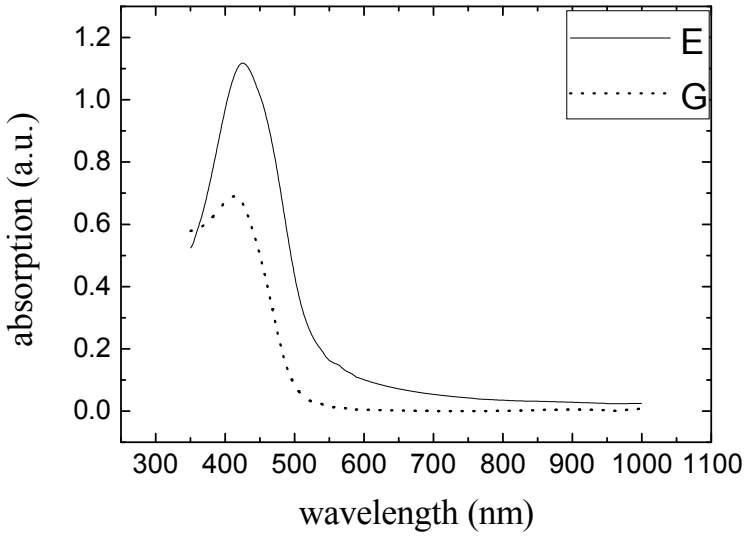

Figure 3.1. The absorption spectrum of the extract of Safflower(Cathumus tincrorius) using ethyl alcohol (E) and polyethylene glycol (G).

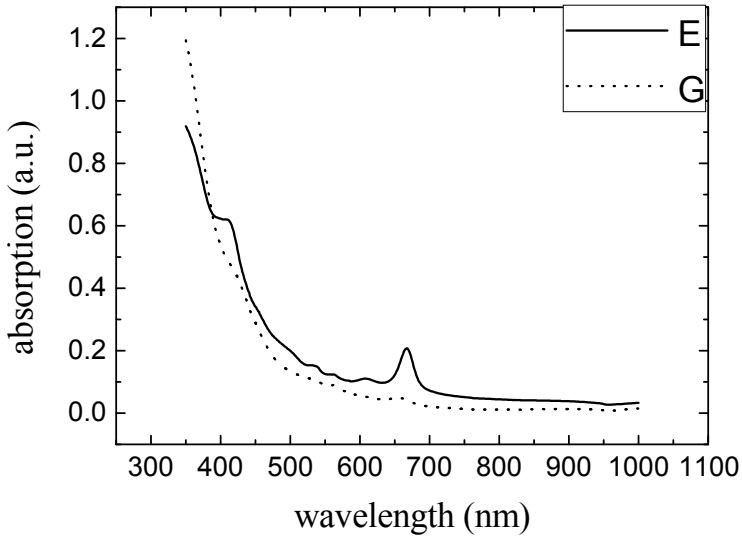

Figure 3.2. The absorption spectrum of the extract of Senna (Cassia angustifolia) using ethyl alcohol (E) and polyethylene glycol (G).

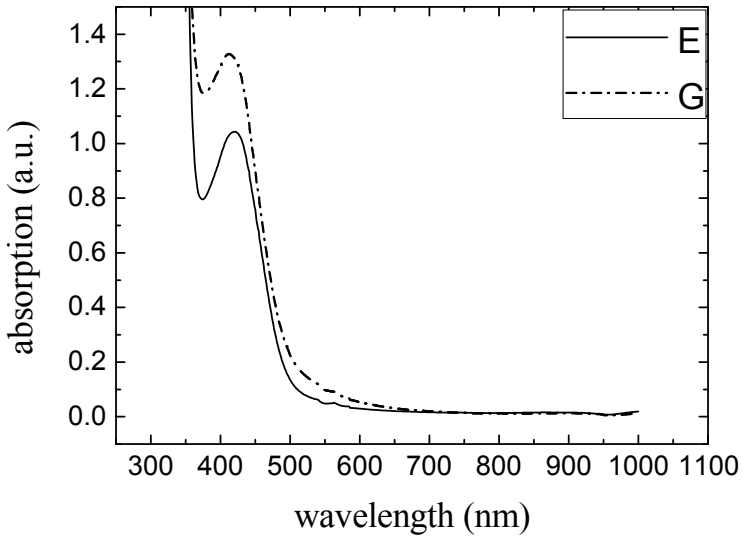

Figure 3.3. The absorption spectrum of the extract of Rheum using ethyl alcohol (E) and polyethylene glycol (G) .

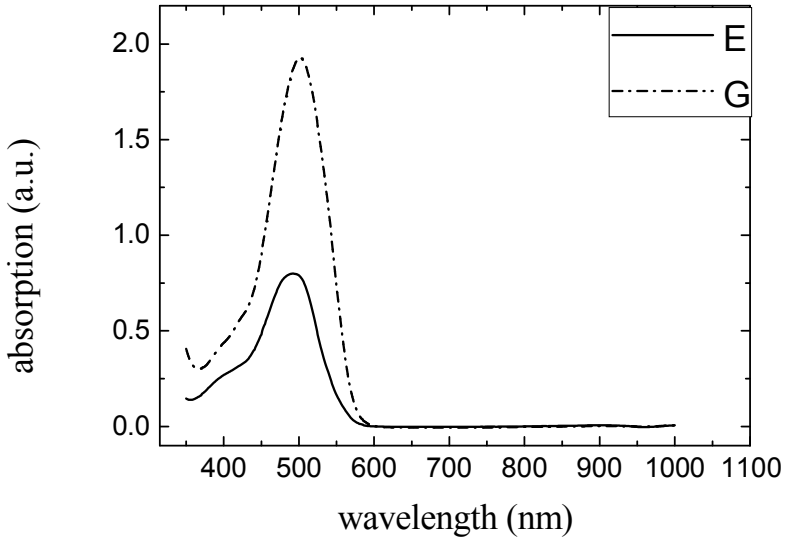

Figure 3.4. The absorption spectrum of the extract of Calumus draca (Dracaena oinnabari) using ethyl alcohol (E) and polyethylene glycol (G).

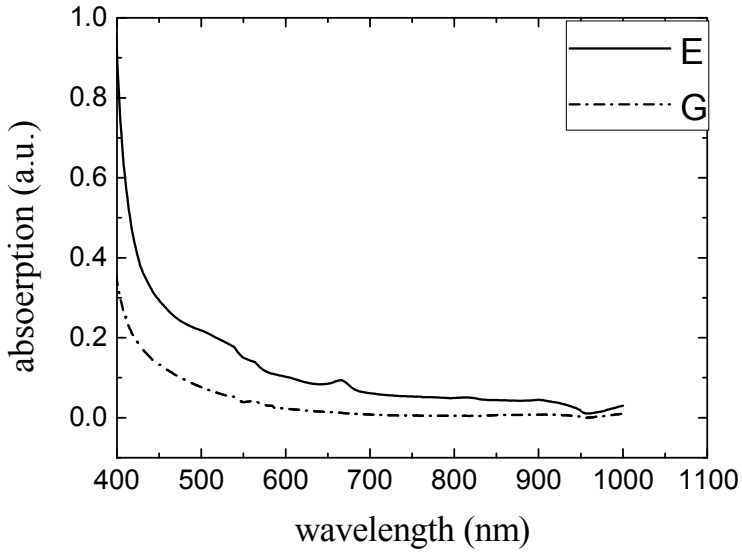

Figure 3.5. The absorption spectrum of the extract of Rosa damascena using ethyl alcohol (E) and polyethylene glycol (G).

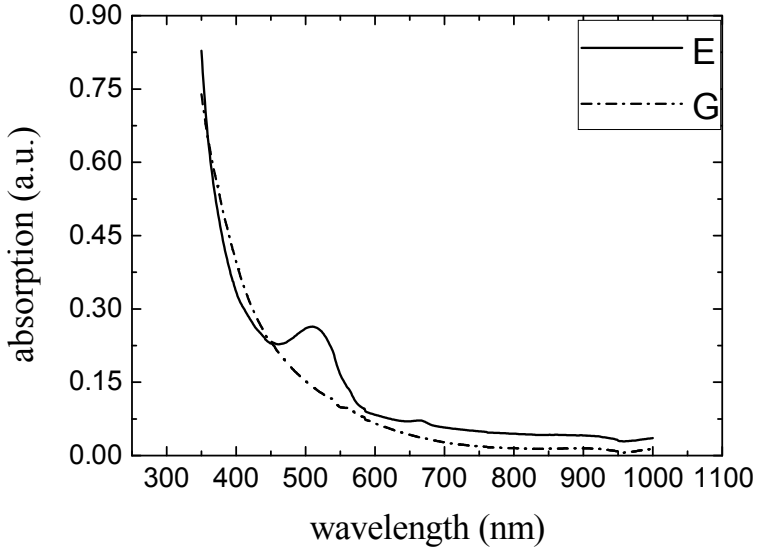

Figure 3.6. The absorption spectrum of the extract of Roselle (Hibiscus sabdarriffa) using ethyl alcohol (E) and polyethylene glycol (G).

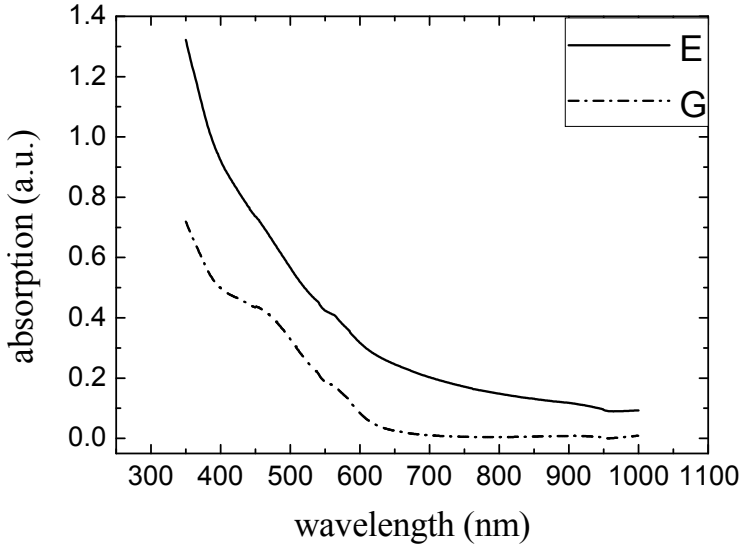

Figure 3.7. The absorption spectrum of the extract of Carya illinoensis using ethyl alcohol (E) and polyethylene glycol (G).

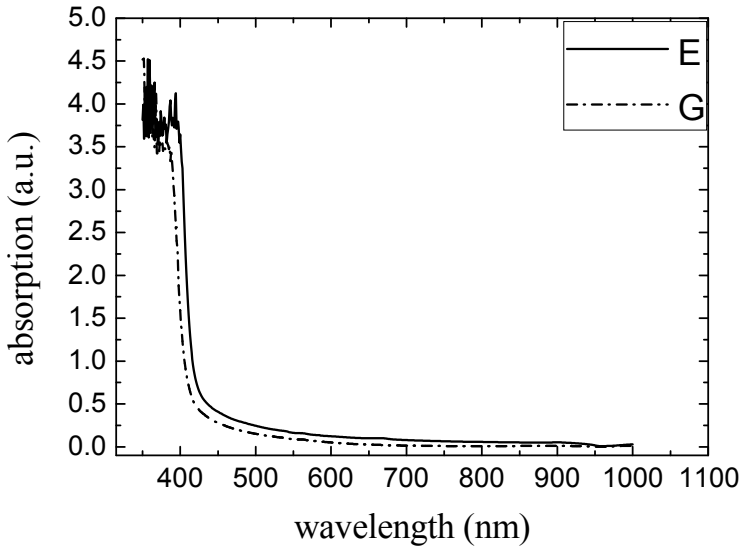

Figure 3.8. The absorption spectrum of the extracts of Runica granatum using ethyl alcohol (E) and polyethylene glycol (G).

3.4.2. Photovoltaic Parameters of Dye Sensitized Solar Cells with Natural Dyes

Two groups of DSSCs have been fabricated with the same dyes. The main difference between the two groups is the counter electrode. In the first group, the counter electrode is fabricated from FTO coated glass with a thin layer of platinum as a catalyst whereas the second group uses a carbon block. In the following the results obtained for the two groups will be presented.

a. Platinum Counter Electrode

In the following, the results obtained for the DSSCs fabricated using eight natural dyes dissolved in ethyl alcohol and polyethylene glycol when platinum is used as a counter electrode are presented. For each dye, the measured current density (J) versus the voltage (V) is presented at three different light intensities. Moreover, each J-V figure shows the result obtained for the same dye when dissolved in two different solvents (ethyl alcohol and polyethylene glycol). For each J-V curve, the power is calculated and plotted versus the applied voltage. In analogy to the J –V curve, each P –V figure shows the calculated power versus the voltage at three different light intensities for the two solvents. Figure 3.9 shows the measured current density versus the voltage of the cell sensitized by Safflowers (Cathumus tincrorius) at light

intensities 80, 100, and 120 klux using platinum electrode for ethyl alcohol and polyethylene glycol as solvents. As the figure shows there is a considerable difference in the DSSC response between the two dye solvents. Using ethyl alcohol as a solvent yields considerable higher values for the open circuit voltage and the short circuit current density. The power is the calculated for each experimented point by simply multiplying the individual current and voltage of the point. The calculated power as a function of the voltage is plotted in Fig. 3.10 for the dye extracted from Safflower (Cathumus tincrorius) for three different light intensities for the two solvents. Figures 3.11, 3.13, 3.15, 3.17, 3.19, 3.21, and 3.23 show respectively the J-V characteristic curves obtained for the fabricated DSSC using Senna, Rheum, Calumus draca, Rosa damascena, Carya illinoensis, Roselle, and Runica granatum. Each curve shows the results obtained under three illuminations. Moreover, each figure illustrates the results obtained for the two solvents except figure 3.21 which corresponds to the Roselle dye since no response is observed to the cell when using polyethylene glycol as a solvent. In a similar manners, Figs. 3.12, 3.14, 3.16, 3.18, 3.20, 3.22, and 3.24 show respectively the calculated power versus the applied voltage of the cells fabricated using Senna, Rheum, Calumus draca, Rosa damascena, Carya illinoensis, Roselle, and Runica granatum.

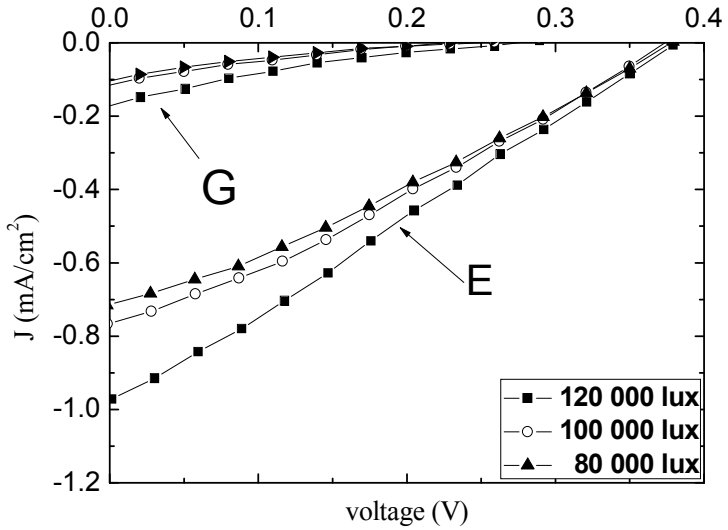

Figure 3.9. Current density–voltage curves for the DSSCs sensitized by Safflower (Cathumus tincrorius) at different light intensities using Pt electrode for two different solvents: E for ethyl alcohol and G for polyethylene glycol.

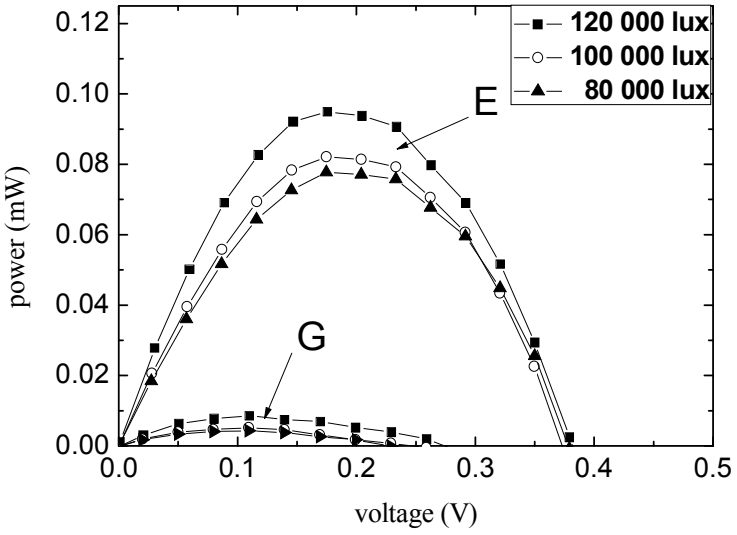

Figure 3.10. Power - voltage characteristics of the DSSCs sensitized by Safflower (Cathumus tincrorius) at different light intensities using Pt electrode for two different solvents: E for ethyl alcohol and G for polyethylene glycol.

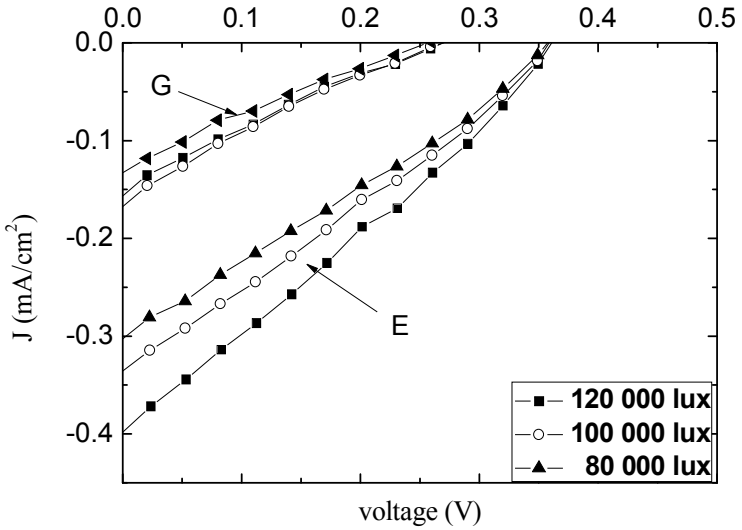

Figure 3.11. Current density–voltage curves for the DSSCs sensitized by Senna at different light intensities using Pt electrode for two different solvents: E for ethyl alcohol and G for polyethylene glycol.

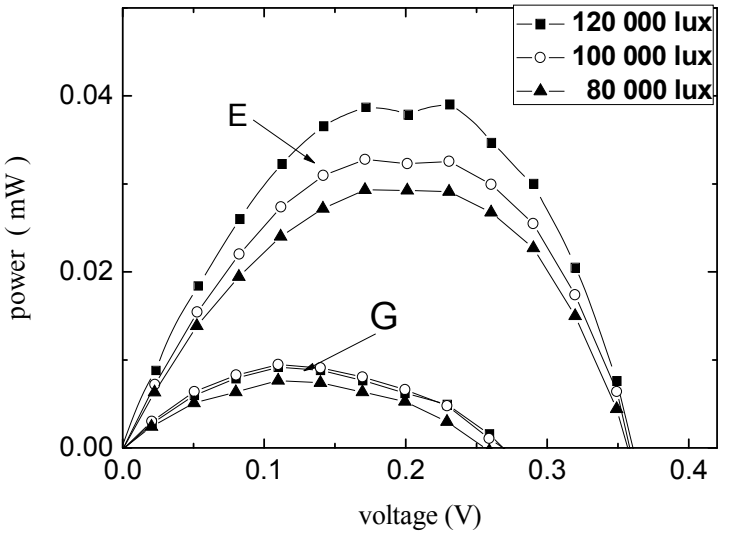

Figure 3.12. Power - voltage characteristics of the DSSCs sensitized by Senna at different light intensities using Pt electrode for two different solvents: E for ethyl alcohol and G for polyethylene glycol.

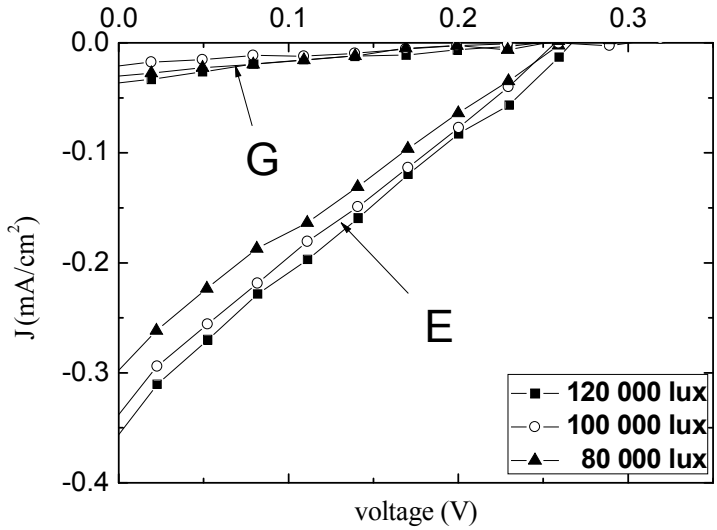

Figure 3.13. Current density–voltage curves for the DSSCs sensitized by Rheum at different light intensities using Pt electrode for two different solvents: E for ethyl alcohol and G for polyethylene glycol.

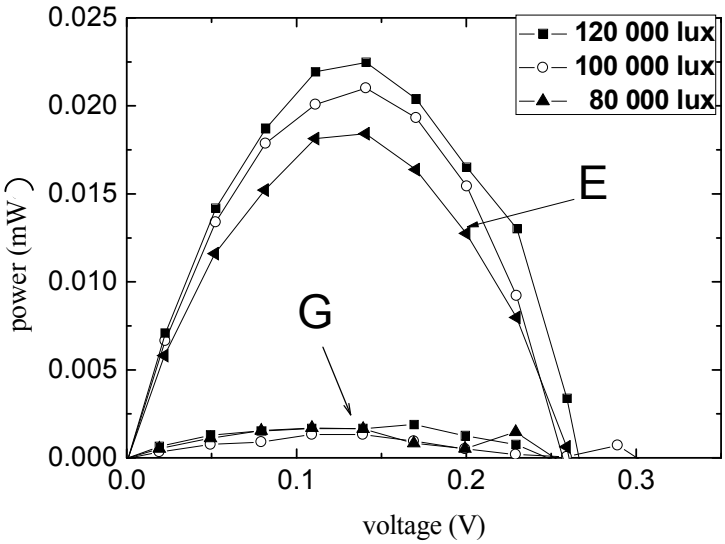

Figure 3.14. Power - voltage characteristics of the DSSCs sensitized by Rheum at different light intensities using Pt electrode for two different solvents: E for ethyl alcohol and G for polyethylene glycol.

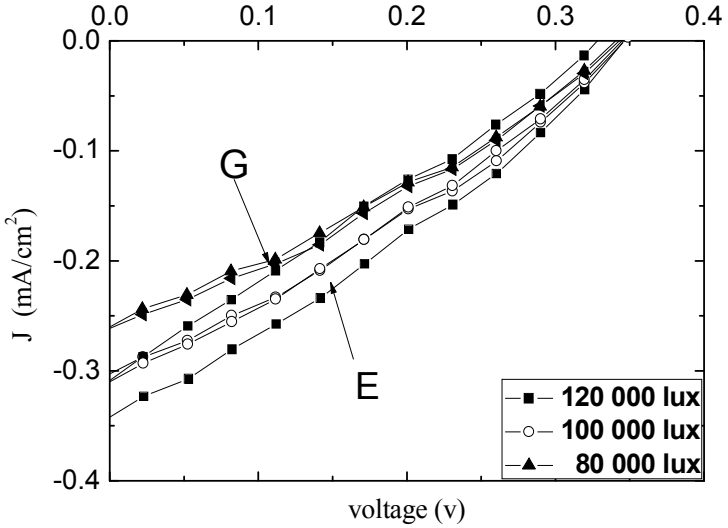

Figure 3.15. Current density–voltage curves for the DSSCs sensitized by Calumus draca (Dracaena oinnabari) at different light intensities using Pt electrode for two different solvents: E for ethyl alcohol and G for polyethylene glycol.

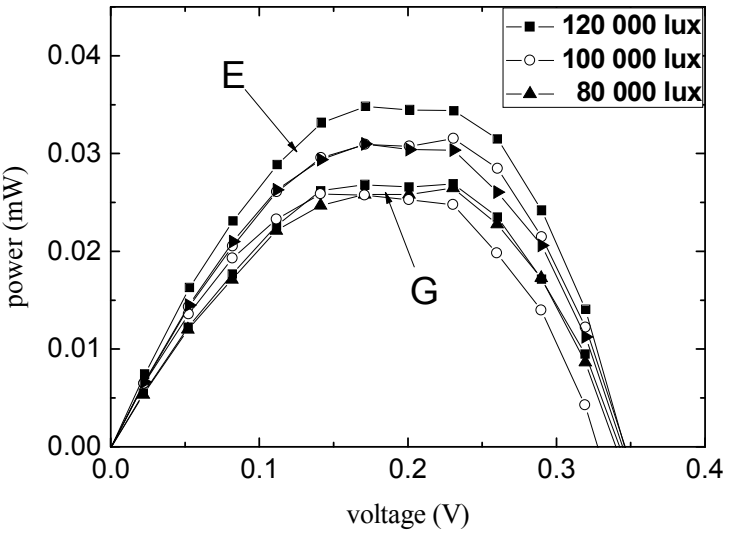

Figure 3.16. Power - voltage characteristics of the DSSCs sensitized by Calumus draca (Dracaena oinnabari) at different light intensities using Pt electrode for two different solvents: E for ethyl alcohol and G for polyethylene glycol.

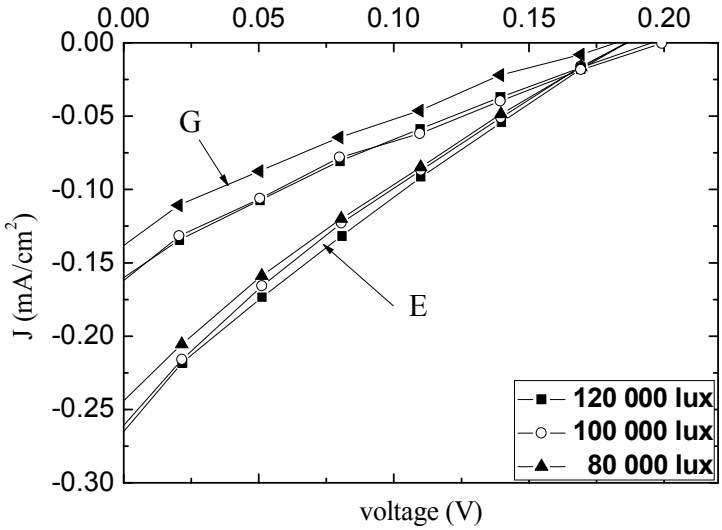

Figure 3.17. Current density–voltage curves for the DSSCs sensitized by Rosa damascena at different light intensities using Pt electrode for two different solvents: E for ethyl alcohol and G for polyethylene glycol.

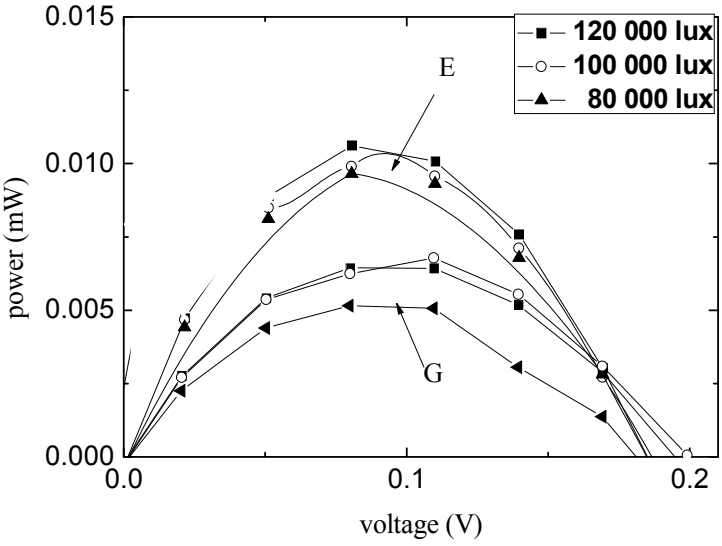

Figure 3.18. Power - voltage characteristics of the DSSCs sensitized by Rosa damascena at different light intensities using Pt electrode for two different solvents: E for ethyl alcohol and G for polyethylene glycol.

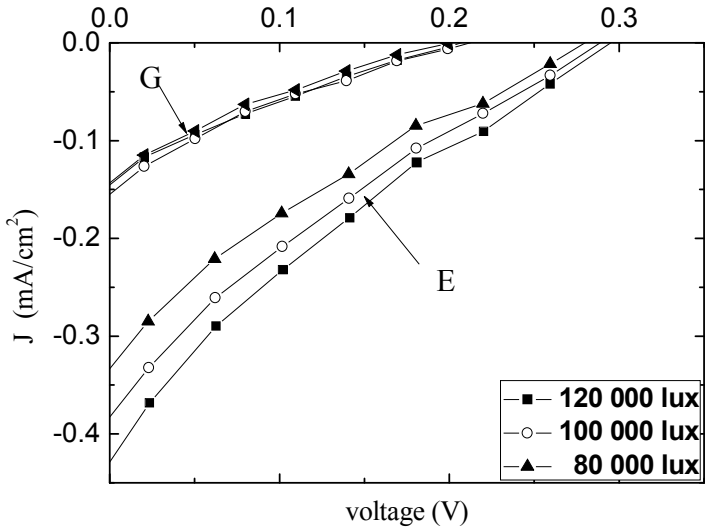

Figure 3.19. Current density–voltage curves for the DSSCs sensitized by Carya illinoensis at different light intensities using Pt electrode for two different solvents: E for ethyl alcohol and G for polyethylene glycol.

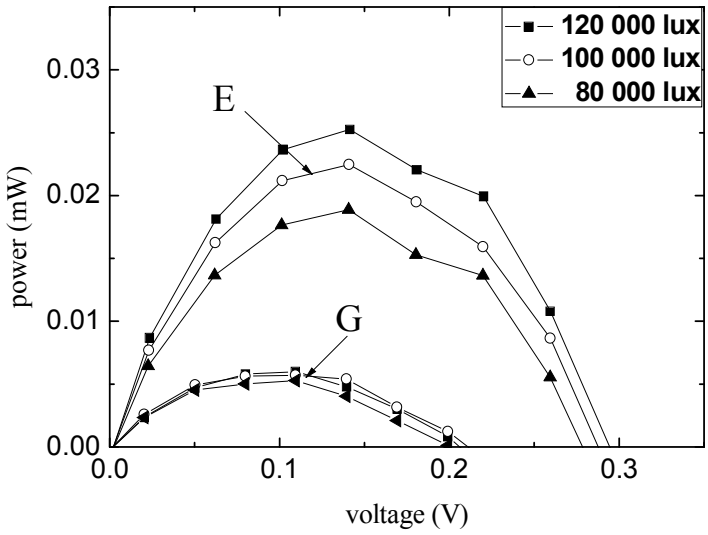

Figure 3.20. Power - voltage characteristics of the DSSCs sensitized by Carya illinoensis at different light intensities using Pt electrode for two different solvents: E for ethyl alcohol and G for polyethylene glycol.

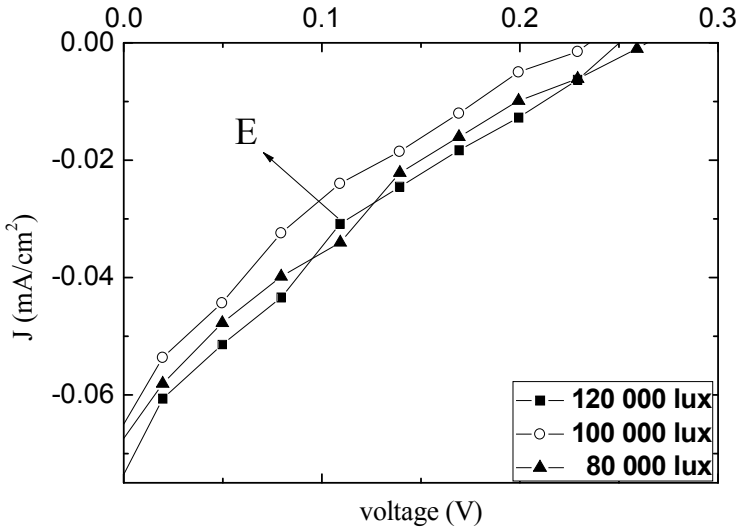

Figure 3.21.Current density–voltage curves for the DSSCs sensitized by Roselle (Hibiscas sabdarriffa) at different light intensities using Pt electrode for two different solvents: E for ethyl alcohol and G for polyethylene glycol.

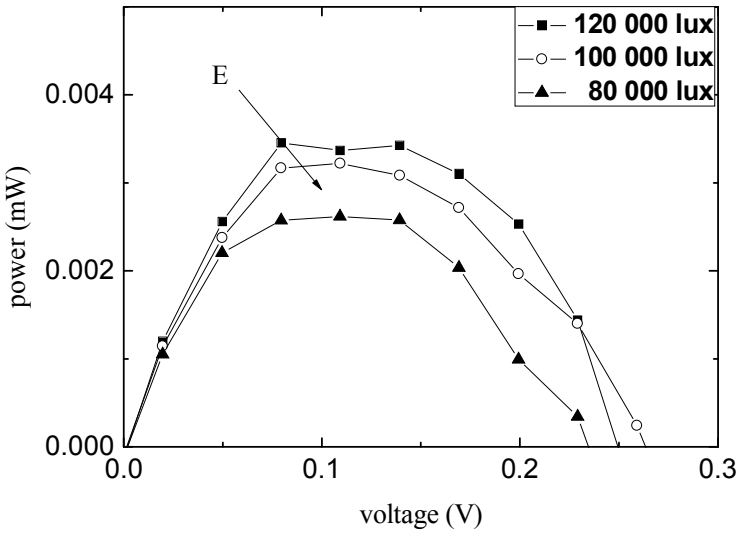

Figure 3.22. Power - voltage characteristics of the DSSCs sensitized by Roselle (Hibiscas sabdarriffa) at different light intensities using Pt electrode for two different solvents: E for ethyl alcohol and G for polyethylene glycol.

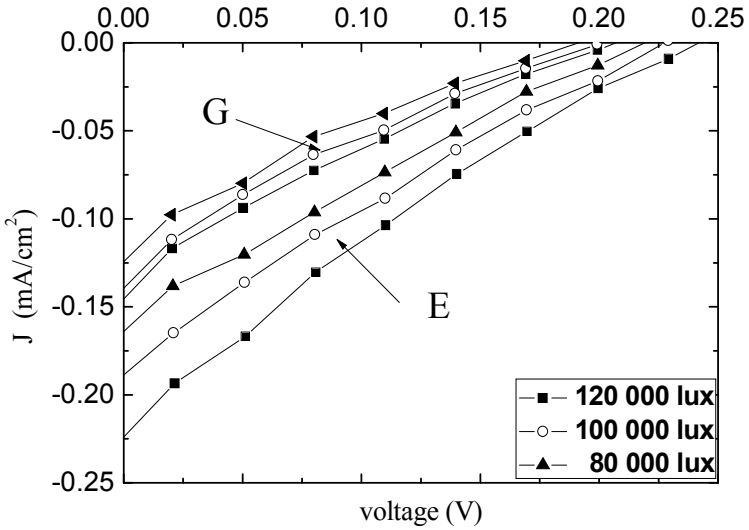

Figure 3.23. Current density–voltage curves for the DSSCs sensitized by Runica granatum at different light intensities using Pt electrode for two different solvents: E for ethyl alcohol and G for polyethylene glycol.

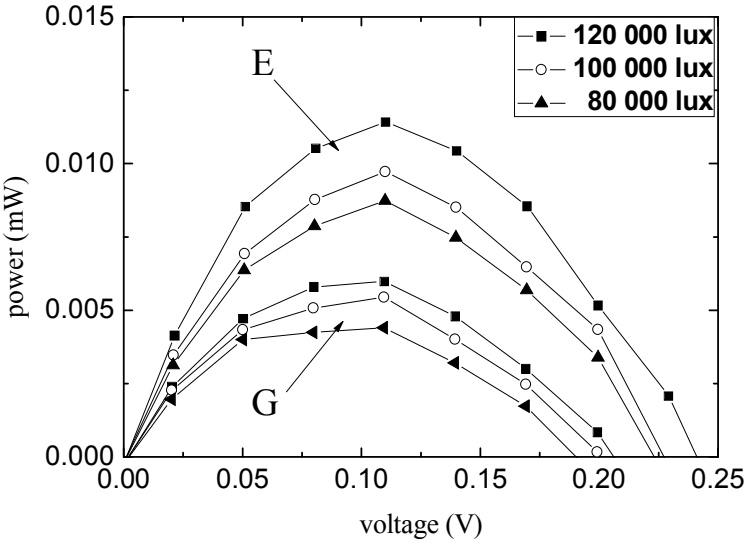

Figure 3.24. Power - voltage characteristics of the DSSCs sensitized by Runica granatum at different light intensities using Pt electrode for two different solvents: E for ethyl alcohol and G for polyethylene glycol.

All measurements where conducted at light intensities of 80, 100, and 120 klux. Values of the short circuit current density (J_{sc}) and open circuit voltage (V_{oc}) were obtained from the J-V curves by estimating the J- axis and V- axis intercepts, respectively. The maximum power point is determined from the P-V curves from which J_m and V_m can be calculated. The fill factor and cell efficiency are the calculated using Eq. (1.4) and Eq. (1.5), respectively. All the photovoltaic parameters of the fabricated DSSCs are tabulated in table 3.1 for the ethyl alcohol solvent and in table 3.2 for the polyethylene glycol. Inspection of these values reveal that there is a clear preference of the performance of the cells fabricated using ethyl alcohol solvent. Moreover, the comparison among all dyes shows that the best dye is the Safflower which corresponded to the highest conversion efficiency. The short circuit current density and the open circuit voltage of Safflower cell where found to be 1mA/cm^2 and 0.371V for the light intensity of 120 klux. In general, the values obtained for η is low compared to the values previously obtained in the literature. The low values of η in our cells may be attributed to the fast charge recombination rate, loss resulting directly for the increased electron mobility [28], or the mismatch between the energy of the excited state of the adsorbed dye and the conduction band edge of ZnO. Moreover, the ground state of dye molecule could be considerably shifted with respect to the redox potential of I^- / I^{-3}.

Table 3.1. Photovoltaic parameters of the DSSCs sensitized by natural dyes extracted with ethyl alcohol as a solvent and Pt as a back electrode.

Dye	Intensity of light	J_{sc} (mA/cm^2)	V_{oc} (V)	J_m (mA/cm^2)	V_m (V)	P_{max} (mW)	FF	η %
Safflower (Cathumus tincrorius)	120,000 Lux	1.0	0.379	0.539	0.17	0.092	0.24	0.094
	100,000 Lux	0.76	0.379	0.469	0.17	0.082	0.28	0.097
	80,000 Lux	0.70	0.379	0.445	0.17	0.077	0.29	0.10
Senna (Cassia angustifolia)	120,000 Lux	0.37	0.349	0.169	0.23	0.039	0.30	0.039
	100,000 Lux	0.31	0.349	0.191	0.17	0.033	0.29	0.039
	80,000 Lux	0.28	0.349	0.145	0.20	0.029	0.29	0.043
Rheum	120,000 Lux	0.310	0.259	0.159	0.14	0.022	0.27	0.022
	100,000 Lux	0.294	0.259	0.149	0.14	0.021	0.27	0.025
	80,000 Lux	0.261	0.259	0.130	0.14	0.018	0.26	0.027
Calumus draca (Dracaena oinnabari)	120,000 Lux	0.31	0.348	0.185	0.17	0.030	0.28	0.030
	100,000 Lux	0.28	0.319	0.156	0.17	0.025	0.28	0.030
	80,000 Lux	0.24	0.319	0.156	0.17	0.026	0.28	0.038

Dye	Intensity of light	J_{sc} (mA/cm^2)	V_{oc} (V)	J_m (mA/cm^2)	V_m (V)	P_{max} (mW)	FF	η %
Rosa damascena	120,000 Lux	0.29	0.169	0.131	0.08	0.016	0.20	0.009
	100,000 Lux	0.28	0.169	0.131	0.08	0.0098	0.22	0.012
	80,000 Lux	0.25	0.169	0.131	0.08	0.009	0.24	0.015
Carya illinoensis	120,000 Lux	0.46	0.299	0.178	0.14	0.025	0.18	0.025
	100,000 Lux	0.41	0.259	0.159	0.14	0.022	0.21	0.026
	80,000 Lux	0.36	0.259	0.134	0.14	0.018	0.20	0.028
Roselle (Hibiscas	120,000 Lux	0.08	0.259	0.035	0.13	0.034	0.23	0.005
	100,000 Lux	0.07	0.259	0.034	0.10	0.029	0.20	0.004
	80,000 Lux	0.07	0.229	0.0185	0.13	0.003	0.15	0.003
Runica granatum	120,000 Lux	0.23	0.229	0.103	0.11	0.011	0.21	0.011
	100,000 Lux	0.19	0.229	0.082	0.11	0.0097	0.20	0.010
	80,000 Lux	0.17	0.229	0.073	0.10	0.0080	0.20	0.011

The Photovoltaic parameters of the DSSCs sensitized with natural dyes and using Pt as a back electrode and using polyethylene glycol(G) as solvent are listed in Table 3.2

Table 3.2. Photovoltaic parameters of the DSSCs sensitized by natural dyes extracted with polyethylene glycol as a solvent and Pt as a back electrode.

Dye	Intensity of light	J_{sc} (mA/cm^2)	V_{oc} (V)	J_m (mA/cm^2)	V_m (V)	P_{max} (mW)	FF	η %
Safflower (cathumus tincrorius)	120,000 Lux	0.18	0.259	0.07	0.109	0.0085	0.16	0.076
	100,000 Lux	0.12	0.229	0.04	0.109	0.0051	0.15	0.052
	80,000 Lux	0.11	0.229	0.039	0.109	0.0042	0.16	0.063
Senna (cassia Angustifolia)	120,000 Lux	0.16	0.264	0.085	0.109	0.0094	0.21	0.009
	100,000 Lux	0.15	0.260	0.083	0.109	0.0091	0.23	0.009
	80,000 Lux	0.13	0.259	0.069	0.109	0.0076	0.22	0.007
Rheum	120,000 Lux	0.038	0.259	0.015	0.169	0.0018	0.25	0.0025
	100,000 Lux	0.031	0.258	0.015	0.109	0.0017	0.20	0.0019
	80,000 Lux	0.022	0.259	0.012	0.109	0.0013	0.22	0.0019
Calumus draca (Dracaena Oinnabari)	120,000 Lux	0.32	0.348	0.202	0.171	0.034	0.31	0.034
	100,000 Lux	0.28	0.348	0.152	0.201	0.030	0.31	0.036
	80,000 Lux	0.24	0.348	0.151	0.170	0.025	0.30	0.038

Dye	Intensity of light	J_{sc} (mA/cm^2)	V_{oc} (V)	J_m (mA/cm^2)	V_m (V)	P_{max} (mW)	FF	η %
Rosa damascena	120,000 Lux	0.17	0.199	0.07	0.109	0.0068	0.22	0.076
	100,000 Lux	0.17	0.199	0.06	0.109	0.0067	0.19	0.078
	80,000 Lux	0.15	0.169	0.06	0.079	0.0051	0.19	0.073
Carya illinoensis	120,000 Lux	0.15	0.199	0.052	0.109	0.0059	0.18	0.0054
	100,000 Lux	0.12	0.199	0.052	0.109	0.0057	0.23	0.0068
	80,000 Lux	0.11	0.199	0.048	0.109	0.0052	0.22	0.0078
Runica granatum	120,000 Lux	0. 12	0.199	0.054	0.109	0.0059	0.25	0.0064
	100,000 Lux	0. 11	0.199	0.049	0.109	0.0054	0.24	0.0064
	80,000 Lux	0.09	0.1999	0.040	0.109	0.0044	0.24	0.0065

b. Carbon Counter Electrode

The results obtained for the DSSCs fabricated using the eight natural dyes dissolved in the two solvents when carbon is used as aback electrode are presented. The measured current density versus the voltage across the cell is illustrated in Figs. 3.25, 3.27, 3.29, 3.31, 3.33, 3.35, 3.37, and 3.39 for the DSSCs sensitized by Safflower (Cathumus tincrorius), Senna (Cassia angustifolia), Rheum, Calumus draca (Dracaena oinnabari), Rosa damascena, Carya illinoensis, Roselle (Hibiscas sabdarriffa), and Runica granatum, respectively. Each figure of these figures shows the J-V curve obtained under three different light intensities for the two solvents except Fig. 3.37 in which the cell exhibited no response when using polyethylene glycol. In a similar manner to the procedure followed for the Pt electrode, the power

is calculated and plotted versus the voltage for all dyes in Figs. 3.26, 3.28, 3.30, 3.32, 3.34, 3.36, 3.38, and 3.40.

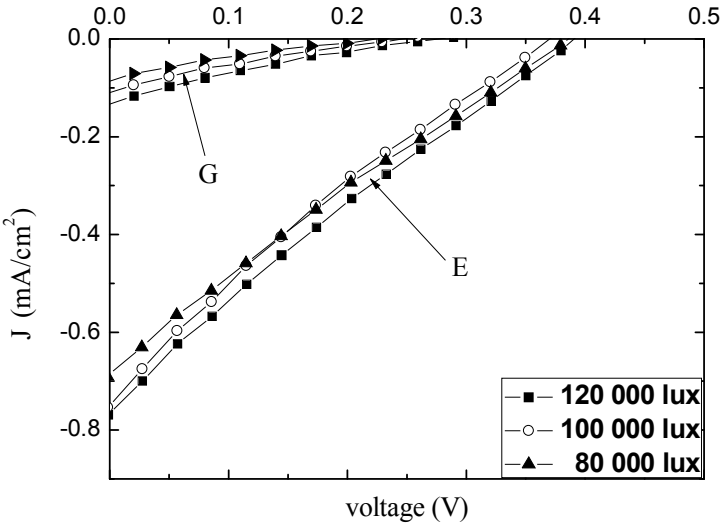

Figure 3.25. Current density–voltage curves for the DSSCs sensitized by Safflower (Cathumus tincrorius) at different light intensities using C electrode for two different solvents: E for ethyl alcohol and G for polyethylene glycol.

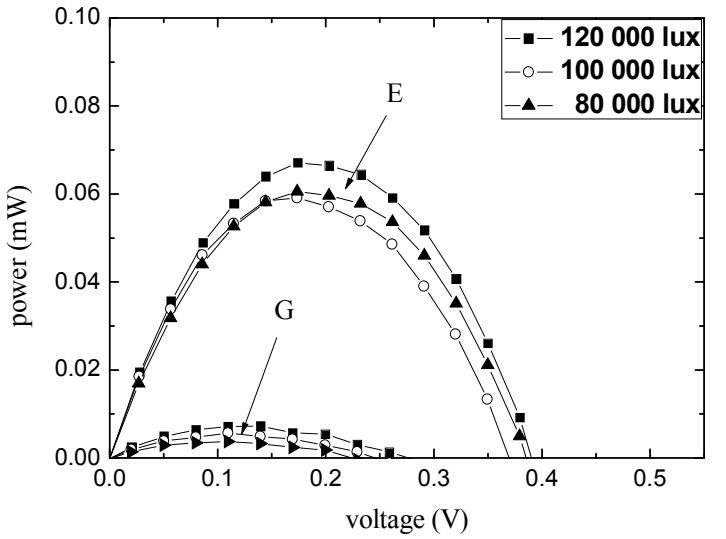

Figure 3.26. Power - voltage characteristics of the DSSCs sensitized by Safflower (Cathumus tincrorius) at different light intensities using C electrode for two different solvents: E for ethyl alcohol and G for polyethylene glycol.

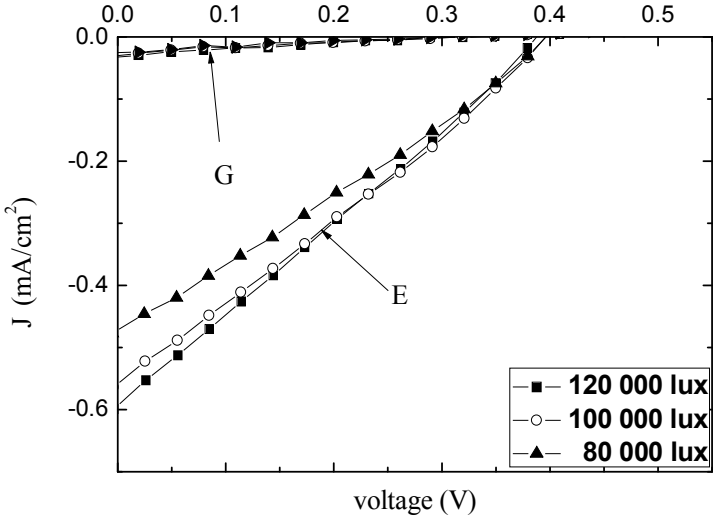

Figure 3.27. Current density–voltage curves for the DSSCs sensitized by Senna at different light intensities using C electrode for two different solvents: E for ethyl alcohol and G for polyethylene glycol.

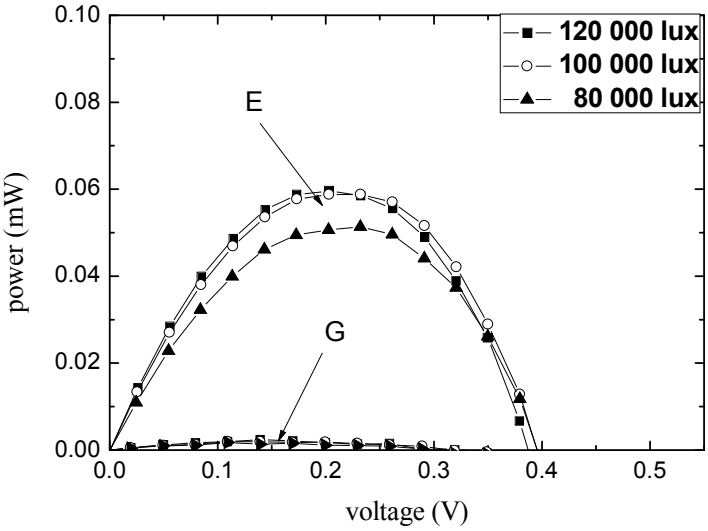

Figure 3.28. Power - voltage characteristics of the DSSCs sensitized by Senna at different light intensities using C electrode for two different solvents: E for ethyl alcohol and G for polyethylene glycol.

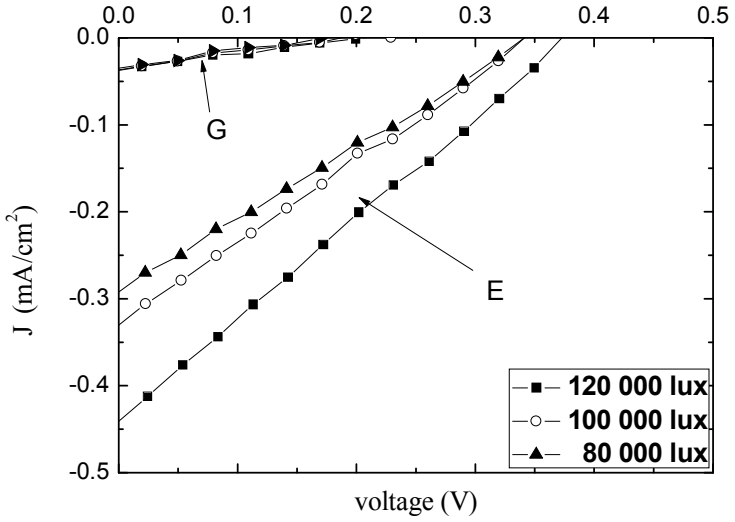

Figure 3.29. Current density–voltage curves for the DSSCs sensitized by Rheum at different light intensities using C electrode for two different solvents: E for ethyl alcohol and G for polyethylene glycol.

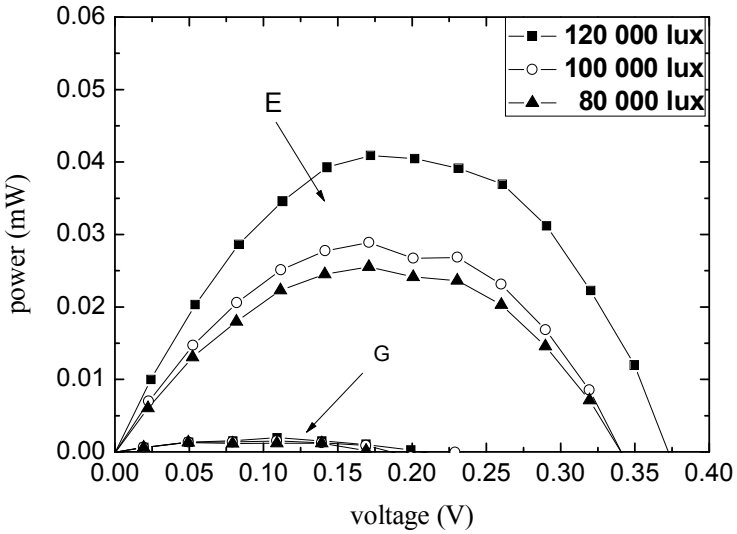

Figure 3.30. Power - voltage characteristics of the DSSCs sensitized by Rheum at different light intensities using C electrode for two different solvents: E for ethyl alcohol and G for polyethylene glycol.

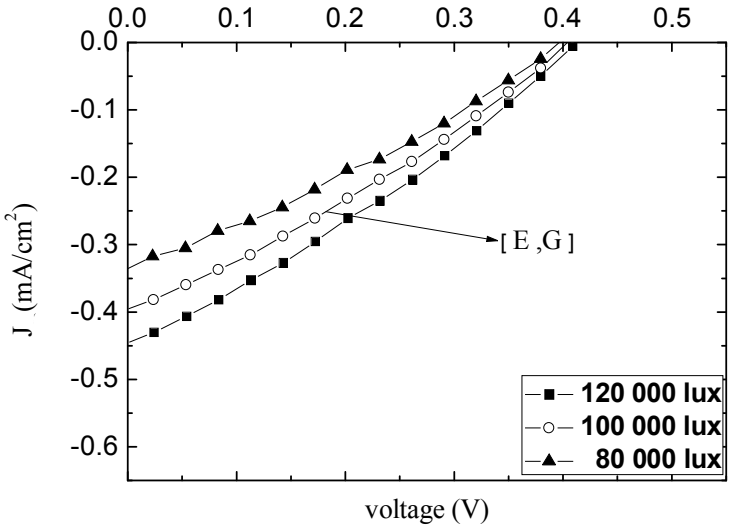

Figure 3.31. Current density–voltage curves for the DSSCs sensitized by Calumus draca (Dracaena oinnabari) at different light intensities using C electrode for two different solvents: E for ethyl alcohol and G for polyethylene glycol.

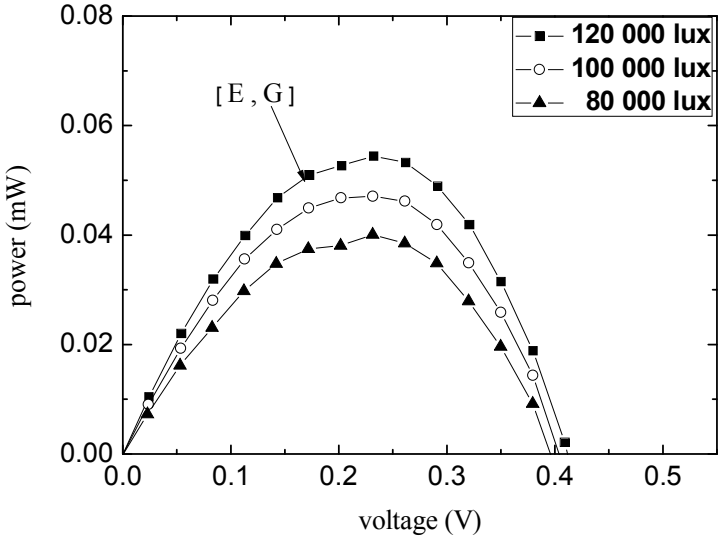

Figure 3.32. Power - voltage characteristics of the DSSCs sensitized by Calumus draca (Dracaena oinnabari) at different light intensities using C electrode for two different solvents: E for ethyl alcohol and G for polyethylene glycol.

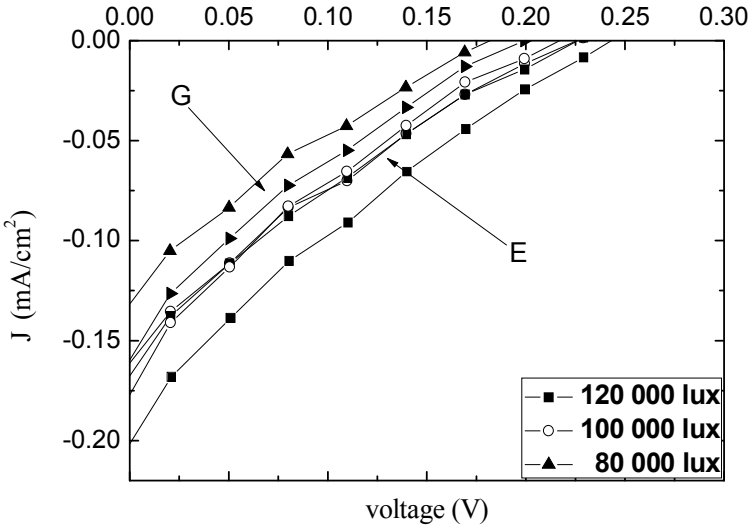

Figure 3.33. Current density–voltage curves for the DSSCs sensitized by Rosa damascena at different light intensities using C electrode for two different solvents: E for ethyl alcohol and G for polyethylene glycol.

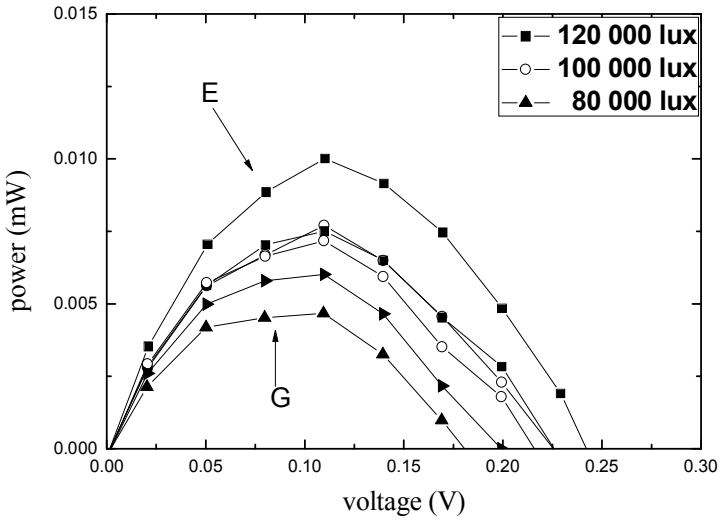

Figure 3.34. Power - voltage characteristics of the DSSCs sensitized by Rosa damascena at different light intensities using C electrode for two different solvents: E for ethyl alcohol and G for polyethylene glycol.

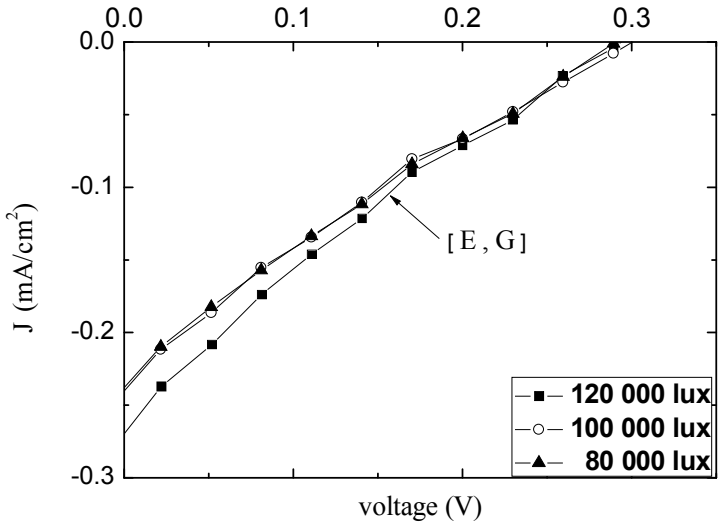

Figure 3.35. Current density–voltage curves for the DSSCs sensitized by Carya illinoensis at different light intensities using C electrode for two different solvents: E for ethyl alcohol and G for polyethylene glycol.

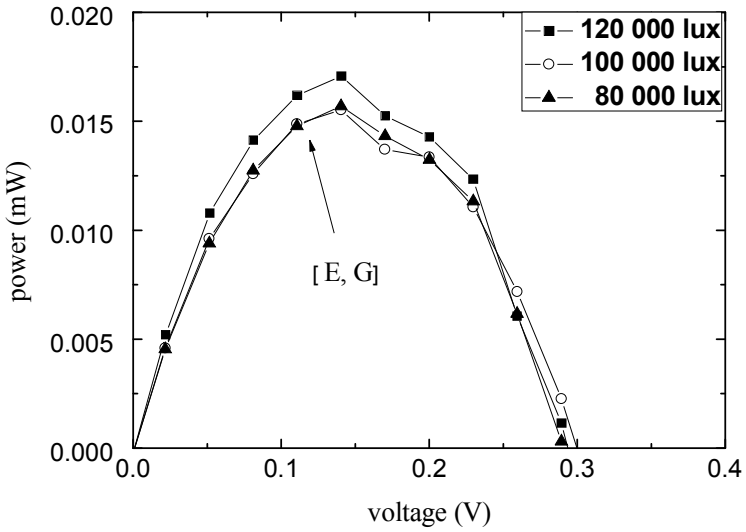

Figure 3.36. Power - voltage characteristics of the DSSCs sensitized by Carya illinoensis at different light intensities using C electrode for two different solvents: E for ethyl alcohol and G for polyethylene glycol.

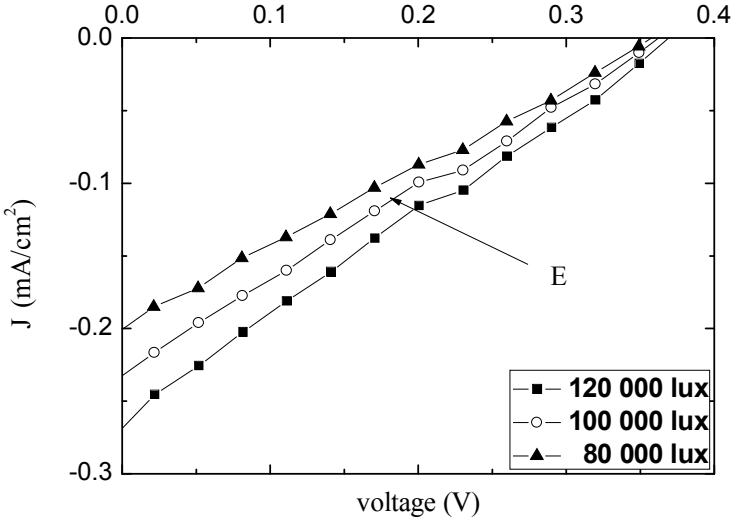

Figure 3.37. Current density–voltage curves for the DSSC sensitized by Roselle (Hibiscas sabdarriffa) at different light intensities using C electrode for a solvents: E for ethyl alcohol .

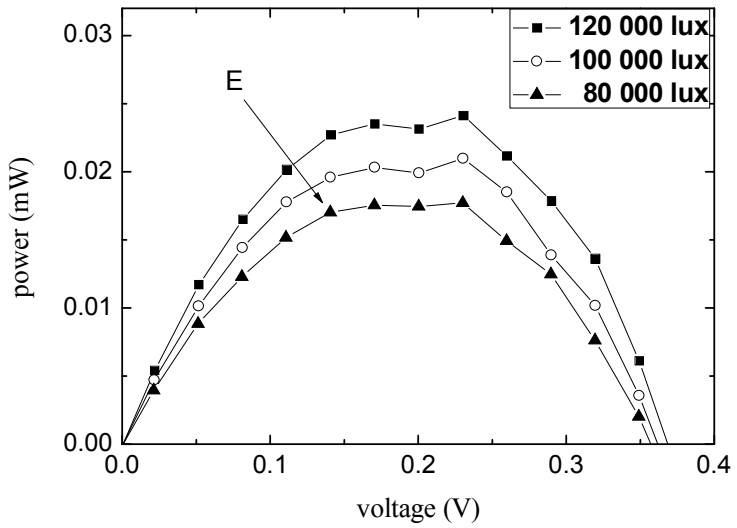

Figure 3.38. Power - voltage characteristics of the DSSC sensitized by Roselle (Hibiscas sabdarriffa) at different light intensities using C electrode for a solvents: E for ethyl alcohol.

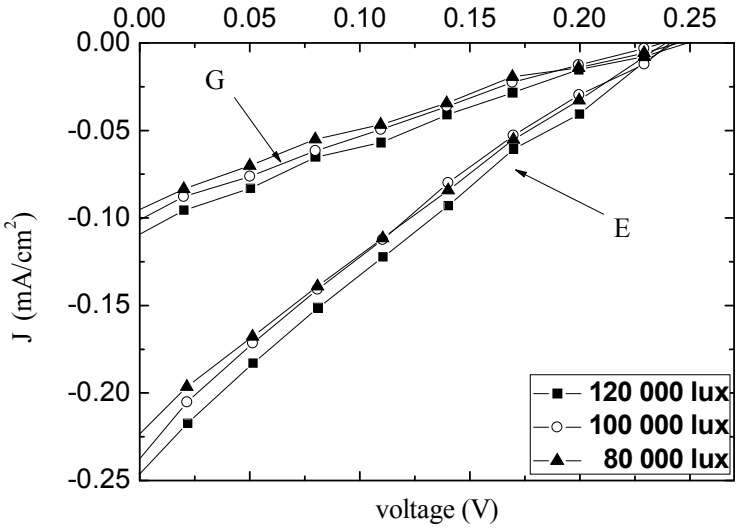

Figure 3.39. Current density–voltage curves for the DSSCs sensitized by Runica granatum at different light intensities using C electrode for two different solvents: E for ethyl alcohol and G for polyethylene glycol.

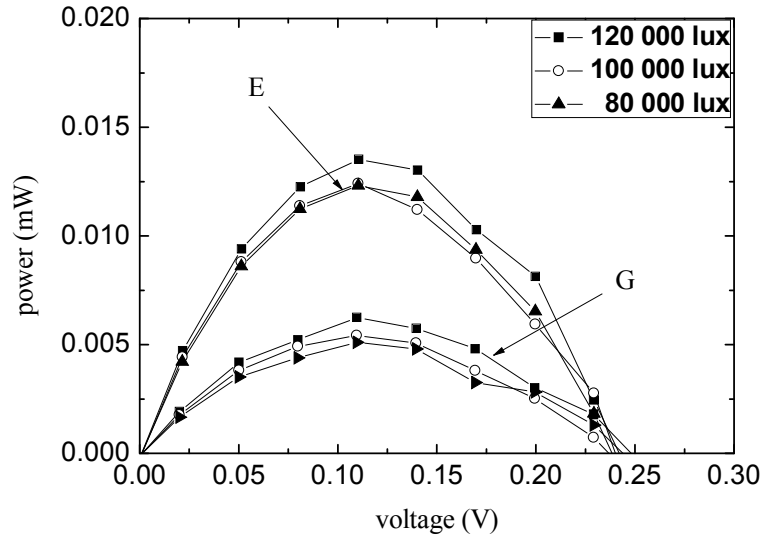

Figure 3.40. Power - voltage characteristics of the DSSCs sensitized by Runica granatum at different light intensities using C electrode for two different solvents: E for ethyl alcohol and G for polyethylene glycol.

The short circuit current density and the open circuit voltage are calculated for each dye and for each solvent. All the photovoltaic parameters (J_m, V_m, P_{max}, η) are also calculated. These values are tabulated in table 3.3 for the ethyl alcohol solvent and in table 3.4 for polyethylene glycol. Comparing the values of table 3.1 with the corresponding ones in table in table 3.3 and the values of table 3.2 with those in table 3.4, the results obtained for the Pt electrode are much higher than that of the carbon electrode. On other hand , the cell parameters obtained for the ethyl alcohol solvent are still better than those for polyethylene glycol as shown in table 3.3 and 3.4. The Safflower dye still exhibits the highest efficiency among all dyes.

Table 3.3. Photovoltaic parameters of the DSSCs sensitized by natural dyes extracted with ethyl alcohol and C as a back electrode.

Dye	Intensity of light	J_{sc} (mA/cm^2)	V_{oc} (V)	J_m (mA/cm^2)	V_m (V)	P_{max} (mW)	FF	η %
Safflower (cathumus tincrorius)	120,000 Lux	0.786	0.380	0.394	0.175	0.0672	0.23	0.068
	100,000 Lux	0.755	0.370	0.354	0.175	0.0622	0.21	0.073
	80,000 Lux	0.695	0.359	0.324	0.175	0.0592	0.22	0.084
Senna (cassia Angustifolia)	120,000 Lux	0.598	0.379	0.282	0.204	0.0603	0.25	0.057
	100,000 Lux	0.564	0.379	0.252	0.202	0.0588	0.23	0.061
	80,000 Lux	0.477	0.379	0.248	0.231	0.0513	0.22	0.085
Rheum	120,000 Lux	0.446	0.349	0.237	0.172	0.0408	0.26	0.040
	100,000 Lux	0.337	0.319	0.168	0.171	0.0288	0.26	0.034
	80,000 Lux	0.269	0.319	0.149	0.170	0.0255	0.25	0.037

Dye	Intensity of light	J_{sc} (mA/cm^2)	V_{oc} (V)	J_m (mA/cm^2)	V_m (V)	P_{max} (mW)	FF	η %
Calumus draca (Dracaena oinnabari)	120,000 Lux	0.448	0.409	0.234	0.231	0.054	0.29	0.054
	100,000 Lux	0.349	0.408	0.203	0.231	0.047	0.32	0.059
	80,000 Lux	0.342	0.408	0.173	0.231	0.046	0.28	0.059
Rosa damascena	120,000 Lux	0.214	0.229	0.090	0.110	0.01	0.20	.0099
	100,000 Lux	0.172	0.229	0.070	0.109	0.0076	0.19	0.0091
	80,000 Lux	0.105	0.169	0.042	0.109	0.0046	0.26	0.0068
Carya illinoensis	120,000 Lux	0.280	0.290	0.121	0.140	0.0170	0.22	0.023
	100,000 Lux	0.249	0.289	0.114	0.140	0.0155	0.23	0.025
	80,000 Lux	0.247	0.289	0.114	0.140	0.0156	0.24	0.026
Roselle (Hibiscas sabdarriffa)	120,000 Lux	0.276	0.379	0.104	0.230	0.0241	0.20	0.016
	100,000 Lux	0.238	0.349	0.019	0.230	0.0209	0.22	0.019
	80,000 Lux	0.206	0.349	0.077	0.230	0.0177	0.22	0.023
Runica granatum	120,000 Lux	0.249	0.258	0.112	0.110	0.0124	0.19	0.012
	100,000 Lux	0.256	0.258	0.122	0.110	0.0135	0.20	0.016
	80,000 Lux	0.233	0.229	0.111	0.110	0.0123	0.21	0.018

The Photovoltaic parameters of the DSSCs (J_{sc} , V_{oc} , FF , η) using C as a back electrode and using polyethylene glycol as a solvent are listed in table 3.4.

Table 3.4. Photovoltaic parameters of the DSSCs sensitized by natural dyes extracted with polyethylene glycol and C as a back electrode.

Dye	Intensity of light	J_{sc} (mA/cm^2)	V_{oc} (V)	J_m (mA/cm^2)	V_m (V)	P_{max} (mW)	FF	η %
Safflower (cathumus tincrorius)	120,000 Lux	0.140	0.259	0.05	0.139	0.007	0.19	0.0069
	100,000 Lux	0.116	0.229	0.05	0.109	0.005	0.20	0.0065
	80,000 Lux	0.093	0.229	0.03	0.109	0.003	0.15	0.0049
Senna (cassia Angustifolia)	120,000 Lux	0.034	0.319	0.017	0.139	0.0023	0.21	0.0023
	100,000 Lux	0.026	0.319	0.017	0.109	0.0019	0.22	0.0022
	80,000 Lux	0.025	0.289	0.016	0.109	0.0017	0.24	0.0026
Rheum	120,000 Lux	0.039	0.199	0.018	0.109	0.0019	0.25	0.0019
	100,000 Lux	0.039	0.199	0.013	0.109	0.0015	0.18	0.0017
	80,000 Lux	0.037	0.169	0.011	0.109	0.0012	0.19	0.0017
Calumus draca (Dracaena Oinnabari)	120,000 Lux	0.448	0.409	0.234	0.231	0.054	0.29	0.054
	100,000 Lux	0.349	0.408	0.203	0.231	0.047	0.32	0.059
	80,000 Lux	0.342	0.408	0.173	0.231	0.046	0.28	0.059

Dye	Intensity of light	J_{sc} (mA/cm^2)	V_{oc} (V)	J_m (mA/cm^2)	V_m (V)	P_{max} (mW)	FF	η %
Rosa damascena	120,000 Lux	0.160	0.229	0.068	0.109	0.0075	0.20	0.007
	100,000 Lux	0.156	0.199	0.065	0.109	0.0071	0.22	0.008
	80,000 Lux	0.143	0.199	0.054	0.109	0.0060	0.20	0.007
Carya illinoensis	120,000 Lux	0.280	0.290	0.121	0.140	0.0170	0.20	0.016
	100,000 Lux	0.249	0.289	0.114	0.140	0.0155	0.22	0.019
	80,000 Lux	0.247	0.289	0.114	0.140	0.0156	0.22	0.023
Runica granatum	120,000 Lux	0.095	0.229	0.056	0.109	0.006	0.28	0.0061
	100,000 Lux	0.087	0.229	0.049	0.109	0.005	0.26	0.0064
	80,000 Lux	0.083	0.229	0.046	0.109	0.005	0.26	0.0075

.

CHAPTWR FOUR

CHEMICAL DYES AS PHOTOSENSITIZERS FOR DYE SENSITIED SOLAR CELLS

In this chapter, DSSCs were prepared using chemical dyes dissolved in ethyl alcohol as a solvent. The ZnO layers were dyed using eight chemical dyes. The absorption spectra of all dyes was performed. The I-V characteristic curves of the fabricated cells were measured and studied. The output power was calculated and plotted. Short circuit current, open circuit voltage, maximum absorption wavelength, maximum power, fill factor, and power conversion efficiency were all presented.

4.1. Absorption Spectra Analysis of Chemical Dyes in Dye Sensitized Solar Cells

Several inorganic, organic and hybrid compounds have been investigated as sensitizer, including porphyrins [29], phtalocyanines [30,31], platinum complexes [32], and fluorescent dyes [33]. Ru-based complexes sensitizers have been widely used because Ru has better efficiency and high durability. However these advantages are offset by their high expense and the tendency to undergo degradation in presence of water. The technical difficulty for the development of the DSSC is now to extend its lifetime and to increase its absorption quantity of sun light**.** Since 1905, Albert Einstein had firstly explained the photoelectric effect mathematically by applying Max Planck's discovery. It was found that the emitted electron only depends on the frequency of incident light. In other words, the output electromotive force of solar cells is determined by the energy of photon ($E = h\nu$). This means the spectral absorption of incident light will influence the measurements of efficiency for solar cells. The fabrication of solar cells should consider the absorption spectrum to fit the incident light for getting efficient generation of electricity [34].

4.2. Material System

The conductive coating typically used is fluorine-doped tin oxide (FTO) preferred over its indium-doped analogue (ITO) for the reasons of lower cost and enhanced stability. Films of nanocrystalline ZnO will be spread on transparent conducting FTO coated glass using doctor blade method. ZnO film is than placed in a solution of dye, which results in the conformal adsorption of a dye monolayer to the film surface. The counter electrode is fabricated from FTO-coated glass, with the addition of a Pt catalyst to catalyse the reduction of the redox electrolyte at this electrode. Platinum thin film is placed on the electrolyte with a spacer.

4.3 Experimental

4.3.1 Chemical Dyes

The following chemical dyes have been used: Alcian blue, Crystal violet, Eosin Y , Carbol fuchsin, Aniline blue, Methyl orange, Fast green and Bromophenol. They were prepared by adding 0.04 gm of dye powder to 20ml of ethyl alcohol. The chromosome solution is left for four hours at room temperature [35].

4.3.2 Preparation of Dye Sensitized Solar Cells

As mentioned in chapter 3, FTO conductive glass sheet was cut into samples of dimensions 0.8cm×1.6cm. The samples were cleaned in a detergent solution using an ultrasonic bath for 15 min, rinsed with water and ethanol, and then dried. The ZnO paste was prepared by adding 0.062 g of ZnO and 0.072 g of polyethylene glycol (G), grinding the mixture for half an hour until a homogeneous paste was obtained. Thin films of nanocrystalline ZnO were spread on the transparent conducting FTO coated glass using doctor blade method, and were placed in an oven at 70 ^{0}C for 20 min. Finally the samples were sintered at 500 ^{0}C for 40 min. Samples were cooled to about 70 ^{0}C before being placed in dyes for one day under dark. The dyed ZnO electrode and the sputtered-platinum counter electrode were assembled to form a solar cell by sandwiching a redox (I^{-}/I^{3}) electrolyte solution. The electrolyte solution

consists of 2ml acetonitrile (ACN) , 8ml propylene carbonate (p-carbonate) , 0.668gm (LiI), and 0.0634gm (I_2).

4.3.3 Characterization and Measurement

a. Absorption Spectra Analysis

The wavelength range of absorption spectra analysis is 350 − 800 nm. UV-VIS absorption measurements of the extracted pigments in ethyl alcohol solution were carried out with a continuous wavelength one beam spectrophotometer.

b. IV Measurements:

The same setup mentioned in subsection 3.3.3(b) was used to measure I-V curve.

4.4. Results and Discussion

4.4.1 Absorption of Chemical Dyes

Figure 4.1 through 4.8 show the UV–VIS absorption spectra of Eosin Y, Alcian blue, Methyl orange, Bromophenol, Carbol fuchsin, Fast green, Aniline blue, and Crystal violet in ethyl alcohol as a solvent. From Fig. 4.1, it can be seen that there is absorption peak at about 520.4 nm for the Eosin Y using ethyl alcohol a solvent. The absorption spectrum of Alcian blue is shows in Fig. 4.2. In the case of ethyl alcohol, the absorption spectrum curve shows a peak at 624.2nm and 671.5nm. As can been seen from Fig. 4.3, there is an absorption peak at 654.4nm for the Methyl orange. Figure 4.4 shows that the Bromophenol exhibits an absorption peak at 426.3nm for ethyl alcohol solvent. In Fig. 4.5, it is shown that Carbol fuchsin extract has a very sharp peak at 550.6nm. Fast green dissolved in ethyl alcohol shows a peak at 619.8nm. Figure 4.7 shows the absorption spectrum of Aniline blue. As can be seen from the figure, the Aniline blue extract shows a peak at 624.8nm. Finally, as Fig. 4.8 shows Crystal violet extract has an absorption peaks in the visible light region at 587.7nm .

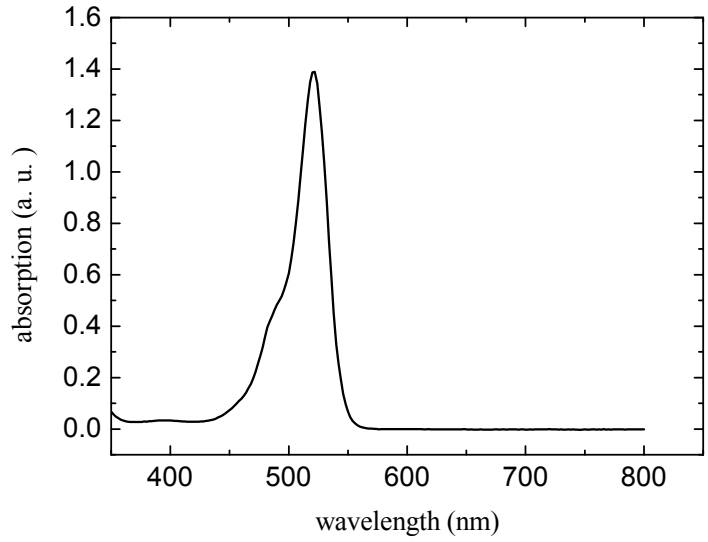

Figure 4.1. The absorption spectrum of the Eosin Y using ethyl alcohol as a solvent

.

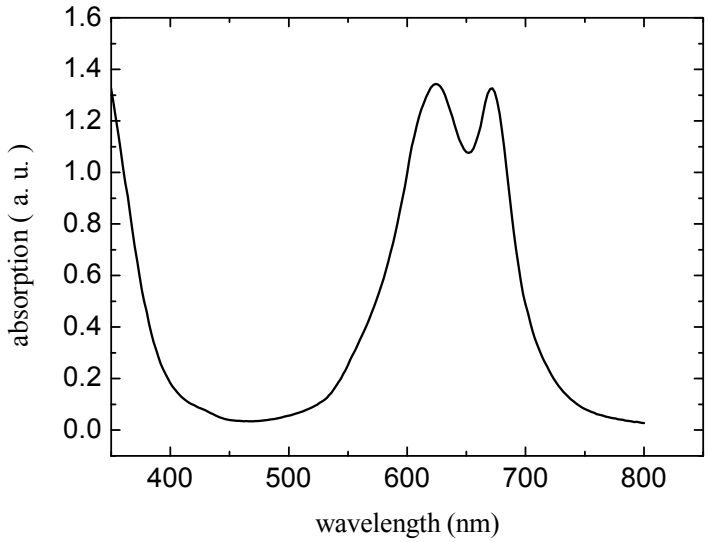

Figure 4.2. The absorption spectrum of the Alcian blue using ethyl alcohol as a solvent.

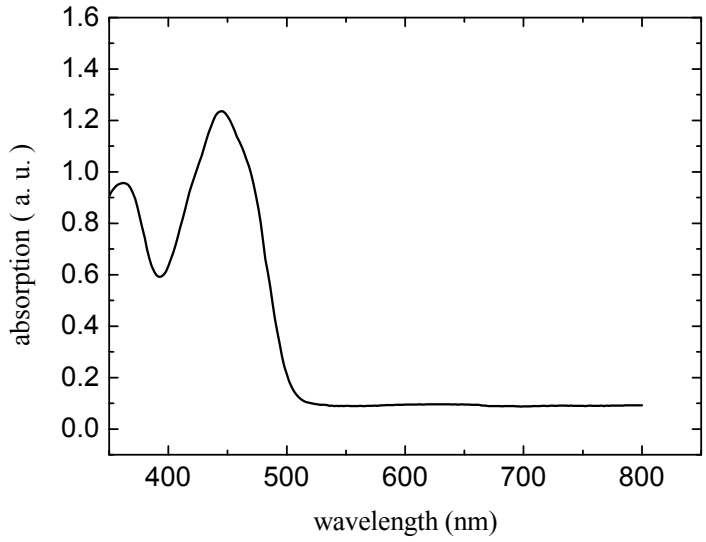

Figure 4.3. The absorption spectrum of the Methyl orange using ethyl alcohol as a solvent .

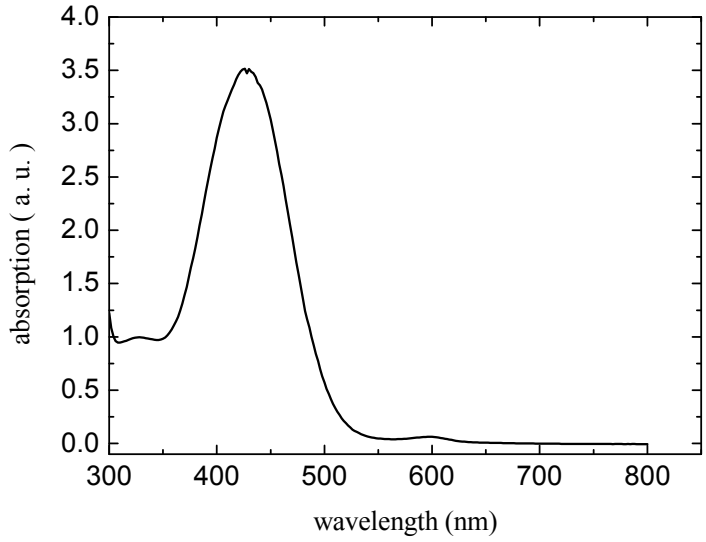

Figure 4.4. The absorption spectrum of the Bromophenol using ethyl alcohol as a solvent.

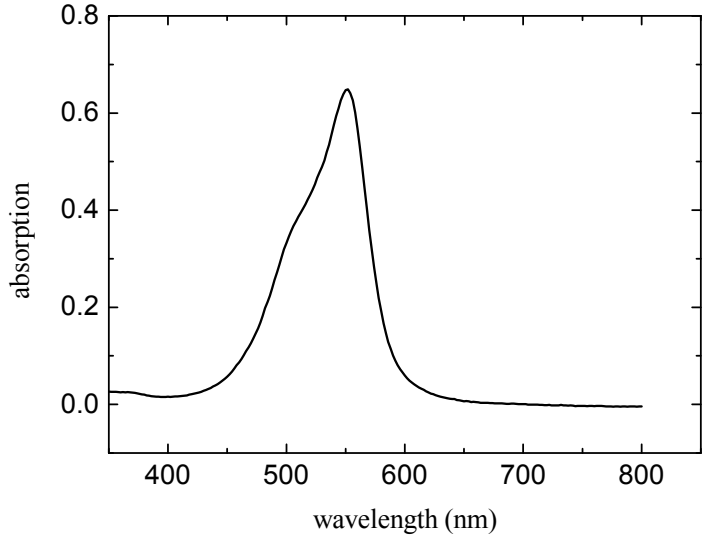

Figure 4.5. The absorption spectrum of the Carbol fuchsin using ethyl alcohol as a solvent .

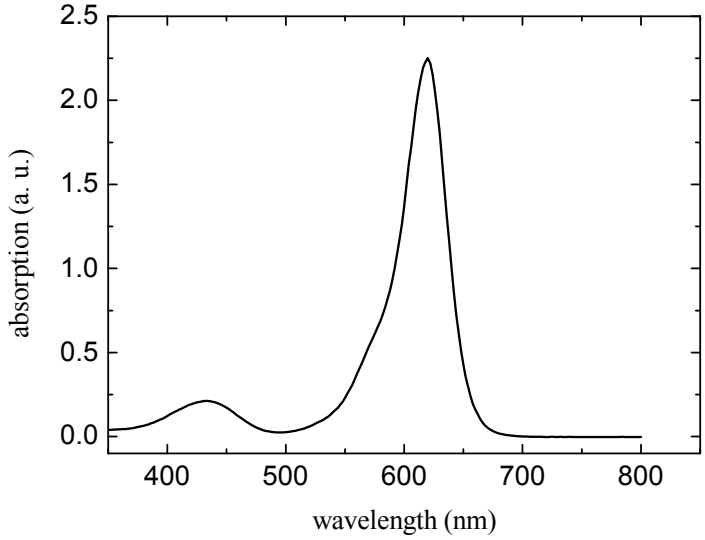

Figure 4.6. The absorption spectrum of the Fast green using ethyl alcohol as a solvent .

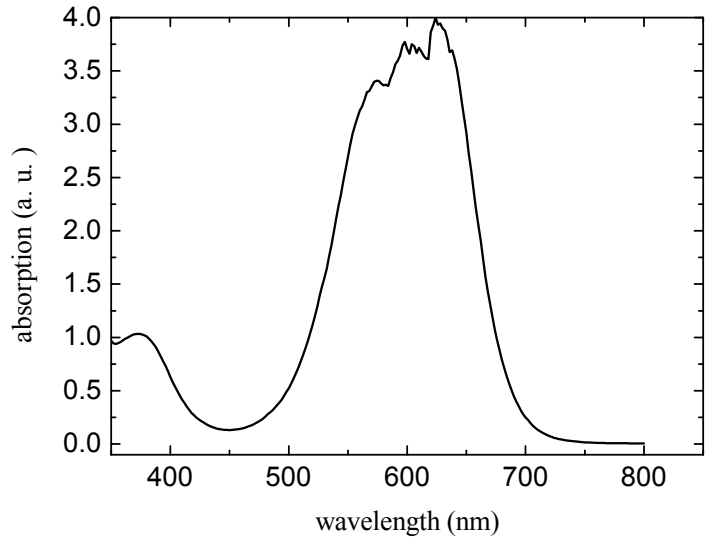

Figure 4.7. The absorption spectrum of the Aniline blue using ethyl alcohol as a solvent .

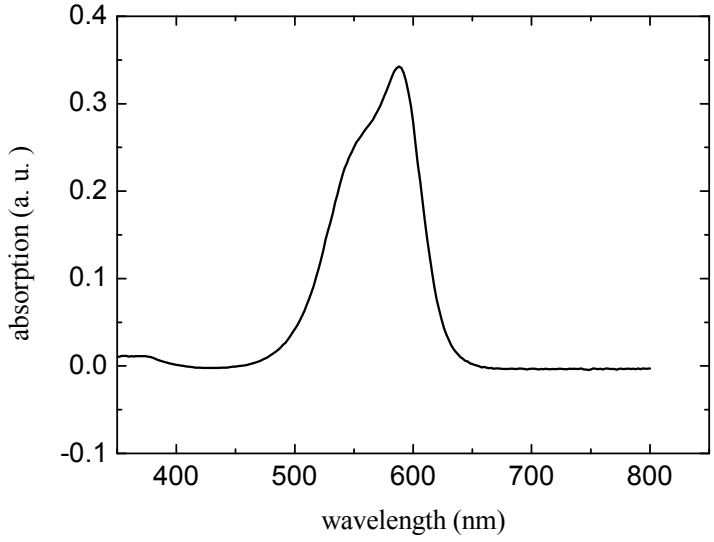

Figure 4.8. The absorption spectrum of the Crystal violet using ethyl alcohol as a solvent .

4.4.2 Photovoltaic Properties of Dye Sensitized Solar Cells Sensitized with Chemical Dyes

In chapter 3, two materials have been used as counter electrodes Pt, and C. The results obtained for Pt were much better than those for C. Thus Pt will be used as a counter electrode. In the following, the results obtained for the DSSCs fabricated using the eight chemical dyes dissolved in ethyl alcohol when the platinum is used as a counter electrode are presented. For each dye, the measured current density (J) versus the voltage (V) is plotted at three different light intensities. For each J-V curve, power (P) is calculated and plotted versus the voltage. Figure 4.9, shows the measured current density versus the voltage of the cell sensitized by Alcian blue at light intensities 80, 100, and 120 klux using platinum electrode for ethyl alcohol as a dye solvent. The power is then calculated for each experimented point by simply multiplying the individual current and voltage of the point. The calculated power as a function of the voltage applied to the cell is plotted in Fig. 4.10. Figures 4.11, 4.13, 4.15, 4.17, 4.19, 4.21, and 4.23 show the J-V characteristic curves obtained for the fabricated DSSC using, Aniline blue, Methyl orange, Crystal violet, Eosin Y, Fast green, Carbol fuchsin, and Bromophenol. Each curve shows the results obtained under illumination of the cell by three different intensities. In a similar manners, Figs. 4.10, 4.12, 4.14, 4.16, 4.18, 4.20, 4.22 and 4.24 show the calculated power versus the of voltage for the cells fabricated using Alcian blue, Aniline blue, Methyl orange, Crystal violet, Eosin Y, Fast green, Carbol fuchsin, and Bromophenol.

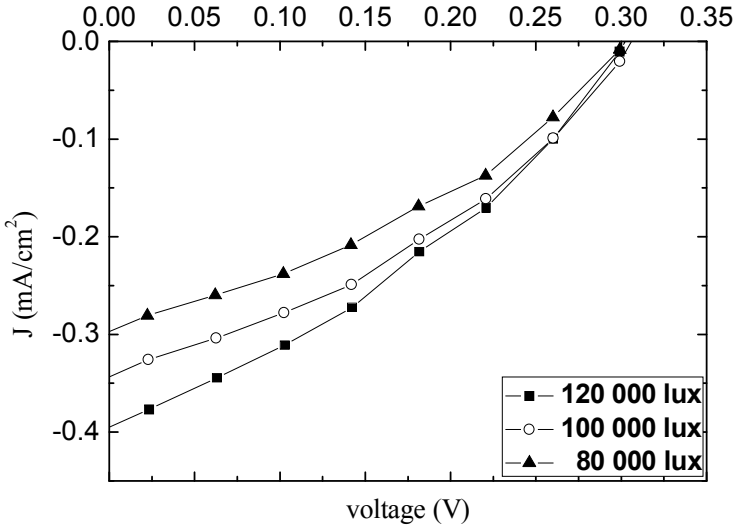

Figure 4.9. Current density–voltage curves for the DSSC sensitized by Alcian blue at different light intensities using Pt electrode.

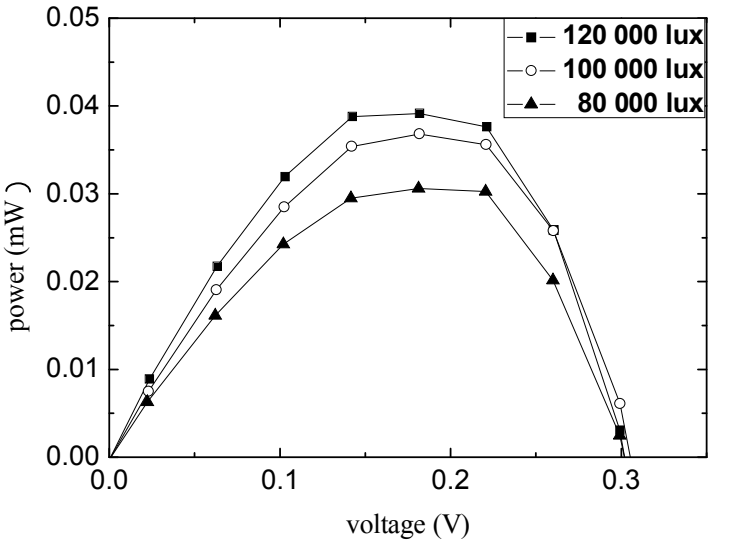

Figure 4.10. Power - voltage characteristics of the DSSC sensitized by Alcian blue at different light intensities using Pt electrode.

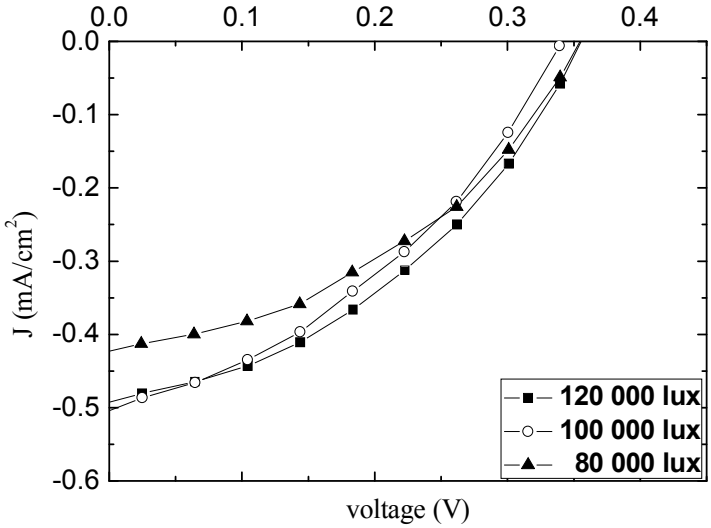

Figure 4.11. Current density–voltage curves for the DSSC sensitized by Aniline blue at different light intensities using Pt electrode.

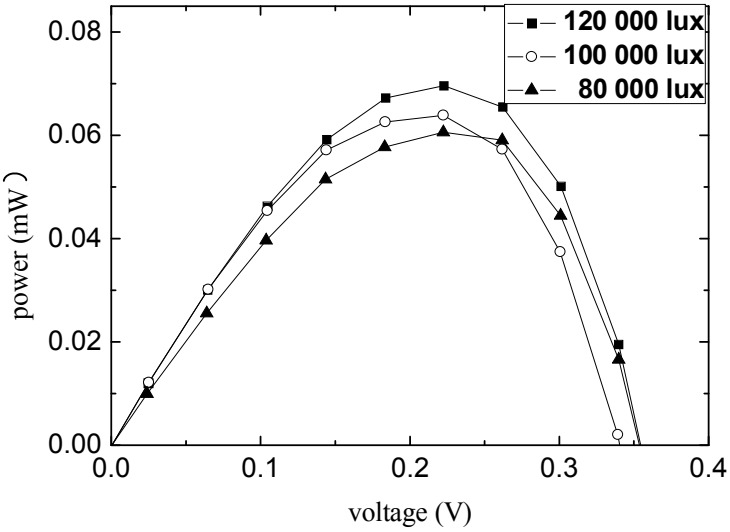

Figure 4.12. Power - voltage characteristics of the DSSC sensitized by Aniline blue at different light intensities using Pt electrode.

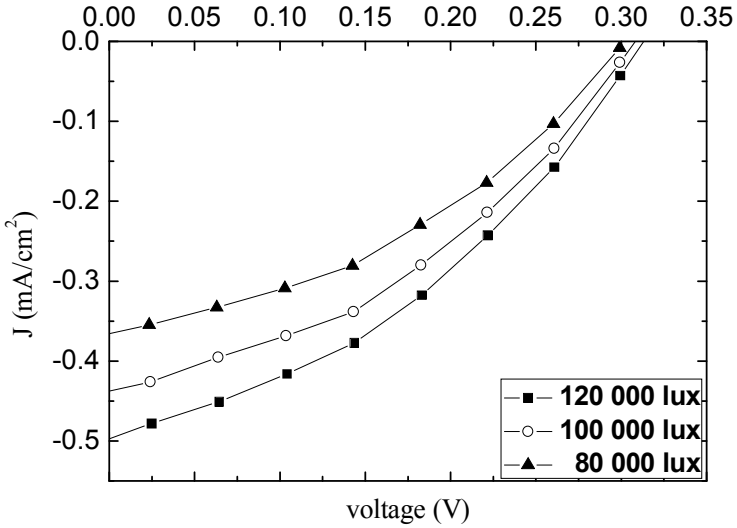

Figure 4.13. Current density–voltage curves for the DSSC sensitized by Methyl orange at different light intensities using Pt electrode.

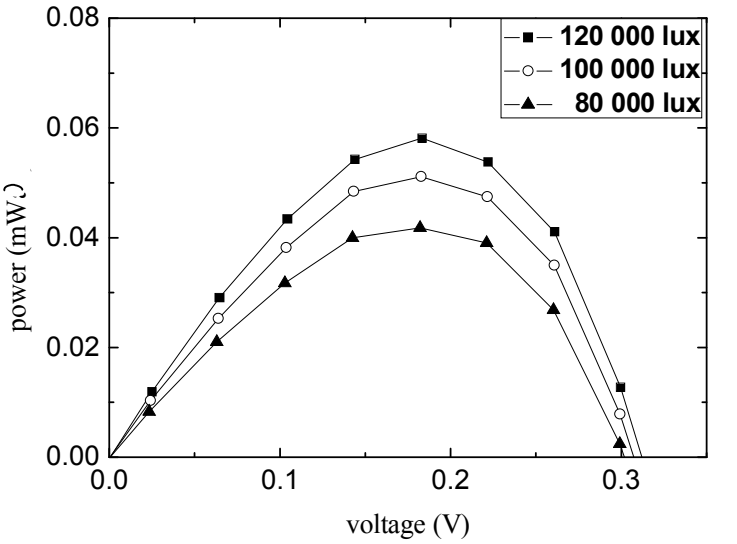

Figure 4.14. Power - voltage characteristics of the DSSC sensitized by Methyl orange at different light intensities using Pt electrode.

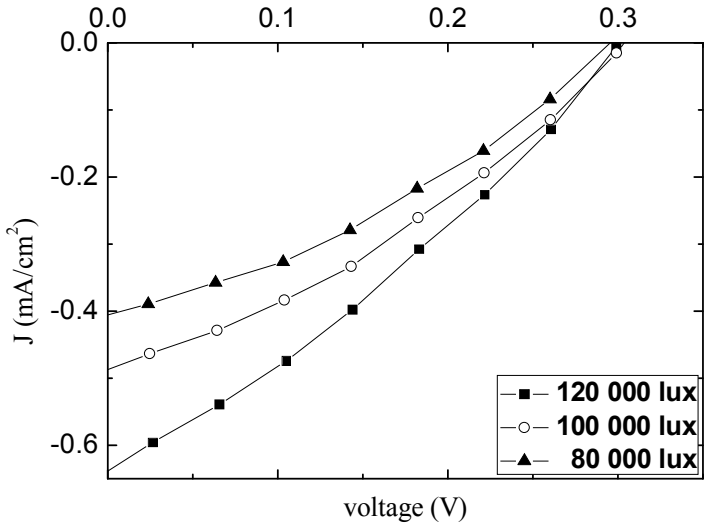

Figure 4.15. Current density–voltage curves for the DSSC sensitized by Crystal violet at different light intensities using Pt electrode.

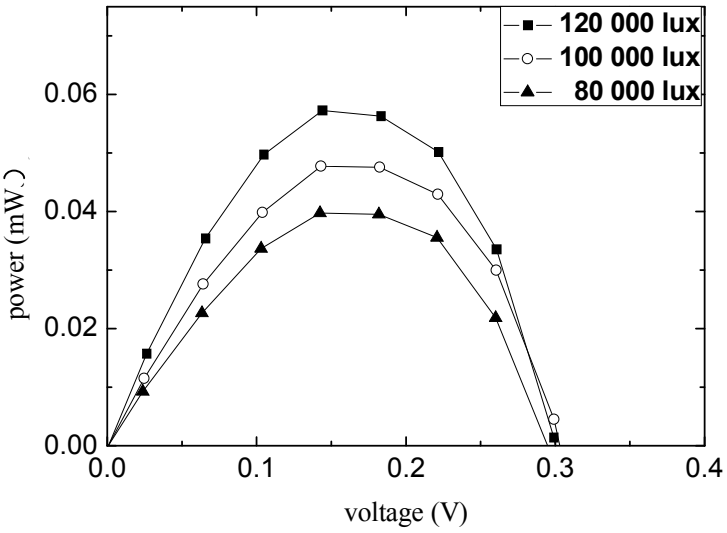

Figure 4.16. Power - voltage characteristics of the DSSC sensitized by Crystal violet at different light intensities using Pt electrode.

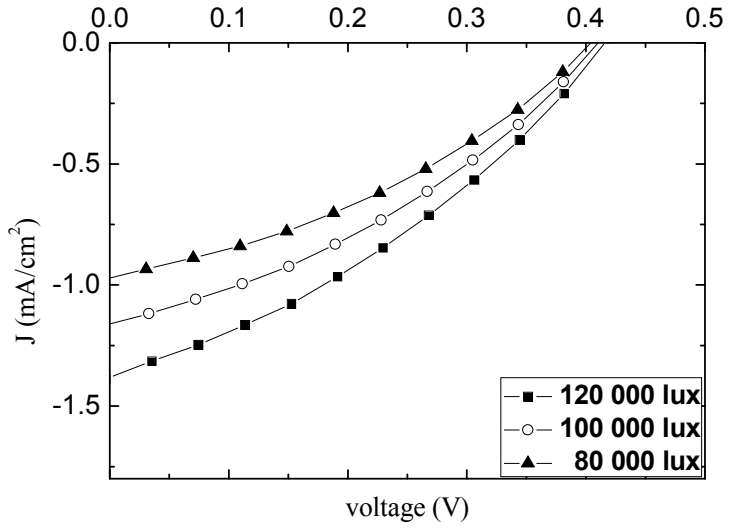

Figure 4.17. Current density–voltage curves for the DSSC sensitized by Eosin Y at different light intensities using Pt electrode.

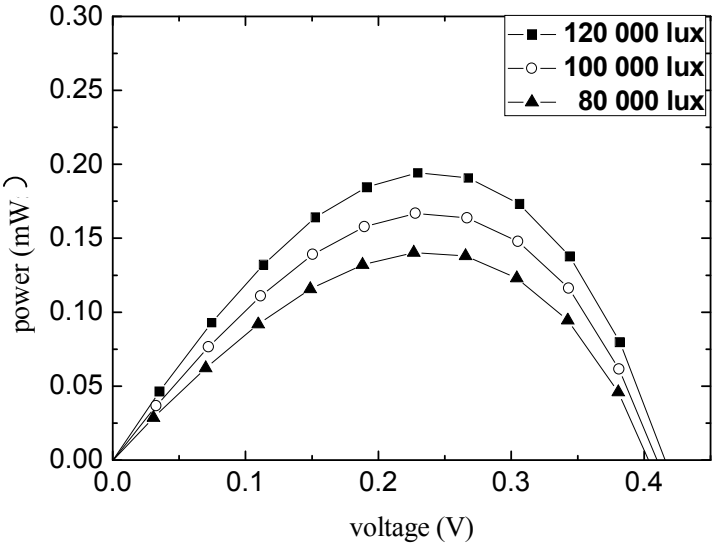

Figure 4.18. Power - voltage characteristics of the DSSC sensitized by Eosin Y at different light intensities using Pt electrode.

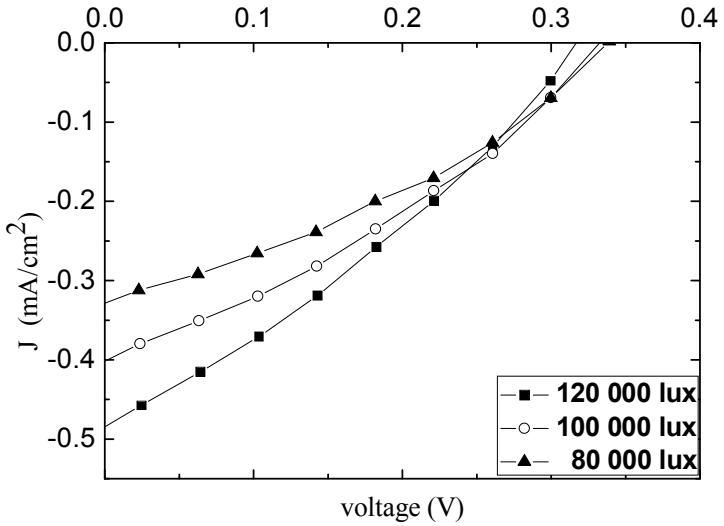

Figure 4.19. Current density–voltage curves for the DSSC sensitized by Fast Green at different light intensities using Pt electrode.

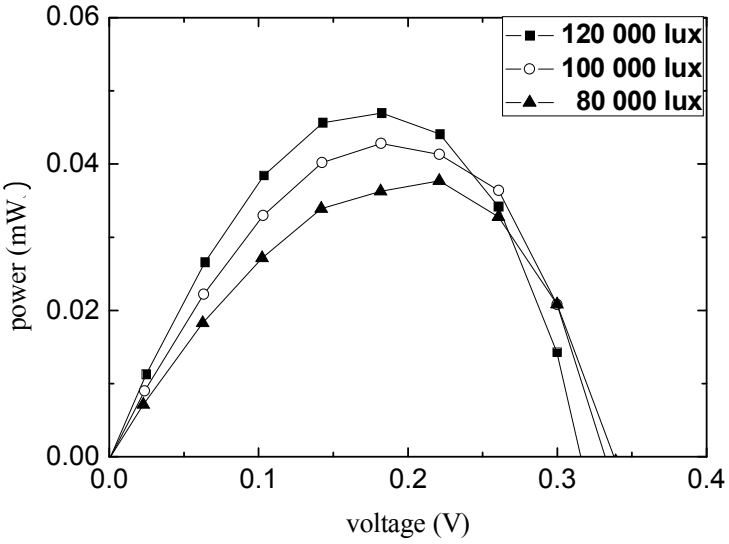

Figure 4.20. Power - voltage characteristics of the DSSC sensitized by Fast Green at different light intensities using Pt electrode.

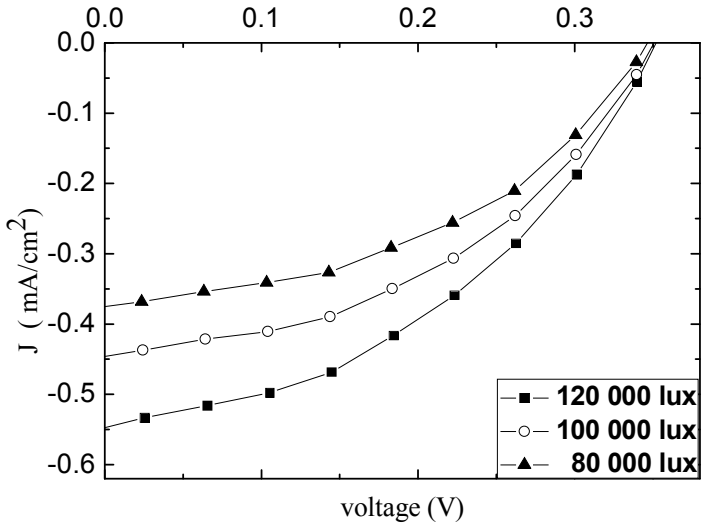

Figure 4.21. Current density–voltage curves for the DSSC sensitized by Carbol Fuchsin at different light intensities using Pt electrode .

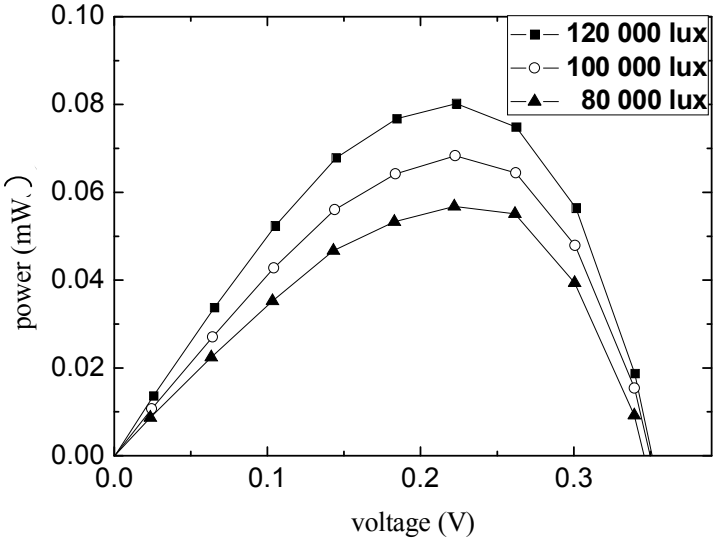

Figure 4.22. Power - voltage characteristics of the DSSC sensitized by Carbol Fuchsin at different light intensities using Pt electrode.

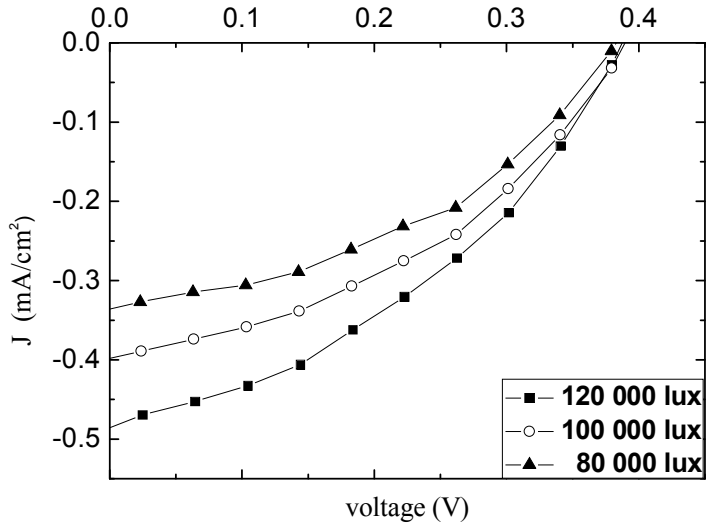

Figure 4.23. Current density–voltage curves for the DSSC sensitized by Bromophenol at different light intensities using Pt electrode.

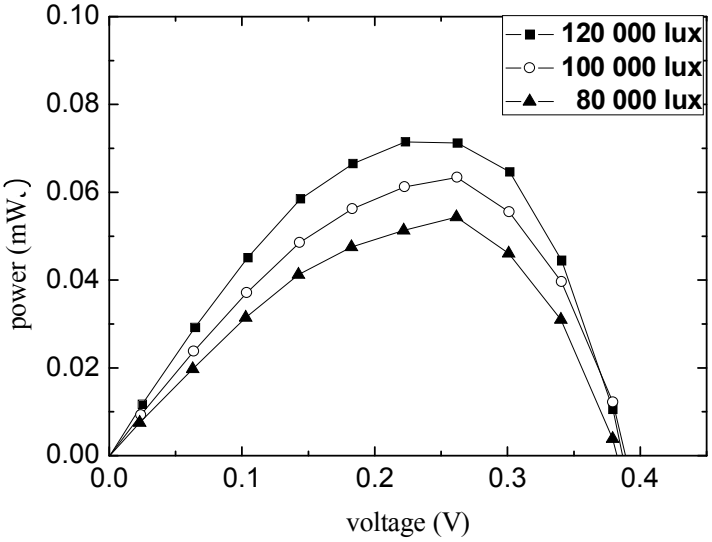

Figure 4.24. Power - voltage characteristics of the DSSC sensitized by Bromophenol at different light intensities using Pt electrode.

All the photovoltaic parameters (J_{sc}, V_{oc}, J_m, V_m, P_{max}, FF, η) of the fabricated DSSCs are tabulated in table 4.1 for the ethyl alcohol solvent. All measurements where conducted at light intensities of 80, 100, and 120 klux. Values of the short circuit current density (J_{sc}) and open circuit voltage (V_{oc}) where obtained from the J-V curves by estimating the J- curve and V- curve intercepts, respectively. The maximum power point is determined from the P-V curves from which J_m and V_m can be calculated. The fill factor and cell efficiency are then calculated using Eq. (1.4) and Eq. (1.5) respectively. Moreover, the comparison among all dyes shows that the best dye is the Eosin Y which corresponds to the highest conversion efficiency. The short circuit current density and the open circuit voltage of Eosin Y cell were found to be 1.39 mA/cm^2 and 0. 421V for the light intensity of 120 klux.

Table 4.1. Photovoltaic parameters of the DSSCs sensitized by chemical dyes dissolved with ethyl alcohol as a solvent and using Pt as a back electrode.

Dye	Intensity of light	J_{sc} (mA/cm^2)	V_{oc} (V)	J_m (mA/cm^2)	V_m (V)	P_{max} (mW)	FF	η %
Alcian Blue	120,000 Lux	**0.37**	**0.299**	**0.27**	**0.142**	**0.038**	**0.34**	**0.038**
	100,000 Lux	**0.32**	**0.299**	**0.20**	**0.181**	**0.036**	**0.37**	**0.043**
	80,000 Lux	**0.28**	**0.299**	**0.16**	**0.181**	**0.036**	**0.34**	**0.043**
Aniline Blue	120,000 Lux	**0.49**	**0.343**	**0.32**	**0.223**	**0.070**	**0.42**	**0.071**
	100,000 Lux	**0.48**	**0.339**	**0.29**	**0.223**	**0.063**	**0.38**	**0.077**
	80,000 Lux	**0.42**	**0.339**	**0.27**	**0.223**	**0.060**	**0.42**	**0.090**
Methyl Orange	120,000 Lux	**0.48**	**0.302**	**0.32**	**0.183**	**0.058**	**0.40**	**0.058**
	100,000 Lux	**0.42**	**0.302**	**0.28**	**0.183**	**0.050**	**0.39**	**0.061**
	80,000 Lux	**0.36**	**0.302**	**0.23**	**0.183**	**0.041**	**0.38**	**0.063**
Crystal Violet	120,000 Lux	**0.61**	**0.304**	**0.40**	**0.146**	**0.057**	**0.31**	**0.057**
	100,000 Lux	**0.49**	**0.302**	**0.34**	**0.142**	**0.047**	**0.36**	**0.057**
	80,000 Lux	**0.40**	**0.301**	**0.29**	**0.144**	**0.040**	**0.34**	**0.062**
Eosin Y	120,000 Lux	**1.39**	**0.421**	**0.84**	**0.227**	**0.19**	**0.32**	**0.195**
	100,000 Lux	**1.17**	**0.409**	**0.73**	**0.229**	**0.167**	**0.34**	**0.200**
	80,000 Lux	**0.94**	**0.404**	**0.62**	**0.224**	**0.140**	**0.36**	**0.208**

Dye	Intensity of light	J_{sc} (mA)	V_{oc} (V)	J_m (mA)	V_m (V)	P_{max} (mW)	FF	η %
Fast Green	120,000 Lux	**0.47**	**0.341**	**0.26**	**0.184**	**0.047**	**0.29**	**0.047**
	100,000 Lux	**0.39**	**0.336**	**0.23**	**0.181**	**0.042**	**0.31**	**0.041**
	80,000 Lux	**0.32**	**0.332**	**0.17**	**0.220**	**0.037**	**0.35**	**0.037**
Carbol Fuchsin	120,000 Lux	**0.54**	**0.341**	**0.36**	**0.223**	**0.080**	**0.45**	**0.080**
	100,000 Lux	**0.44**	**0.341**	**0.31**	**0.223**	**0.068**	**0.46**	**0.082**
	80,000 Lux	**0.38**	**0.338**	**0.25**	**0.221**	**0.056**	**0.43**	**0.082**
Bromophenol	120,000 Lux	**0.48**	**0.385**	**0.32**	**0.264**	**0.072**	**0.38**	**0.071**
	100,000 Lux	**0.40**	**0.379**	**0.28**	**0.263**	**0.063**	**0.48**	**0.073**
	80,000 Lux	**0.33**	**0.378**	**0.23**	**0.262**	**0.054**	**0.48**	**0.060**

CHAPTER FIVE

OPTIMIZATION OF THE ZINC OXIDE LAYER FOR DYE SENSITIZED SOLAR CELLS

In this chapter, The DSSC dyed with the best two dyes found in chapter three and chapter four will be optimized. Two parameter are studied in details to find out the optimum values corresponding to the highest conversion efficiency. These parameters are the sintering temperature and thickness of the ZnO layer.

5.1 The Best Dyes

It is found that the Safflower is the best dye among the eight natural dyes presented in chapter three, and Eosin Y is the best chemical dye among the chemical dyes presented in chapter four. In the following, the properties of these dyes are presented.

a. Safflower

Safflower (Cathumus tincrorius) has the molecular Formula $C_{43}H_{42}O_{22}$. It's a member of the family of Compositae or Asteraceae. Safflower was the Latinized synonym of the Arabic word quartum, or gurtum, which refers to the color of the dye extracted from safflower flowers. The English name safflower probably evolved from various written forms of usfar, affore, asfiore, and saffiore to safflower. Safflower flowers are known to have many medical properties for curing several chronic diseases and they are widely used in Chinese herbal preparations [36]. Safflower oil is characterized by the presence of a high proportion of n-6 polyunsaturated fatty acids that include linoleic (approximately 75%), oleic (13%), palmitic (6%), stearic (3%), and other minor straight-chained fatty acids [37]. Alpha and gamma tocopherol content have also been found [38]. The chemical structure of safflower is shown in Fig. 5.1.

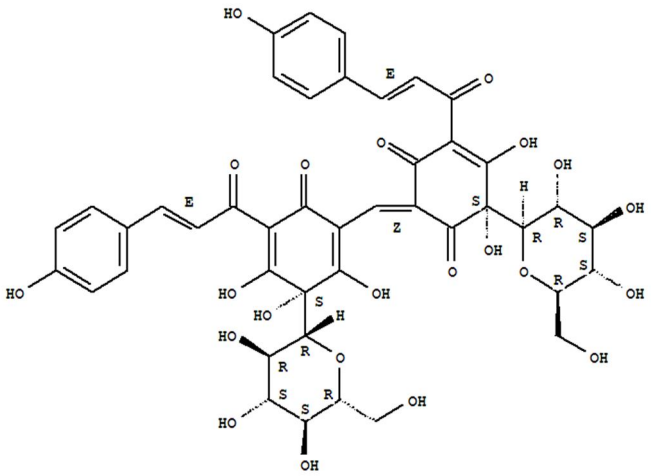

Figure 5.1. Chemical structure of safflower (Cathumus tincrorius).

b. Eosin Y

There are several dyes named eosin, and specifically the one most commonly used to counter stain hemalum is Eosin Y. Eosin Y has molecular formula $C_{20}H_8Br_4O_5$ and molecular weight of 647.89. Eosin Y is a pink water soluble acid dye which also displays yellow-green fluorescence [39]. Eosin Y was used in the fields of dyeing, printing, printing ink, and fluorescent pigment. Eosin Y is used in paint and dye industries because of its vivid color. The toxic nature of the dye is still not quantified much but its high content in living systems is proved to be harmful [40, 41]. The chemical structure of Eosin Y is shown in Fig. 5.2.

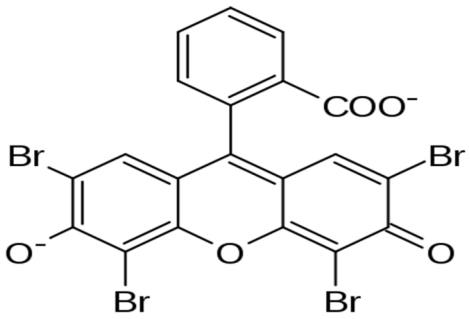

Figure 5.2. Chemical structure of Eosin Y.

5.2 Optimization of Sintering Temperature

5.2.1. Preparation of Dye Sensitized Solar Cells at Different Temperatures

Seven sets of samples were prepared. Each set was sintered at a specific temperature. After depositing the ZnO paste on the FTO substrates, the first set was sintered at 250 ^{0}C, the second set at 300 ^{0}C, the third set at 350 ^{0}C, the fourth set at 400 ^{0}C, the fifth set at 450 ^{0}C, the sixth set at 500 ^{0}C, and the seventh set at 600 ^{0}C. Sintering time was 40 min for all sets. Two cells from each set were dyed with safflower and other two cells from each set were dyed with Eosin Y.

5.2.2. Results and Discussions

Figure 5.3, shows the current density–voltage for the DSSCs prepared at different sintering temperatures sensitized by Eosin Y. As can be seen from the figure the output characteristics of the DSSC show quasi-linear behavior at 250, 300, 350, 500, and 600 ^{0}C temperatures and slightly super linear deviation at 400 and 450 ^{0}C. The figure shows that the optimum temperature that corresponds to the highest value of V_{oc} and J_{sc} is 450 ^{0}C. All values of open circuit and short circuit current corresponding to all temperatures are tabulated in table 5.1. In a similar manner, Fig. 5.4 shows the current versus the voltage of DSSCs sensitized by safflower and sintered at temperatures 250, 300, 350, 400, 450, 500, and 600 ^{0}C. Two important features can be seen from the figure. First, the J-V curve shows a quasi- linear be behavior of all temperatures. Second, the optimum temperature is 400 ^{0}C at which the highest value for V_{oc} and J_{sc} were obtained. Table 5.2 shows all values of V_{oc} and J_{sc} obtained at different temperatures. As can be seen, at temperatures higher than 450 ^{0}C, dying process does not work well because the paste becomes nonporous. Moreover, at low temperatures (< 400 ^{0}C), the paste is not dyed well because of these conclusions can be applied to both natural and chemical dyes. Finally, temperatures between 400 – 450 ^{0}C are recommended as optimum temperatures for sintering DSSCs based on ZnO.

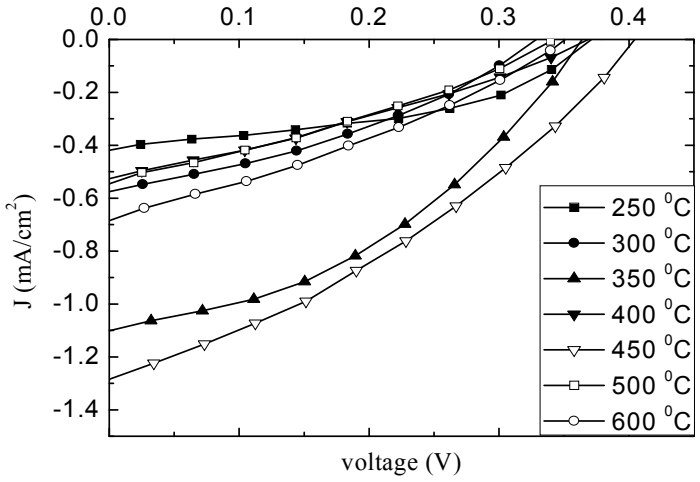

Figure 5.3. Current density–voltage curves for the DSSCs prepared at different sintering temperatures and sensitized by Eosin Y and using Pt a back electrode.

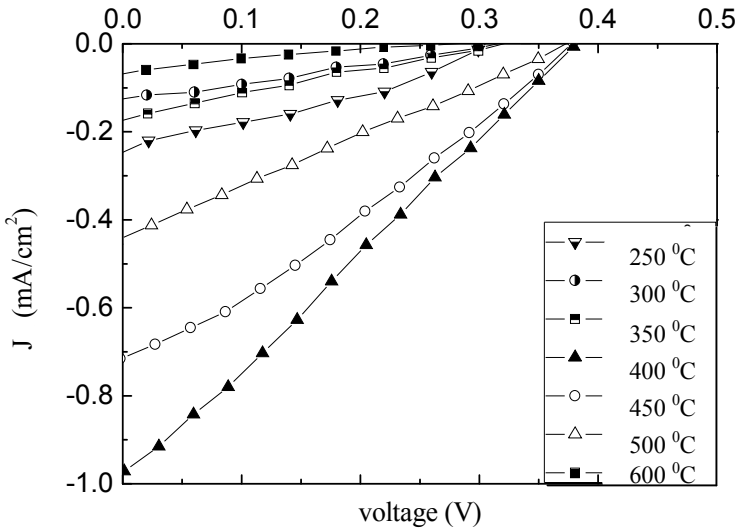

Figure 5.4. Current density–voltage curves for the DSSCs prepared at different sintering temperatures and sensitized by safflower and using Pt a back electrode.

Table 5.1. Photovoltaic parameters of the DSSCs sintered at different temperatures and sensitized by Eosin Y dye.

Temperature (^{0}C)	250	300	350	400	450	500	600
J_{sc} (mA/cm^2)	0.41	0.58	1.10	0.67	1.30	0.54	0.67
V_{oc} (V)	0.322	0.330	0.362	0.330	0.402	0.347	0.339

Table 5.2. Photovoltaic parameters of the DSSCs sintered at different temperatures and sensitized by safflower dye.

Temperature (^{0}C)	250	300	350	400	450	500	600
J_{sc} (mA/cm^2)	0.24	0.12	0.17	0.97	0.71	0.44	0.07
V_{oc} (V)	0.229	0.229	0.230	0.380	0.350	0.299	0.259

The short circuit currents and open circuit voltage versus the seven sintering temperatures are, respectively, shown in Fig. 5.5 (a) and Fig. 5.5 (b) for the DSSCs dyed with Eosin Y. Both figures show peaks at 400 ^{0}C sintering temperature. Fig. 5.6 (a) and Fig. 5.6 (b) show the same for the DSSCs sensitized by safflower. The figure shows peak at 450 ^{0}C sintering temperature.

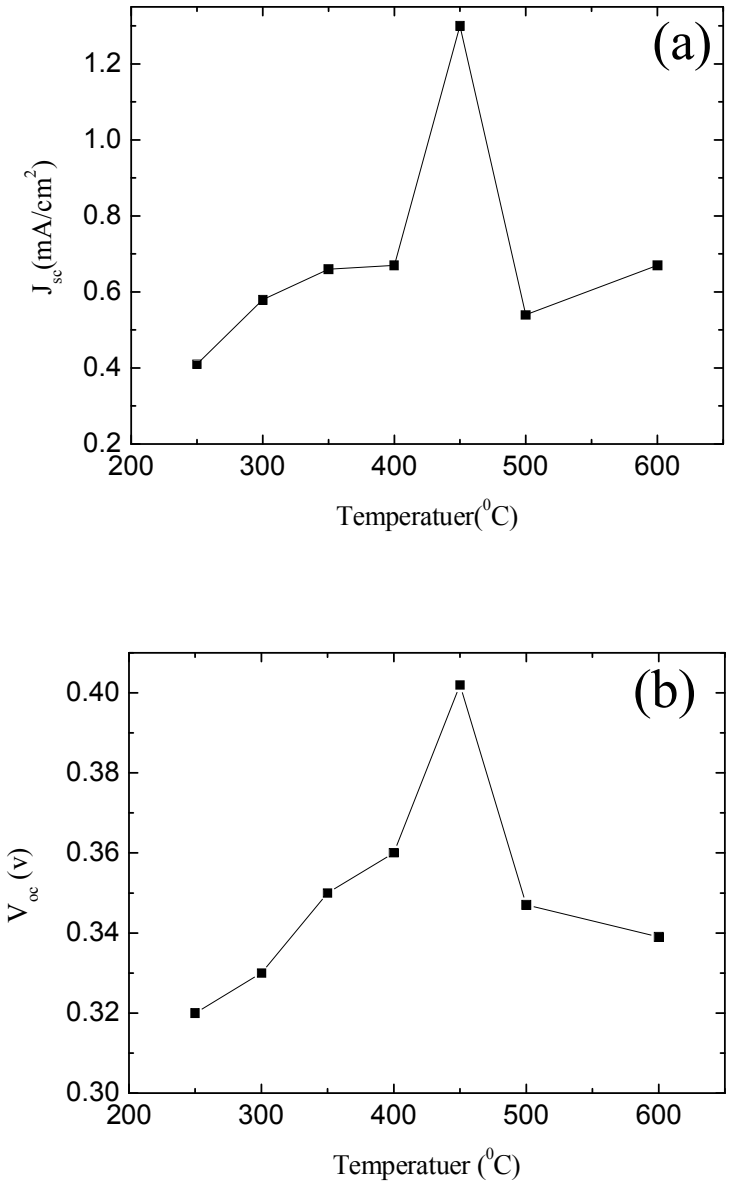

Figure 5.5. Variation of (a) short circuit current density and (b) open circuit voltage as a function sintering temperature of the ZnO photo-anodes, using Eosin Y as a sensitizer.

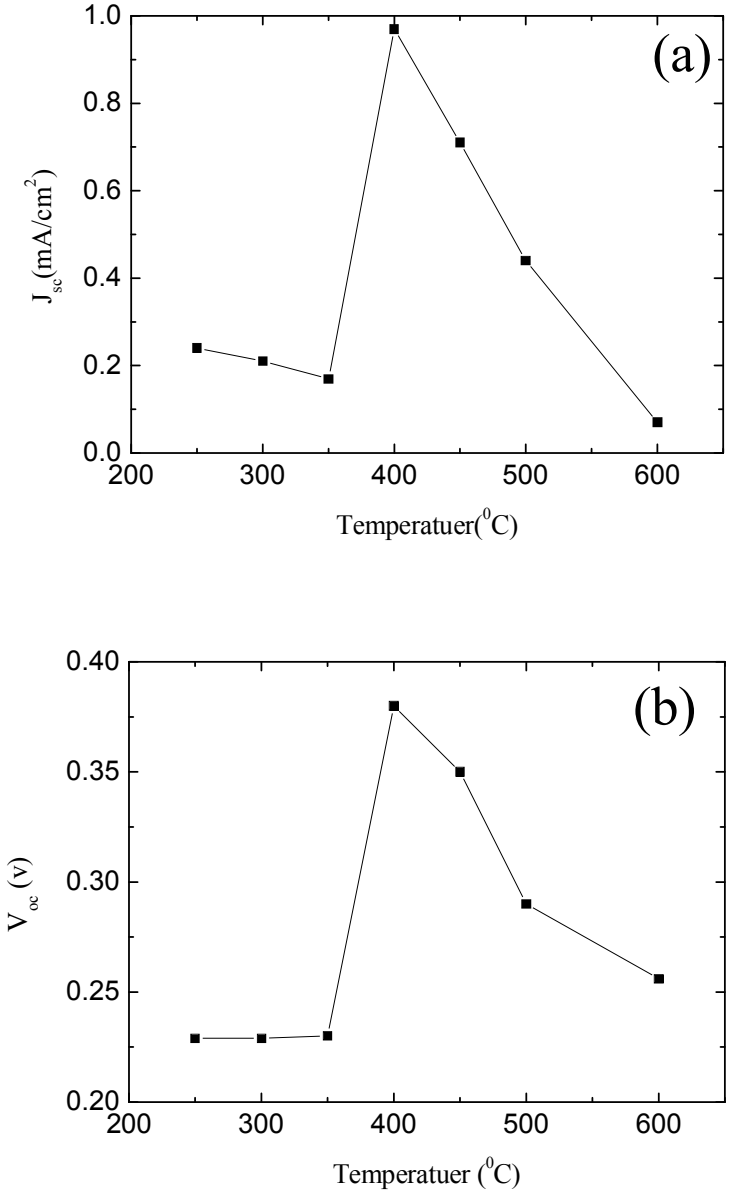

Figure 5.6. Variation of (a) short circuit current density and (b) open circuit voltage as a function sintering temperature of the ZnO photo-anodes, using safflower as a sensitizer.

5.3. Optimization of the Thickness of ZnO Layer

5.3.1. Preparation of Dye Sensitized Solar Cells with Different Thicknesses

Six sets of sample were prepared. The main difference between them was the thickness of the ZnO layer which is donate by D. The different thicknesses were obtained by changing the weight of ZnO powder in the paste. In the DSSCs fabricated

in the previous chapters, 0.072g of ZnO was added to 0.62g of polyethylene glycol. In this work, weights of 0.072, 0.062, 0.052, 0.042, 0.032, and 0.022g of ZnO were added to 0.062g of polyethylene glycol to prepare the different sets. All sets, were sintered of 400 ± 5 ^{0}C for 40 min. Two cells from each set were dyed with safflower and other two cells were dyed by Eosin Y.

5.3.2. Measurements and Techniques

The thickness of ZnO layer was measured using a general microscope based on the depth of focus. General microscope have a strong longitudinal (the Z- direction) resolving power down to a few micrometers. To measure the require thickness a notch is made within the ZnO layer with plastic sharp tip. The ZnO layer is than placed on the X-Y stage of the microscope. The image is focused on the bed of the notch through the observation of very fine dust (or ZnO) particles and reading R_1 of the fine adjustment dial is recorded. Slowly turn the fine adjustment knob until the top layer comes into focus and the reading R_2 on the scale is recorded. The distance D which the vertical stage moved is simply the thickness of the ZnO layer[43].

$$D = R_1 - R_2 \tag{5.1}$$

This method is accurate within the depth of focus of a microscope which is given by:

$$\Delta Z = \frac{\lambda}{4n[1-\sqrt{1-\left(\frac{NA}{n}\right)^2}\,]} \tag{5.2}$$

Where λ is the wavelength used, n is the index of reflation of the medium between the objective and the specimen under study, NA is the numerical aperture of the objective .

In this study, the sample is illuminated with white light centered at 550nm and an objective with NA=0.65 is used. Thus, the thickness measurement is accurate within ±5.2× 10^{-7} m.

5.3.3. Results and Discussions

DSSCs prepared at different ZnO photo-anode thicknesses are then assembled using at Pt as a counter electrode. The J-V measurements are then carried out. Figure 5.7 shows the J-V relation for six DSSCs prepared at different ZnO layer thickness and sensitized by Eosin Y. As can be seen from the figure the highest J_{sc} in obtained for the cell of thickness of 7.5 μm whereas the highest V_{oc} in found for the cell of thickness 2.2μm. To find out the optimum thickness, we calculated P_{max} and η for all cells. Table (5.3) shows all the photovoltaic parameters of DSSCS prepared at different ZnO layer thicknesses and sensitized by Eosin Y. The table shows clearly that a thickness of 7.5 μm is the optimum one. In Fig. 5.8, the J-V curves for the DSSCs fabricated at different ZnO layer thickness and sensitized by safflower are shown. In a similar manner to the conclusion reached for DSSCs sensitized by Eosin Y, the thickness of 7.5μm represents the optimum layer thickness which in this case correspond to the highest V_{oc} and J_{sc} .

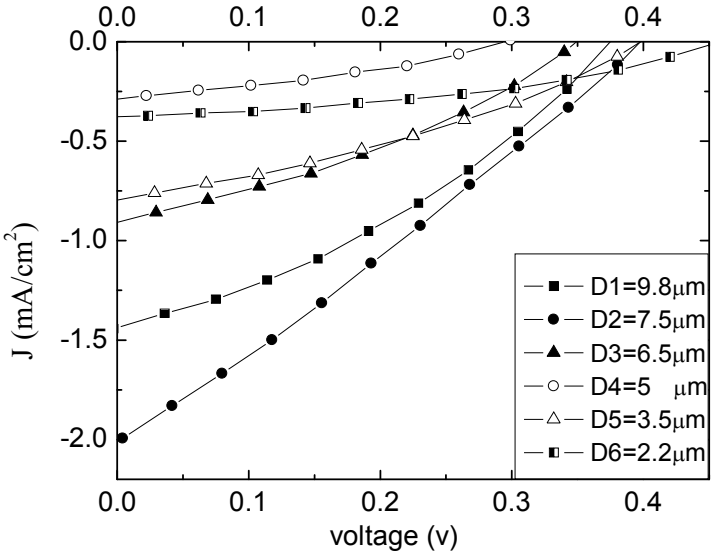

Figure 5.7. Current density–voltage curves for the DSSCs prepared at different sintering thicknesses and sensitized by Eosin Y.

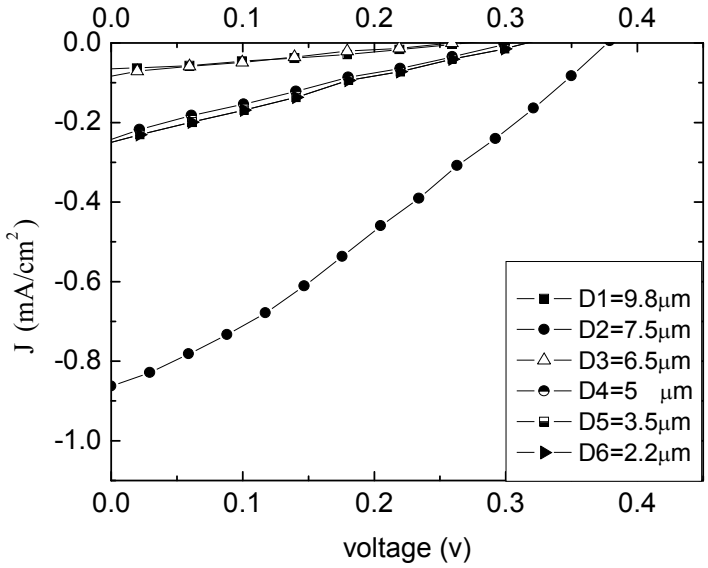

Figure 5.8. Current density–voltage curves for the DSSCs prepared at different sintering thicknesses and sensitized by safflower**.**

Table 5.3. Photovoltaic parameters of the DSSCs sensitized by Eosin Y dyes, at different ZnO thicknesses.

ZnO Thickness (μm)	**2.2**	**3.5**	**5**	**6.5**	**7.5**	**9.8**
J_{sc} (mA/cm^2)	**0.38**	**0.77**	**0.27**	**0.87**	**2.03**	**1.39**
V_{oc} (V)	**0.355**	**0.380**	**0.364**	**0.344**	**0.402**	**0.345**
P_{max} (mW)	**0.07**	**0.10**	**.087**	**0.10**	**0.21**	**0.187**
η %	**0.069**	**0.107**	**0.108**	**0.159**	**0.275**	**0.109**

The conversion efficiencies (η), maximum power (P_{max}), short circuit current densities (J_{sc}) and open circuit photo-voltages (V_{oc}) for the different DSSCs using various ZnO thicknesses at the photo-anode are summarized in Table 5.4.

Table. 5.4. Photovoltaic parameters of the DSSCs sensitized by safflower dyes, at different ZnO thicknesses.

ZnO Thickness (µm)	**9.8**	**7.5**	**6.5**	**5**	**3.5**	**2.2**
J_{sc} (mA/cm^2)	**0.075**	**0.88**	**0.33**	**0.07**	**0.22**	**0.23**
V_{oc} (V)	**0.266**	**0.370**	**0.269**	**0.262**	**0.303**	**0.303**
P_{max} (mW)	**0.006**	**0.09**	**0.021**	**0.004**	**0.017**	**0.018**
η %	**0.005**	**0.095**	**0.02**	**0.005**	**0.01**	**0.01**

The short circuit current, open circuit voltage, maximum power, and conversion efficiency versus the thicknesses of the ZnO layer are, respectively, shown in Figs. 5.9 (a), 5.9 (b), 5.10 (a), and 5.10 (b). All these parameters exhibit a peak at a layer thickness of 7.5µm. These figure correspond to DSSCs sensitized by Eosin Y. Figures 5.11 and 5.12 show the same for DSSCs sensitized by safflowers.

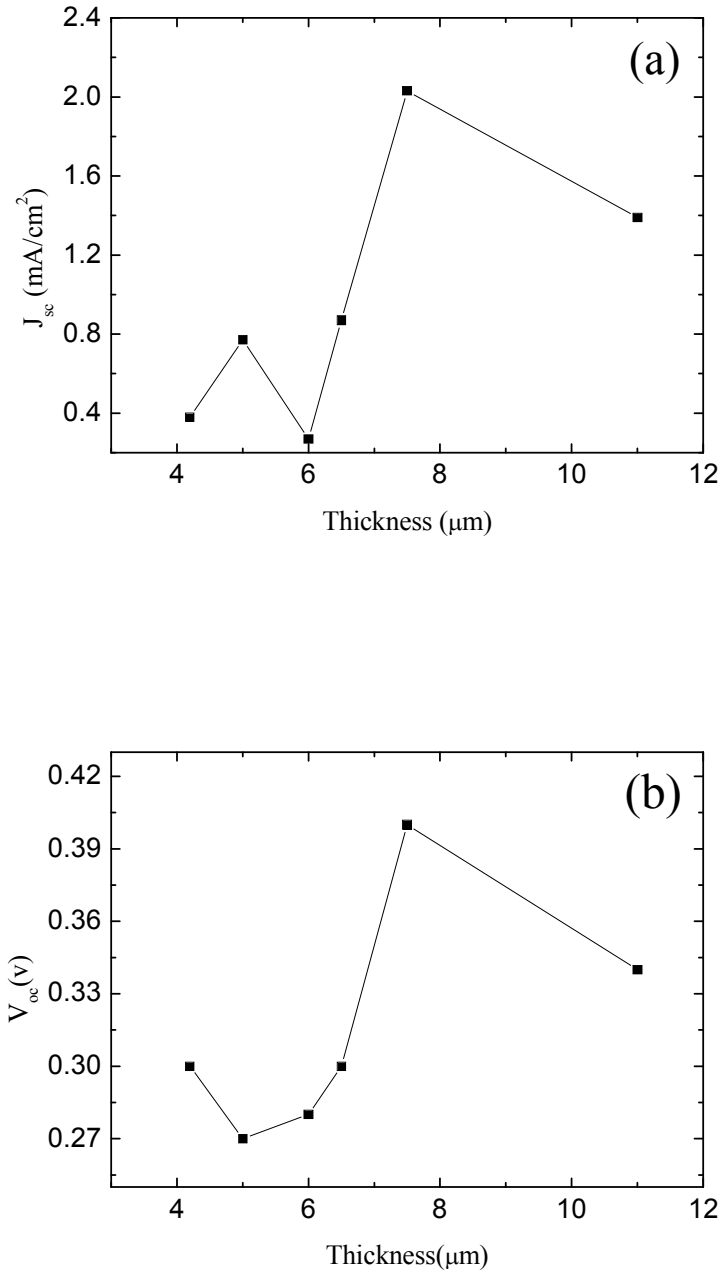

Figure 5.9. Variation of (a) short circuit current density and (b) open circuit voltage as a function of ZnO layer thicknesses of the photo-anodes, using Eosin Y as a sensitizer.

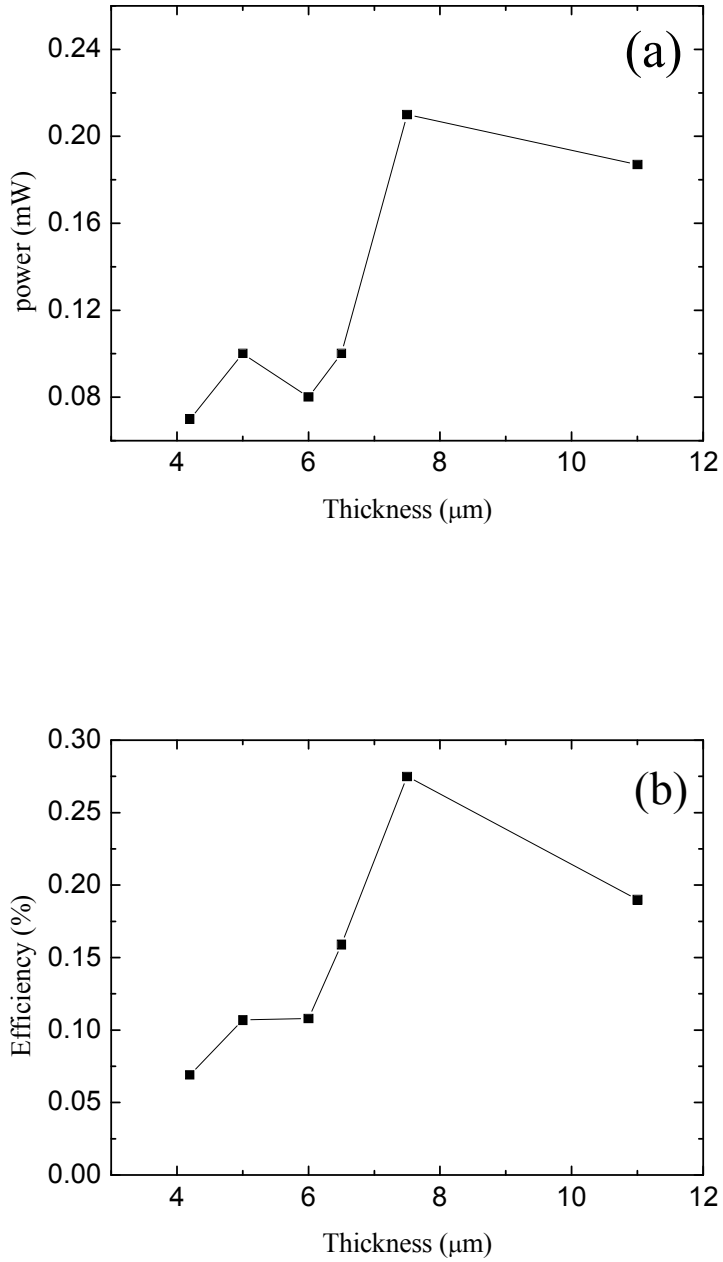

Figure 5.10. Variation of (a) power and (b) efficiency as a function of ZnO layer thicknesses of the photo-anodes, using Eosin Y as a sensitizer

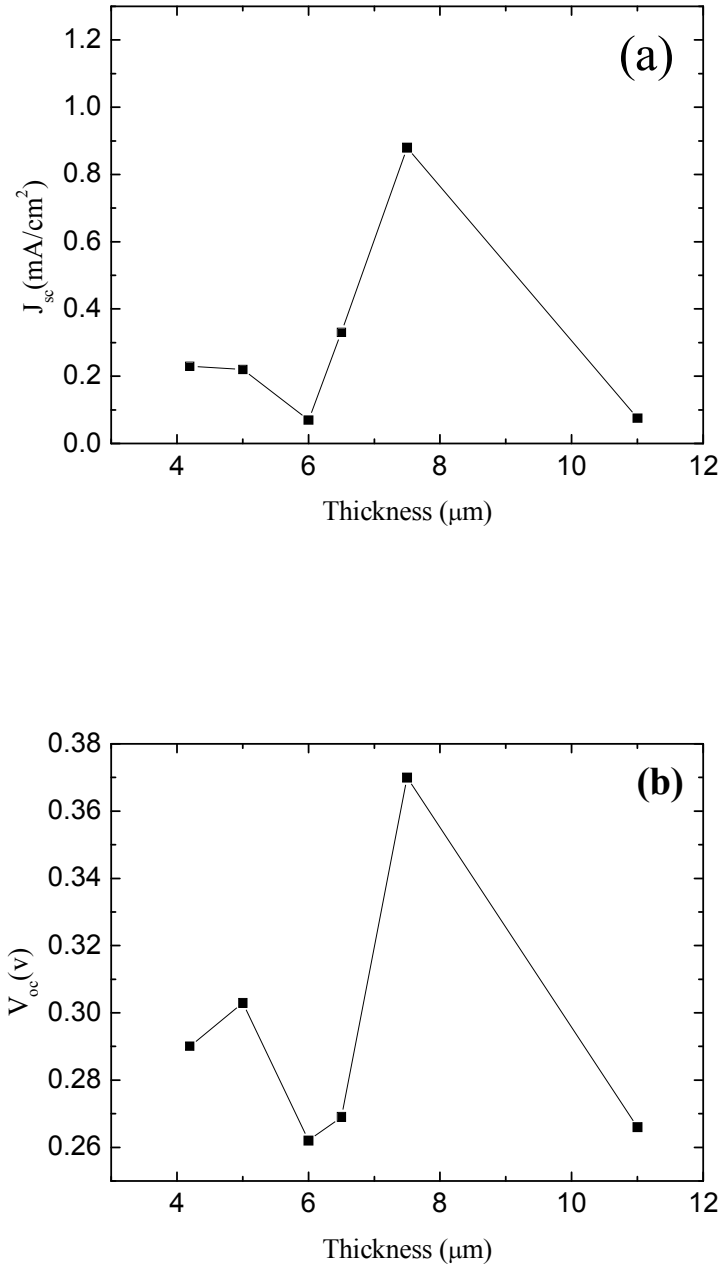

Figure 5.11. Variation of (a) short circuit current density and (b) open circuit voltage as a function of ZnO layer thicknesses of the photo-anodes, using safflower as a sensitizer.

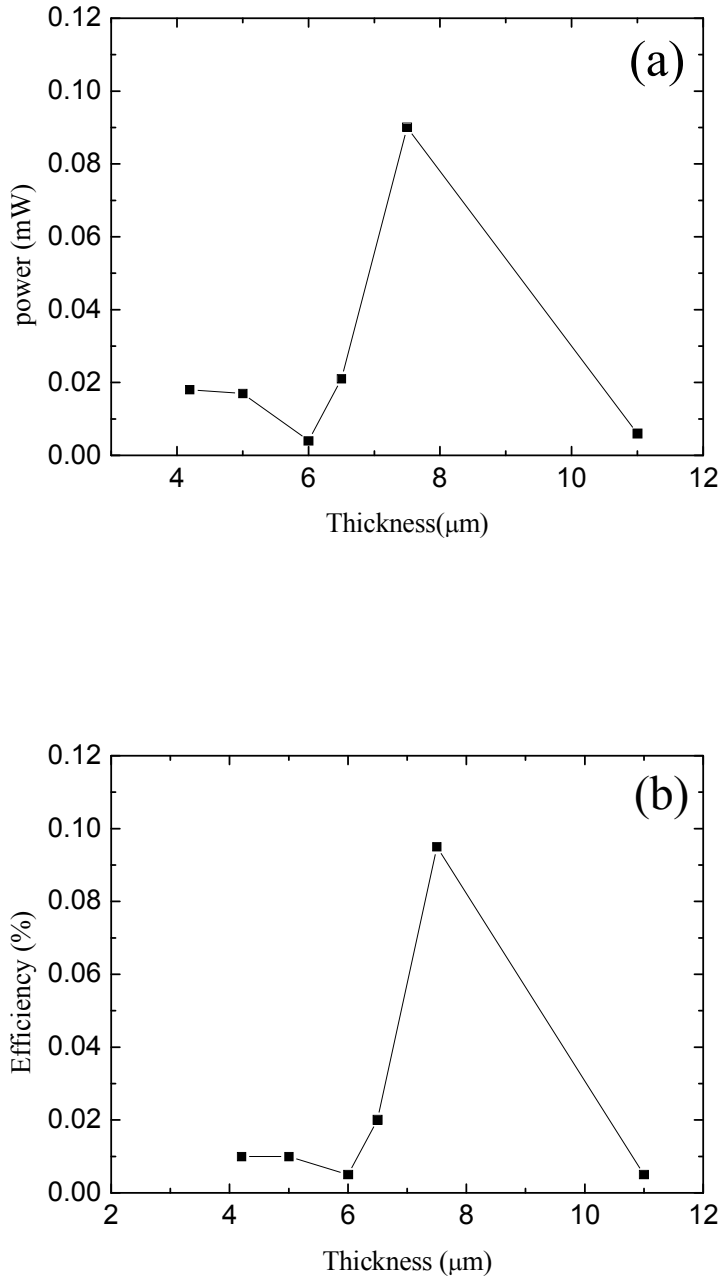

Figure 5.12. Variation of (a) power and (b) Efficiency as a function of ZnO layer thicknesses of the photo-anodes, using safflower as a sensitizer.

5.4 Absorption Spectra of Eosin Y and Safflower on ZnO Nanoparticles

Eosin Y shows an intense absorption peak in the visible region at 520.4 nm which corresponds to the maximum absorption peak of the Eosin Y monomer (see Fig. 4.1). When ZnO layer was dyed with Eosin Y, the spectrum was carried out a gain. Fig. 5.13 shows the UV–VIS spectra of Eosin Y absorbed on ZnO film. The absorption

spectra which Eosin Y adsorbed on ZnO is obviously wider and very small shifted compared with that in ethyl alcohol solution. When Eosin Y was adsorbed on the ZnO film, the peak was observed which means that the interaction between the dyes and the cationic ZnO surface was observed. The interaction was formed through a chemical bond. Similarly, when the ZnO layer is dyed with safflower, the absorption spectrum is carried out a gain. Fig. 5.14 shows the UV–VIS spectra of safflower adsorbed on ZnO film together with that of safflower in ethyl alcohol . The peak is observed to be widen and shifted toward lower wavelength.

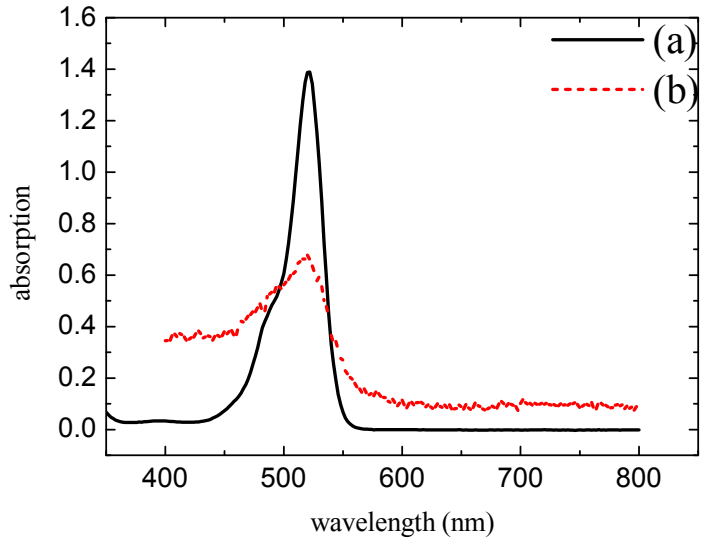

Figure 5.13. The absorption spectrum of (a) Eosin Y in ethyl alcohol and (b) Eosin Y adsorbed on ZnO layer.

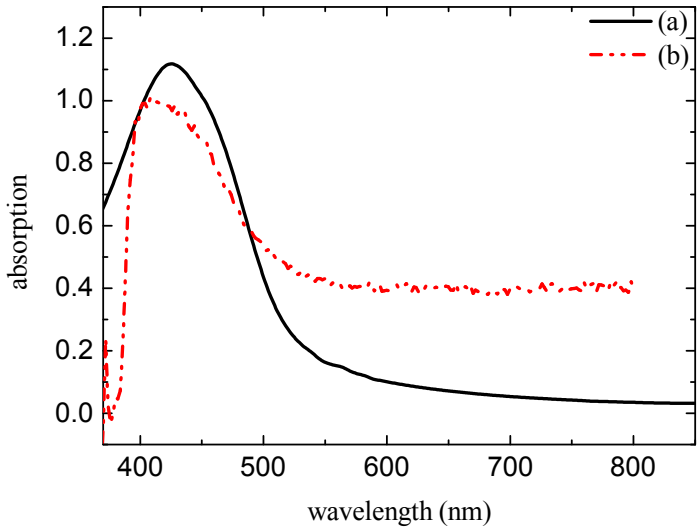

Figure 5.14. The absorption spectrum of (a) safflower in ethyl alcohol and (b) safflower adsorbed on ZnO layer.

Conclusion

The work in this thesis sought to better understand and demonstrate the necessary steps needed to make solar energy as economically viable as fossil fuels. The chosen system to study was the dye sensitized solar cell. DSSCs have the potential to be cheaper than other solar cells and just as efficient.

In chapter 1 and 2, some of the concepts and fundamentals of solar cells such as solid state solar cells, semiconductors, light absorption, photovoltaic processes in a solar cell, operating principle in DSSCs, materials of a DSSC have been studied. The basic differences between the DSSC and p-n- junction solar cells have been presented. Factors that affect the efficiency of the DSSC have been pointed out.

In chapter 3, natural dyes were extracted from seeds, leaves, flowers and roots of plants. The ZnO layer was dyed using eight natural dyes, A set of dye-sensitized solar cells were assembled using two dye solvents and two materials as a back electrode. The fabricated cells were examined under three different light intensities.

The following results have been obtained:

- Using ethyl alcohol to extract natural dyes and carbon as a back electrode, J_{sc} from 0.214 mA/cm^2 to 0.786 mA/cm^2 and V_{oc} from 0.258V to 0.385V at intensities equal (80-100-120klux).
- Using polyethylene glycol as a solvent and carbon as a back electrode the results were founded as, the J_{sc} from 0.031 mA/cm^2 to 0.409 mA/cm^2 and V_{oc} from 0.140V to 0.400V at intensities equal (80-100-120 klux).
- Using ethyl alcohol as a solvent and platinum as a back electrode the results were founded as, the J_{sc} from 0.08 mA/cm^2 to1 mA/cm^2 and V_{oc} from 0.169V to0.379V at intensities equal (80-100-120klux).
- Using polyethylene glycol as a solvent and platinum as a back electrode the results were founded as, the J_{sc} from to 0.03 mA/cm^2 to 0.18 mA/cm^2 and V_{oc} from 0.199V to 0.348V at intensities equal (80-100-120klux).

In chapter 4, eight chemical dyes were used as sensitizer for DSSCs. Eight dyes such as Alcian blue, Crystal violet, Eosin y, Carbol fuchsin, Aniline blue, Methyl orange, Fast green and Bromophenol were investigated and using ethyl alcohol as solvent only. And we were used platinum as back electrode and ethyl alcohol as solvent of

dyes the results were founded as, the J_{sc} from 0.33 mA/cm^2 to 1.38 mA/cm^2 and V_{oc} from 0.300 V to 0.421V at intensities equal (80-100-120klux).

In chapter 5, the optimum sintering temperature and thickness for ZnO past was studied which we were dyed with safflower as natural dye and Eosin y as a chemical dye have been used. The optimum sintering temperature was found to be 425 ±5 ^{0}C. The optimum thickness for ZnO layer was found to be 7.5 ±5.2× 10^{-7} μm.

References

[1] D. Walker, "Corrole Sensitized Solar Cells", Cal. I. of Technology, Pasadena, California, 2011

[2] K. Lovegrove and K. Weber, "Solar Energy - Power for the new Millennium," Australian National University - Centre for Sustainable Energy Systems, http://online.anu.edu.au/engn/solar/solarth/ct.html, 1999.

[3] B. Sørensen, "Renewable Energy", 1st edn., Academic Press, London, 1979.

[4] R.L. Sizmann, P. Köpke and R. Busen, "Solar power plants", 17-83, editor: C.-J. Winter, R.L. Sizmann and L.L. Vant-Hull, "Solar Radiation Conversion" Springer-Verlag, Berlin, Heidelberg, 1991.

[5] S.R. Wenham, M.A. Green and M.E. Watt, "Applied Photovoltaics", Bridge Printery, 1994.

[6] D.M. Chapin, C.S. Fuller and G.L. Pearson, "A New Silicon p-n Junction Photocell for Converting Solar Radiation into Electrical Power ", J. Appl. Phys., 25, 676-677, 1954.

[7] J. Nelson ," The Physics of Solar Cell", 13-16, 2003.

[8] D.G.Wolfbauer, " The Electrochemistry of Dye sensitized solar cell ,their sensitizer and their redox shuttles", Department of chemistry, monash, clayton3168, Melbourne, Australia, 1997.

[9] B. O'Regan and M. Grätzel, " A low cost high-efficiency solar cell based on dye-sensitized colloidal TiO2 films", Nature, 353, 737-740, 1991.

[10] M. K. Nazeeruddin, et al., " Conversion of Light to Electricity by cis-X2Bis(2,2'-bipyridyl-4,4'- dicarboxylate) ruthenium(II) Charge-Transfer Sensitizers (X = Cl-, Br-, I-, CN- and SCN-) on Nanocrystalline TiO2 Electrodes", J. Am. Chem. Soc., 115, 6382-6390, 1993.

[11] A. Tolvanen, "Characterization and manufacturing techniques of dye sensitized solar cell", Master of science in technology, 2003.

[12] M. Toivola, "DYE-SENSITIZED SOLAR CELLS ON ALTERNATIVE SUBSTRATES", Master of science in technology, 2010.

[13] A. Luque , S. Hegedus "Handbook of Photovoltaic Science and Engineering", Master of science in technology, 664-665, 2002.

[14] J. Halme, " Dye-sensitized nanostructured and organic photovoltaic cells: technical review and preliminary tests", Master of science in technology, 2002.

[15] C. Klein., M. K. Nazeeruddin, D. D. Censo, P. Liska, M. Grätzel, "Inorganic Chemistry", 4216,43, 2004.
[16] G. Wolfbauer, et al., "A channel flow cell system specifically designed to test the efficiency of redox shuttles in dye sensitized solar cells", Solar Energy Materials & Solar Cells, 70, 85-101, 2001.
[17] A. Stanley, et al., " Minimizing the dark current at the dye-sensitized TiO2 electrode, Solar Energy Materials & Solar Cells", 52, 141-154, 1998.
[18] G. Smestad, et al., " Testing of dye-sensitized TiO2 solar cells I: Experimental photocurrent output and conversion efficiencies", Solar Energy Materials & Solar Cells, 32, 3, 259-272, 1994.
[19] M. K. Nazeeruddin, et al., " Conversion of Light to Electricity by cis-X2Bis(2,2'-bipyridyl-4,4'- dicarboxylate)ruthenium(II) Charge-Transfer Sensitizers (X = Cl-, Br-, I-, CN- and SCN-) on Nanocrystalline TiO2 Electrodes", J. Am. Chem. Soc., 115, 6382-6390, 1993.
[20] G. Chmiel, et al., " Dye sensitized solar cells (DSC): Progress towards application", 2nd World Conference and Exhibition on Photovoltaic Solar Energy Conversion, 6-10 July Vienna Austria, 1998.
[21] S. Lee, et al., " Modification of electrodes in nanocrystalline dye-sensitised TiO2 solar cells, Solar Energy Materials and Solar Cells", 65, 193-200, 2001.
[22] E. Olsen, et al., " Dissolution of platinum in methoxy propionitrile containing Li/I2", solar energy materials and solar cells 63, 267-273, 2000.
[23] G. Calogero, G. D. Marco, S. Cazzanti, S. Caramori، R. Argazzi, A. D. Carlo, C. A. Bignozzi, Int. J. Mol. Sci11 254–267, 2010.
[24] C.G. Garcia, A. S. Polo, and N. Y. Murakami Iha, J. Photochem. Photobiol, A, 160, 87–91, 2003.
[25] R. G.Gordon, "Criteria for Choosing Transparent Conductors", MRS Bulletin, Aug., 52-57, 2000.
[26] S. Hao, J. Wu, Y. Huang, and J. Lin, "Natural dyes as photosensitizers for dye-sensitized solar cell" Solar Energy, 80(2006): 209-214, 2006.
[27] A. S. Polo and N. Y. M. Iha "Blue sensitizers for solar cells: Natural dyes from Calafate and Jaboticaba", Solar Energy Materials and Solar Cells, 90(2006): 1936-1944, 2006.
[28] J. M. Kroon, N. J. Bakker, H. J. P. Smit, P. Liska, K. R. Thampi, P. Wang, S. M. Zakeeruddin, M. Grätzel, A. Hinsch, S. Hore, U. Würfel، R. Sastrawan, J. R. Durrant,

E. Palomares, H. Pettersson, T. Gruszecki، K. Skupien, and G. E. Tulloch, "Nanocrystalline dye-sensitized solar cells having maximum performance, Progress in Photovoltaics Research and Applications, Progress in Photo- voltaic", 15, 1, 1-18, 2006.

[29] F. Odobel, E. Blart, M. Lagrée, "Porphyrin dyes for TiO_2 sensitization", J Mater Chem, 13,502 510, 2003.

[30] M.K. Nazeeruddin, R. Humphry-Baker, M .Grätzel, D .Wohrle, G .Schnurpfeil, G .Schneider, A .Hirth, N .Trombach, "Efficient near-IR sensitization of nanocrystalline TiO_2 films by zinc and aluminum phthalocyanines", J Porphyrins Phthalocyanines. 3:230–237, 1999.

[31] J .He, A. Hagfeldt, SE .Lindquist," Phthalocyanine-Sensitized nanostructured TiO_2 electrodes prepared by a novel anchoring method", Langmuir. 17:2743–2747, 2001.

[32] A. Islam, H. Sugihara, K. Hara, LP .Singh, R. Katoh, M. Yanagida, Y .Takahashi, S .Murata" Dye sensitization of nanocrystalline titanium dioxide with square planar platinum(II) diimine dithiolate complexes" Inorganic Chemistry, 40:5371–5380, 2001.

[33] J.M .Rehm, G.L .McLendon, Y .Nagasawa, K .Yoshihara, J. Moser, M. Grätzel," Femtosecond electron-transfer dynamics at a sensitizing dye-semiconductor (TiO_2) interface", J Physic Chem,100:9577–9588, 1996.

[34] D.A. Neamen, "Semiconductor Physics and Devices", Richard D. IRWIN, Inc., 1992.

[35] E. Yamazaki, M. Murayama, N. Nishikawa, N. Hashimoto, M. Shoyama, O. Kurita, "Utilization of natural carotenoids as photosensitizers for dye-sensitized solar cells", Sol. Energy 81, 512–516, 2007.

[36] D. Li, and H.H. Mundel, "Safflower Carthamus tinctorius L Promoting the Conservation and Use of Underutilized and Neglected Crops. 7. Institute of Plant Genetics and Crop Plant Research", Gatersleben/International Plant Genetic Resources Institute, Rome, 1996.

[37] J.S .Kwon, J.T .Snook, G.M .Wardlaw, D.H.Hwang, "Effects of diets high in saturated fatty acids, canola oil, or safflower oil on platelet function, thromboxane B2 formation, and fatty acid composition of platelet phospholipids", Am J Clin, Nutr;54(2):351-358, 1991.

[38] C. M. john, "The anti-inflammatory properties of safflower oil and coconut oil may be mediated by their respective concentrations of vitamin E", J Am Coll Cardiol , 49(17):1825-1826, 2007.

[39] M. Perez, F.Torrades, X.Domenech, J.Peral, "Fenton and photo-Fenton oxidation of textile effluents", *Water Res*, **36**, 2703-2710, 2002.

[40] Y. Xie, F. Chen, J.He, Z.Jincai, H.Wang, "Photoassisted degradation of dyes in the presence of Fe3+ and H2O2 under visible irradiation", *Photochem Photobiol J*, 136, 235-240, 2000.

[41] M.S.Lucas, J.A.Peres, " Decolorization of the azo dye reactive black 5 by Fenton and photo-Fenton oxidation, *Dyes Pigments*", **71**, 235-243, 2006.

[42] P. Teesetsopon1, S. Kumar1 and J. Dutta, "Photoelectrode Optimization of Zinc Oxide Nanoparticle Based Dye-Sensitized Solar Cell by Thermal Treatment", International Journal of electrochemical science Int. J. Electrochem. Sci., 7 4988 – 4999, 2012.

[43] I.T. Young, R. Zagers, L.J. van Vliet, J. Mullikin, F. Boddeke, H. Netten, "Depth-of-Focus in microscopy, in:SCIA'93", Proc. of the 8th Scandinavian Conference on Image Analysis, Tromso, Norway, 493-498, 1993.